ABSTRACT

Title of Document: CHROMOPHORIC DISSOLVED ORGANIC MATTER (CDOM) IN THE OCEAN: OPTICAL PROPERTIES AND RELATION TO CDOM STRUCTURE AND SOURCE

Andrea Anna Sherma Andrew
Doctor of Philosophy, 2014

Directed By: Professor Neil V. Blough, Department of Chemistry and Biochemistry

CDOM is a ubiquitous component of the dissolved organic matter pool which absorbs UV and visible light. Owing to its optical properties it plays a critical role in photochemistry and biogeochemistry in aquatic systems. Extensive data exist on the optical properties of CDOM from both terrestrial and coastal environments, yet the open oceans have been under-sampled. Consequently, the source and structural basis of marine CDOM optical properties are still debated. To address this, CDOM optical properties were acquired for both untreated and sodium borohydride (NaBH4) reduced natural waters and C18 extracts for waters of the Equatorial Atlantic Ocean. The similarities and differences were examined relative to optical data obtained for CDOM from terrestrial sources. Ocean CDOM was found to comprise of a marine CDOM

component (absorbs and emits in the UV), as well as a terrestrial CDOM component (absorbs in the UV-Vis, and emits in the visible).

CDOM concentrations in oceans are low and seawater contains high salt concentrations, impeding the use of some analytical techniques. These salts can be removed by solid phase extraction which results higher concentrations of organic matter. The extent to which the C18 extracts represent the whole water samples was examined. Our data indicate that the optical properties of the extracted material is largely representative of the original CDOM.

It is generally suggested that optical measurements for CDOM be acquired as close to the time of collection as possible. However, CDOM is commonly stored at 4°C in the dark and there is no consensus regarding the effect of storage on CDOM. To address this, the effect of storage on the optical properties of CDOM samples stored for 6 years was examined. Taking into account standard deviation in optical measurements, it was concluded that the storage protocol did not significantly affect CDOM optical properties.

In situ production has been suggested as one of the main sources of CDOM in oceans. The optical properties of DOM produced by one of the most abundant bacteria in oceans (*P. ubique*) was examined. The results indicate that under our incubation conditions CDOM is not produced.

CHROMOPHORIC DISSOLVED ORGANIC MATTER (CDOM) IN THE OCEAN: OPTICAL PROPERTIES AND RELATION TO CDOM STRUCTURE AND SOURCE

By

Andrea Anna Sherma Andrew

Dissertation submitted to the Faculty of the Graduate School of the
University of Maryland, College Park, in partial fulfillment
of the requirements for the degree of
Doctor of Philosophy
2014

Advisory Committee:
Professor Neil V. Blough, Chair
Professor Alice C. Mignerey
Professor George R. Helz
Professor Amy S. Mullin
Professor Sujay S. Kaushal

Dedication

To My Family,

particularly my mother and father, Angela and Eustace Andrew.

Daddy I wish you were here for this.

Acknowledgements

So many people have contributed to my success to this point in my career. It is almost too overwhelming to think of the number of people that I sincerely wish to pay gratitude to.

Foremost, I would like to express my sincere gratitude to my advisor Dr Neil V. Blough for his continuous support throughout my Ph. D research. Because of you I have had so many wonderful experiences (going out at sea, working with so many people on collaborative projects). Without your knowledge, guidance, constructive comments, encouragement, and most of all patience, this work would not have been possible.

My supervisor Dr. Rossana Del Vecchio, has been a great source of knowledge and insight during this process. I sincerely want to thank her for all the many discussions regarding analyzing and presenting data, for editing my not so great first drafts, and most importantly for teaching me the skills to interpret the data in terms of the big picture.

Thank you to the rest of my thesis committee: Professor Alice Mignerey, Professor Amy Mullin, Professor George Helz and Professor Sujay Kaushal.

Special thanks to the crew of the R/V Endeavor, who took care of me at sea and brought me back home safely, and to all the people who assisted me in sample collection and processing.

I thank my fellow lab mates Yi Zhang, Tara Schendorf, Dan Baluha, Kelli Golanoski, Lynne Heighton and Kevin Khoech for their stimulating discussions, and being there for me during the fun times and the not so great times, particularly during my knee surgery. It meant everything to me that I could count on you guys for anything.

I would like to thank my family for the unwavering support financially, emotionally and spiritually. You guys pushed me through this even when I didn't feel that I could make it, and believed in me when I didn't believe in myself.

Last but not least, I would like to say a very special thank you to Doile, who has been by my side throughout this journey. Your support meant everything to me.

Table of Contents

List of Tables

List of Figures

Chapter 1: Chromophoric Dissolved Organic Matter (CDOM) - Background and significance

1.1 What is CDOM?

Natural organic matter (NOM) is composed of organic compounds from the remains of once-living organisms such as plants and animals and their waste products in the environment. Dissolved organic matter (DOM) is operationally defined as the fraction of NOM present in surface and ground water that passes through a 0.2um filter. The fraction of the total DOM that absorbs light is referred to as chromophoric dissolved organic matter (CDOM), but in the past has often been called gelbstoff, gilvin and yellow substance. The organic matter isolated from CDOM using solid phase extraction techniques is termed "humic substances" (HS). HS can be further subdivided into humic and fulvic acids based on extraction techniques employed. Fulvic acids are soluble at all pH values, whereas humic acids are only soluble above pH 2 (Figure 1 - 1).

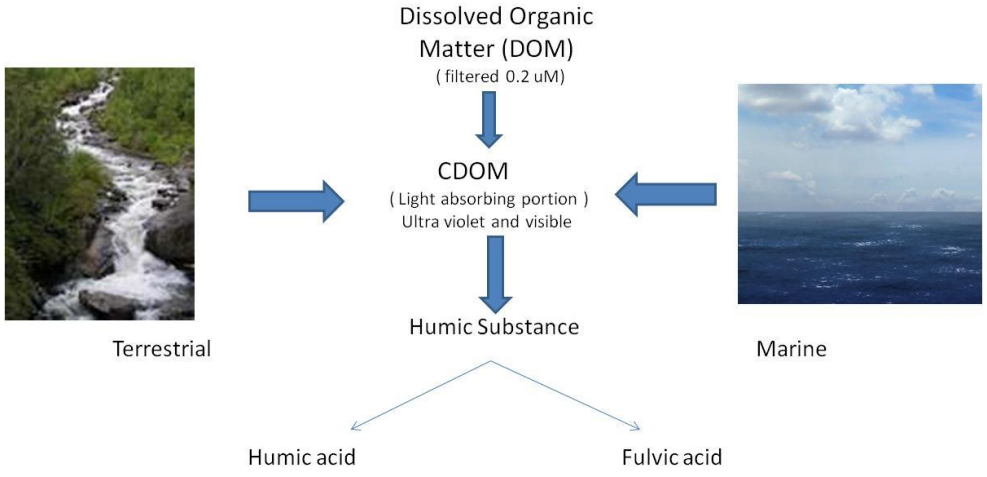

Figure 1 - 1: The relationship between DOM, CDOM and humic substances

1.2 Environmental significance

DOM in oceans is one of the world's largest bioactive reservoirs of carbon and plays a major role in the carbon cycle and global climate (Hansell et al., 2009). Although evidence suggests that CDOM represents a small fraction of the DOM pool, absorption of light in aquatic environments is primarily due to dissolved (CDOM) and particulate organic matter (phytoplankton pigments and detritus) and hence the need to better understand this DOM fraction. CDOM greatly influences the aquatic light field and the biogeochemistry of both fresh and marine waters due to its unique optical properties and ubiquitous presence in natural waters. It absorbs solar radiation in the ultraviolet and visible wavelength regimes, with strongest absorption at short wavelengths, ranging from the blue to ultraviolet (UVA/B) (Blough and Del Vecchio, 2002; Blough and Zepp, 1995; Bricaud et al., 1981). CDOM can thus provide protection from damaging UV radiation for phytoplankton and other light-sensitive organisms (Blough and Del Vecchio, 2002; Coble, 2007; Whitehead et al., 2000). In areas influenced by rivers, increased absorption of visible light by CDOM can affect the amount and quality of photosynthetically active radiation (PAR) available to phytoplankton ultimately influencing primary production (Blough et al., 1993; DeGrandpre et al., 1996; Vodacek et al., 1997; Vodacek et al., 1995). CDOM is also photoreactive (Mopper and Kieber, 2002; Moran and Zepp, 1997) resulting in the production of photochemical intermediates which ultimately lead to CDOM 'bleaching' or loss of absorption (Del Vecchio and Blough, 2002; Vodacek et al., 1997; Whitehead et al., 2000) thus altering the aquatic light field (Del Vecchio and Blough, 2004b; Nelson and Siegel, 2002). These photochemical reactions can result in

the production of biologically-available low molecular weight compounds (Kieber et al., 1989; Mopper and Kieber, 2002; Moran and Zepp, 1997) that can fuel the growth of micro-organisms. The bioavailability of trace metals can also be influenced due to direct photochemistry or reactions with reactive oxygen species (Blough and Del Vecchio, 2002). Light absorption by CDOM can also result in the photochemical production of a number of important trace gases such as CO_2 and CO, as well as the photosensitized loss of gases such as dimethyl sulfide (Mopper and Kieber, 2002; Nelson and Siegel, 2002).

CDOM also interferes with satellite remote sensing retrievals of chlorophyll-a concentrations that are needed to estimate ocean primary productivity. Chlorophyll-a has a strong absorption band in the blue portion of the electromagnetic spectrum that may be obscured by CDOM absorption, because they both absorb in the same wavelength regime (Del Castillo, 2005). Also, as a result of CDOM's influence on ocean color and the improvements of satellite ocean color sensors and data interpretation, CDOM has also been employed as a tracer of upper ocean biogeochemical processes and water mass mixing (Chen and Gardner, 2004; Del Vecchio et al., 2009; Nelson and Siegel, 2013; Stedmon et al., 2010)

1.3 Optical properties

1.3.1 Absorbance

Since CDOM absorbs and emits light in the ultraviolet and visible portion of the electromagnetic spectrum, absorption and fluorescence spectroscopy is commonly used

to investigate its optical properties. CDOM absorption spectra are featureless and decrease exponentially toward longer wavelengths (Bricaud et al., 1981; Green and Blough, 1994) (Figure 1 - 2). The absorption spectrum is usually parameterized as an exponential function of the form

$$a(\lambda) = a(\lambda_0)e^{-S(\lambda-\lambda_0)} \qquad \text{(Eqn. 1)}$$

where $a(\lambda)$ and $a(\lambda_0)$ are absorption coefficients at wavelength λ and reference wavelength λ_0. S, the spectral slope, defines how rapidly the absorption decreases with increasing wavelength. Absorption coefficients are calculated from the relation

$$a(\lambda) = 2.303A(\lambda)/l \qquad \text{(Eqn. 2)}$$

where A is the optical density measured across pathlength l(meters), and 2.303 is the conversion factor between base 10 logarithm and natural logarithm.

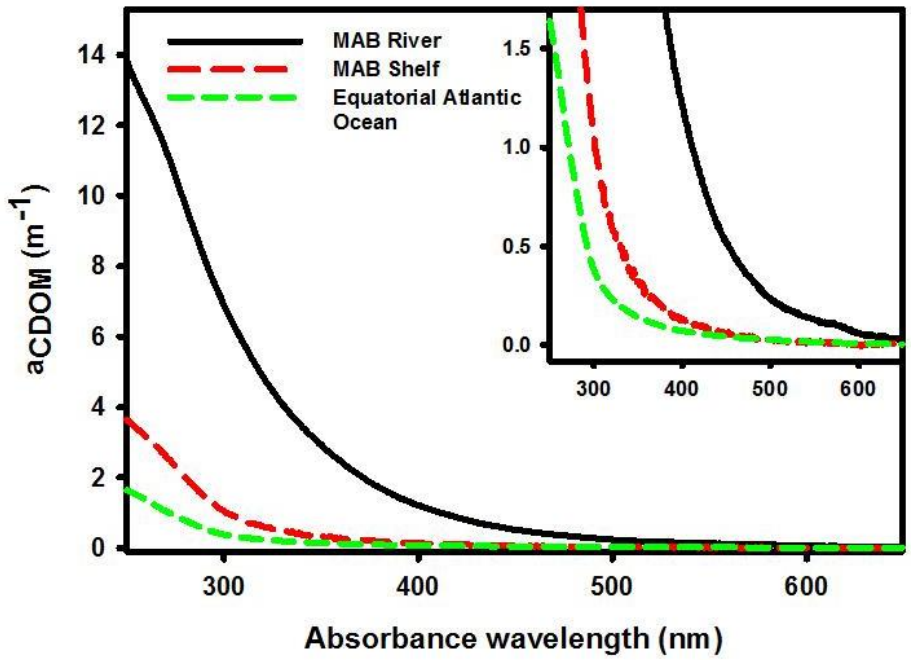

Figure 1 - 2: Absorption spectrum for surface CDOM samples from the Middle Atlantic Bight (MAB) river and shelf and from the equatorial Atlantic Ocean (Station 14- 2.99° S, 9.99° W). Inset - expanded scale for a_{CDOM} values 0 – 1.7 m^{-1}

CDOM absorption and spectral slope (S) values vary spatially and temporally and can provide useful information about sources and nature of CDOM. Larger absorption coefficients are generally exhibited by fresh waters and for coastal waters receiving large fresh water inputs, relative to oligotrophic seawaters. Conversely, coastal and fresh water environments exhibit smaller S values as a result of the larger absorption contribution in the visible wavelength regime, relative to oligotrophic waters (Nelson and Siegel, 2002). The higher degree of aromaticity and complexity within CDOM from fresh and coastal waters results in more absorption towards longer wavelength and thus smaller S values relative to marine CDOM (Del Castillo, 2005). Although S varies with source, it can also be altered through biological (Moran et al., 2000) and chemical processing (e.g. solar irradiation and reduction) of the source material (Del Vecchio and Blough, 2002; Helms et al., 2008) or even mixing (Del Castillo, 2005).

1.3.2 Fluorescence

The emission spectrum of CDOM is very broad and unstructured, similar to absorbance spectrum (Figure 1 - 3: each colored line). Emission intensity decreases, while its maximum continuously red-shifts with increasing excitation wavelength (Figure 1 - 3: black arrow & inset), suggesting the presence of numerous absorbing centers. This unusual relationship between excitation wavelength, emission intensity and emission maxima, highly underscore the complexity of CDOM. As a result, excitation-emission matrix spectra (EEMS) (Figure 1 - 3) are usually employed to provide a more complete picture of CDOM fluorescence emission properties.

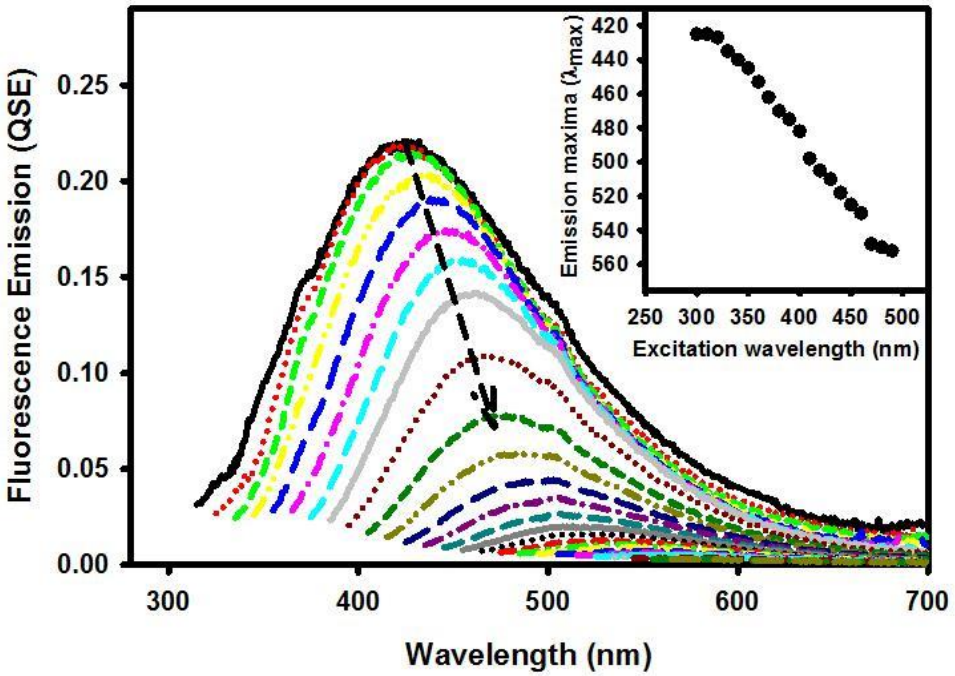

Figure 1 - 3 EEMS for a CDOM surface sample from the MAB region in August 2006 (excited from 300 - 550 nm). Emission intensities are reported in quinine sulfate equivalents (QSE), obtained by normalizing the sample EEMS with the emission of 1ppb Quinine sulfate excited at 350 nm (fluorescence standard). Inset: wavelength of maximun emission at excitation wavelengths 300 - 500 nm)

EEMS are obtained by collecting individual emission spectra at successively longer excitation wavelengths (Figure 1 - 3: each spectrum is a different color). These spectra are then combined in one plot, which displays fluorescence emission intensity as a function of excitation and emission wavelength. EEMS can be used to characterize and identify the various groups of fluorescing components which comprise CDOM (Coble, 1996; Coble et al., 1990; Kowalczuk et al., 2005), thus providing additional information about the possible sources and nature of CDOM. EEMS can thus be a valuable tool when analyzing the various fluorescent components of CDOM and the changes resulting from

mixing, biological degradation or production, and photo-bleaching that may occur in the environment.

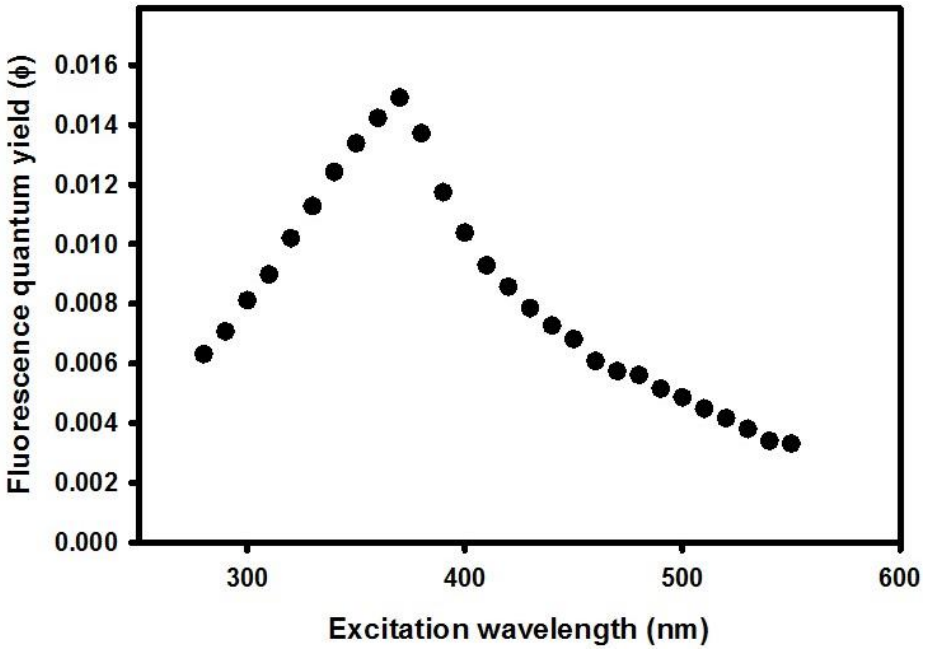

Figure 1 - 4: Wavelength dependence of quantum yield for a surface CDOM sample (river) from the MAB region in August 2006.

1.3.3 Quantum yield

The fluorescence quantum yield (QY or ϕ) is defined as the ratio of photons emitted to those absorbed and represents another tool for characterizing CDOM from different locales. Similar to absorbance and fluorescence emission, the wavelength dependence of quantum yield is also very distinctive. The maximum QY values are generally obtained with excitation wavelengths between 360 and 400 nm, and decreases at both shorter and longer excitation wavelengths (Figure 1 - 4). QY values are generally low, on the order of 0.1 – 2.5% depending on source (Andrew et al., 2013; Boyle et al., 2009; Green and Blough, 1994).

1.4 Sources and sinks

Although CDOM occurs naturally in all aquatic environments, it has generally been classified into two general types, terrestrial and marine, based on its optical properties and possible origin. However, how much the optical properties vary in aquatic systems due to differences in the source of CDOM as opposed to the chemical and biological processing of a given source material remains highly uncertain. Terrestrial CDOM is usually observed in rivers, estuaries and coastal waters receiving large river inputs. In these locales, absorption coefficients vary linearly and inversely with salinity, indicative of a fresh water source, while the values of S are usually comparable with those observed for river end-members. Recent work has also shown excellent correlations between terrestrial CDOM absorbance at 350 nm and lignin phenols, suggesting that it originates from a lignin source (Hernes and Benner, 2003; Stenson et al., 2003; Stubbins et al., 2010), and to a smaller extent tannins (Maie et al., 2008; Sleighter and Hatcher, 2008). Changes in optical properties begin to become evident in higher salinity waters, suggestive of a transition between terrestrially dominated regions and more marine like regions. This may be as a result of the replacement of the terrestrial CDOM with a marine form or from photochemical or biological processing of the terrestrial source material, or a combination of these factors.

Although much headway has been made regarding the source of terrestrial CDOM, the primary source of marine CDOM (away from river dominated margins and in open oceans) is still a highly debated issue. Further hindering the determination of the source of marine CDOM is the fact that marine environments have historically been under

sampled. Unlike terrestrial CDOM, absorption coefficients observed for marine CDOM are usually very low (~0.1 - 0.2 m^{-1} at 355 nm) , and exhibit no clear correlation with salinity (Ferrari and Dowell, 1998). Lack of correlation of a_{CDOM} with salinity suggests that terrestrial input may only be a small fraction or that other sources may be involved in marine CDOM production. Some researchers have postulated that the primary source of marine CDOM is in situ biological production from marine source materials (Steinberg et al., 2004; Yamashita and Tanoue, 2004) by as yet ill-defined formation mechanisms/processes. Other researchers suggest that it is in part the result of chemical modification and dilution of residual terrestrial material (humic substances) during transport to the ocean (Hernes and Benner, 2006; Murphy et al., 2008). Recent work has shown that although there are some differences in the optical properties of terrestrial and marine CDOM, there are however very striking similarities (Andrew et al., 2013).

Although a significant volume of river water is continuously being discharged to oceans and seas introducing an appreciable amount of CDOM, the oceans are not as colored (Blough and Del Vecchio, 2002). There is a discernible difference in CDOM absorption values between these two environments. This suggests that there must be one or more significant transformational processes that act as sinks of CDOM and the contribution from in situ production in oceans is very small. Early studies indicated that loss of terrestrial CDOM could result from flocculation and precipitation. However later studies have shown that these loss methods appear to be inconsequential based on the conservative or quasi-conservative mixing observed for estuaries (Blough et al., 1993; Del Castillo et al., 1999). Further, direct bacterial degradation does not appear to be a

significant sink (Moran et al., 2000). However, more recent studies indicate that photochemical degradation (photo bleaching) and photo-degradation coupled with bacterial uptake have been shown to act as substantial sinks of CDOM (Del Vecchio and Blough, 2004b; Kieber et al., 1989; Spencer et al., 2009; Vodacek et al., 1997).

1.5 Structural basis of optical properties

Several spectroscopic analytical techniques have been employed to gain structural information about CDOM (Kujawinski et al., 2004; Mopper et al., 2007) and indicate that CDOM contains a variety of structures including carboxylic acids, carboxyl-rich molecules, substituted phenols, ketones, aldehydes and quinones, to name a few (Nebbioso and Piccolo, 2013; Sulzberger and Durisch-Kaiser, 2009). Although results from ultra-high resolution mass spectrometry (Kujawinski et al., 2009) and fluorescence spectroscopy (Andrew et al., 2013) suggest a primarily lignin-base origin for terrestrial CDOM and the humic-like component of marine CDOM, the molecular basis for its optical properties is still a grey area, due to the complexity of these optical properties. In this regard, two models have been proposed to explain the optical properties of terrestrial CDOM; the superposition model and the electronic interaction model (EI). The superposition model theorizes that these optical properties are the result of the linear sum of absorption and emission spectra of individual non-interacting chromophores found within CDOM. In contrast, the EI model attributes these optical properties in part to electronic interactions (for example energy and electron transfer) (Figure 1 - 6) between chromophores within partially-oxidized oligomeric/polymeric hydroxyl-/methoxy

aromatics such as lignin, tannins and polyphenols (Boyle et al., 2009; Del Vecchio and Blough, 2004a). These interactions lead to new emission properties which cannot be explained by a simple sum of the spectra of individual chromophores. Within this model, a fraction of electronic charge may be transferred between electron-rich donors and electron deficient acceptors in physical proximity to each other creating new, lower energy optical transitions or charge transfer (CT) bands. These CT bands extend the absorbance spectra to longer wavelengths than that observed for local donor and acceptor moieties (Figure 1 - 5), providing an explanation for the long wavelength, near UV and visible absorption and emission properties of CDOM. UV absorption and near visible emission is dominated by known aromatic structures (hydroxyl/methoxy-aromatics) within these partially-oxidized oligomeric/polymeric hydroxyl-/methoxy aromatics.

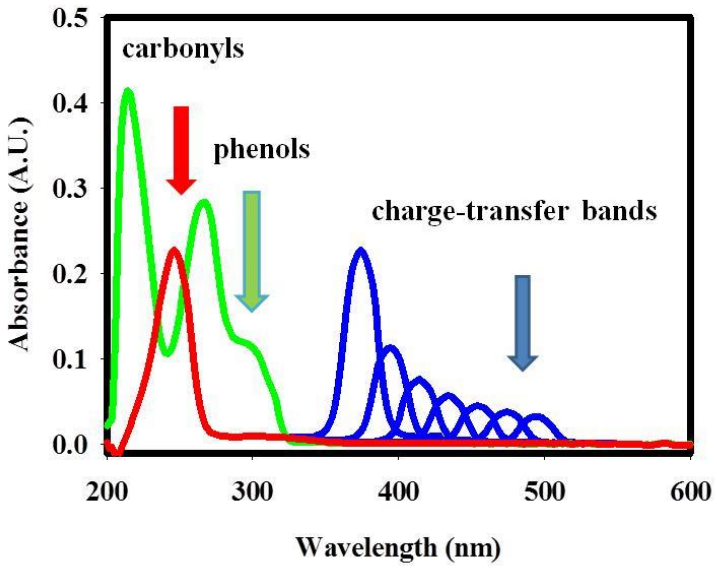

Figure 1 - 5: Electronic Interaction Model: the absorbance spectrum of quinones (red line) and phenols (green line) interact electronically to form charge transfer bands (blue line) that extend the absorption spectra to longer wavelengths.

Extensive studies have provided evidence that the optical properties of CDOM cannot be described by a simple superposition of absorption and emission spectra of non-interacting chromophores. Instead, results support the EI model as a more plausible explanation for the optical properties of terrestrial CDOM (and humic substances) (Boyle et al., 2009; Del Vecchio and Blough, 2004a; Ma et al., 2010) and the humic-like component of marine CDOM (Andrew et al., 2013). Within the context of a lignin based origin for terrestrial CDOM, the long wavelength absorbance and emission is proposed to result from interactions between hydroxy- or methoxy- aromatic electron donors such as phenols and methoxylated phenols and electron acceptors such as quinones and/or aromatic ketones/aldehydes contained within partially oxidized lignin precursors (Figure 1 - 6). While the ultraviolet absorption and near-visible emission is thought to arise principally from the aromatic structures known to be a part of lignin (local donor states, (Lin and Kringstad, 1970; Lundquist et al., 1978)).

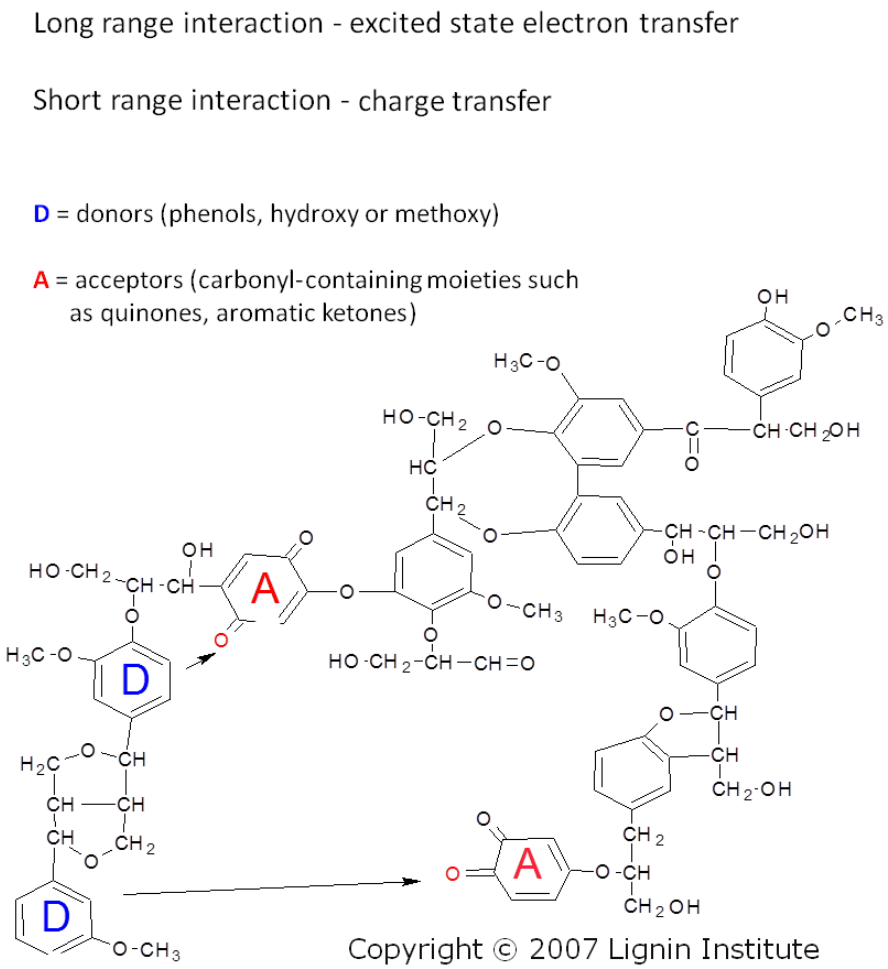

Figure 1 - 6: Possible electronic interactions between donors (hydroxy-/methoxy-aromatics) and acceptors (quinones, aromatic ketones) within a partially oxidized lignin fragment

To investigate the validity of the EI model, studies have employed laser photobleaching measurements (Del Vecchio and Blough, 2004a), steady-state and time resolved emission measurements (Boyle et al., 2009) and most recently chemical treatments, specifically borohydride ($NaBH_4$) reduction (Andrew et al., 2013; Golanoski et al., 2012; Ma et al., 2010). Sodium Borohydride ($NaBH_4$) is a selective reductant of carbonyl containing compounds. It effectively reduces aldehydes and ketones to alcohols; and quinones to hydroquinones, through hydride transfer (Figure 1 - 7).

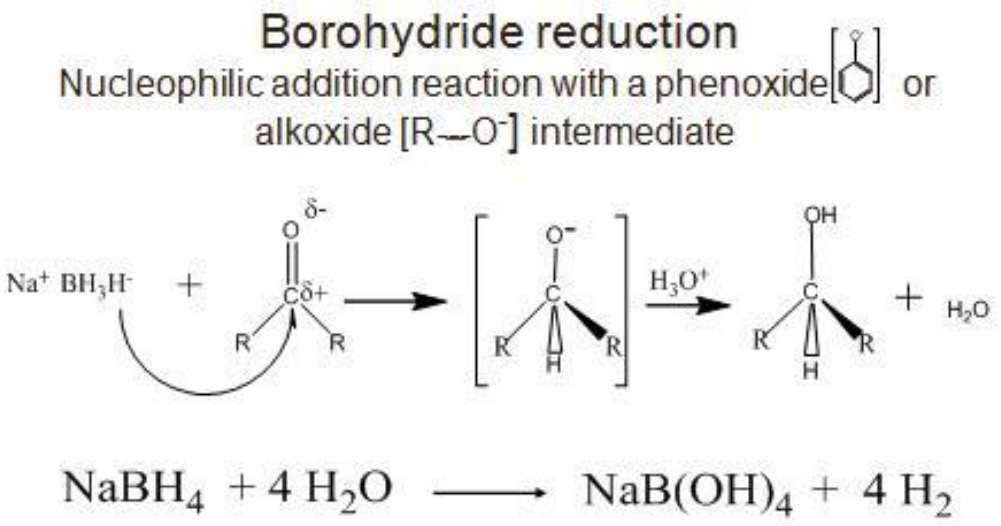

Figure 1 - 7: Borohydride reduction under nitrogen at 25ºC

The reduction of these carbonyl containing compounds (acceptor moieties) within CDOM structure should in principal result in (a) the interruption of charge-transfer interactions, and therefore loss of long wavelength absorbance and emission, and (b) enhanced, blue-shifted emission from local donor states that are no longer quenched because of the removal of acceptor moieties. Consistent with these expectations, sodium borohydride reduction of terrestrial (Ma et al., 2010) and marine (Andrew et al., 2013) CDOM results in the preferential loss of long wavelength absorption and a concomitant increase and blue shift in fluorescence emission intensity (Figure 1 - 8), suggestive that the EI model provides a valid basis for the observed optical properties.

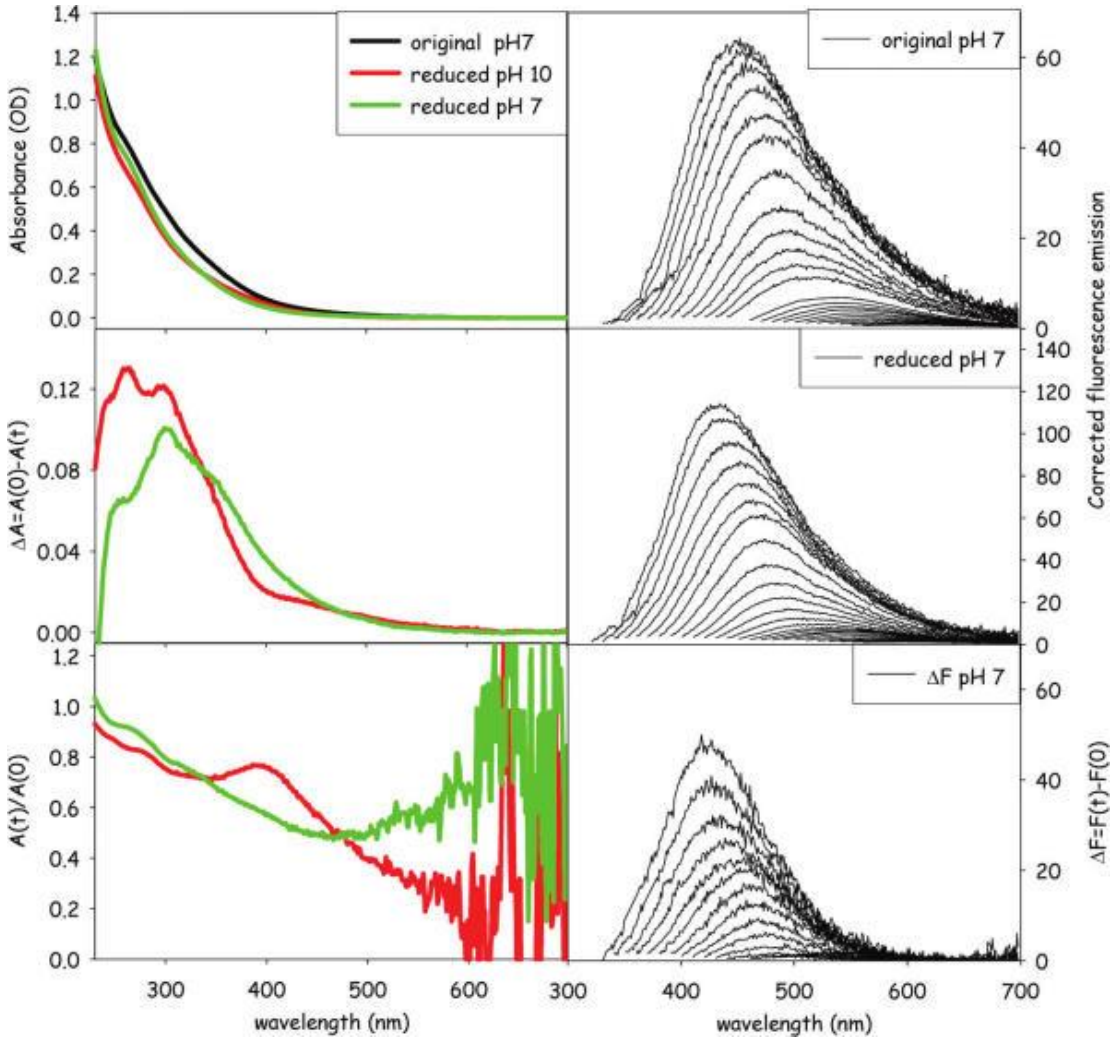

Figure 1 - 8: Changes in optical properties for SRFA (50 mg/L, pH 7) following $NaBH_4$ reduction (~5 mg, 2 h after addition). ΔA > 0 indicates loss of absorbance while ΔF > 0 represents gain of fluorescence signal (Ma et al., 2010).

Thus, by directly comparing the changes in optical properties of pre- and post- reduced CDOM samples from different environments, information about the similarities and or differences in photo-physical properties can provide much insight into the underlying molecular basis for the optical properties and by extension structure and source.

1.6 Purpose and summary of research

Great headway has been made over the years with regard to the optical properties of terrestrial and marine CDOM, but research is still lacking in the area of source and structure determination, particularly for marine CDOM. Compounding this question of structure and source, as mentioned previously, is the fact CDOM from marine environments has historically been far less sampled. Over the last several years (Mopper et al., 2007; Nelson and Siegel, 2013) research in this area has burgeoned in order to examine this question and is one of the main focuses of the work presented in this thesis (Chapter 2). Research done in the few marine environments that have been sampled has made conclusions solely based on correlations between one or two parameters without any complimentary structural or chemical measurements to support conclusions (Swan et al., 2009; Yamashita and Tanoue, 2008) which may be misleading. To address this issue, a comprehensive study of the optical properties of CDOM from the Atlantic Ocean was undertaken. The optical properties (both absorption and emission) and changes in these properties upon chemical modification were examined and compared to results obtained from previous research on CDOM from terrestrial environments. This work provided great insight into the source of marine CDOM, by demonstrating the remarkable spectroscopic similarities between marine and terrestrial CDOM. The results provided evidence of the occurrence in marine waters of a major terrestrial CDOM component that absorbs in the UV and visible and emits in the visible, as well as marine CDOM components that absorb and emit in the UV. Further, the results underscored that the simultaneous acquisition of complete spectral absorption and emission properties,

combined with chemical tests (C-18 extractions, borohydride reduction) can provide a far clearer picture of the sources and cycling of CDOM within the oceans.

Extremely low CDOM absorption values are typically observed in open oceans, particularly the surface, and sometimes may present a challenge in obtaining statistically relevant/valid data from these whole water samples. Although optical measurements can usually be obtained from these samples, other measurements may require sample concentration or removal of salts. Thus, concentration and isolation of CDOM from the whole water sample is a common practice. This has been accomplished using many methods which include the use of cartridges pre-packed with XAD ion-exchange resins, silica C18 sorbents and more recently PPL (modified styrene divinylbenzene polymer type sorbents), as well as reverse osmosis coupled with electrodialysis (RO/ED). C18 solid phase extraction is currently one of the most widely used techniques, taking advantage of the hydrophobic and acidic nature of humic materials which form a major component of CDOM. This has allowed for improved optical characterization of humic substances in open ocean, and has facilitated the use of techniques such as NMR and ultra-high resolution mass spectrometry providing vital structural information (Hertkorn et al., 2006; Mopper et al., 2007) It is unlikely that open ocean CDOM is entirely composed of water soluble organic acids, consequently, the question arises as to the extent this extracted material represents the whole water sample, and its utility in addressing these still unanswered questions about marine CDOM. Until now, a comprehensive study comparing the optical and chemical properties of the whole water CDOM sample and its extracted humic material had not been undertaken, which is the

subject of the work presented in chapter 3. This information is essential in determining the utility of extracted humic material as a proxy for elucidating the structural basis for CDOM optical properties and possible source.

To this end, the extraction efficiencies of C18 cartridges in relation to CDOM optical properties for samples from the Middle Atlantic Bight (MAB) and the Equatorial Atlantic Ocean (EAO) were investigated. Additionally, observed changes in the optical properties upon chemical reduction with sodium borohydride for C18 extracts and corresponding whole water sample were examined and compared. Overall, the results of this work revealed that the optical properties of the original CDOM samples and the corresponding extracted material did not vary significantly. Moreover, remarkably similar changes in optical properties of C18 extracts and corresponding CDOM sample were observed upon $NaBH_4$ reduction suggesting a common chemical nature for these materials. Some discrete emission bands were however observed in a few CDOM samples which were not extracted by C18 cartridges, and appeared to be unaffected by borohydride reduction. Such bands exhibited a very different optical signature than the bulk CDOM and resistance to sodium borohydride reduction suggesting a different chemical nature for these bands. This indicates that some care has to be taken when extrapolating conclusions from the extracts to the whole natural organic material.

The samples used for the study described above (work presented in chapter 3) were collected on several cruises in 2006 in the Middle Atlantic Bight region. The whole water samples have been in storage in acid washed glass bottles in the dark at 4ºC up till

present, while extracts were stored frozen over this period. Although this is a common practice (for shorter time periods), there is no consensus on maximum storage times. Further, little work has been done to examine to the long term storage effects on CDOM optical properties. Researchers have mentioned that there are no measurable effects of storage for short periods of time (3 months) (Wurl, 2009a), but have not systematically examined this nor have they looked at the effect over much longer periods. The work presented in chapter 4 provides results of a comprehensive study of the storage effects (6 years) on CDOM optical properties. This information is very important to the community in light of the fact that sample storage is a common practice, and it is sometimes very difficult (both expensive and time consuming) to re-sample locations. Knowledge of the stability of CDOM samples under current storage practices could provide vital information on the usability of these samples for a greater number of studies over a longer period of time. Results from this work suggest that CDOM from the MAB stored at 4°C in the dark was chemically stable for extended time scales, but susceptible to sedimentation and precipitation of some of the organic material.

The work presented in Chapter 5, examines the optical properties of CDOM produced by *Pelagibacter ubique* during growth in an incubation experiment. *Pelagibacter ubique* is a member of the ubiquitous SAR11 clade of bacteria, one of the largest fractions of bacterial cells in Surface Ocean. This work was part of a collaboration project which also examined the molecular composition of the DOM produced by SAR11 using FTICR-MS. The goal of this work was to investigate and explore the idea that in situ production by bacteria may possibly be one of the sources of marine CDOM, as suggested by many

studies. The results did not provide any evidence to suggest that CDOM, with long wavelength emission properties, is produced by *Pelagibacter ubique* under our specific incubation conditions.

Chapter 2: Chromophoric dissolved organic matter (CDOM) from the Equatorial Atlantic Ocean: Optical properties and their relation to CDOM structure and source

2.1 Overview

Extensive data exist on the optical properties of CDOM from terrestrial and coastal environments, yet the open oceans have been historically under-sampled. Consequently, the source and structural basis of marine CDOM optical properties are still debated. To address this issue, detailed optical measurements were acquired for both untreated and sodium borohydride ($NaBH_4$) reduced natural waters and C18 extracts (C18-OM) across the Equatorial Atlantic Ocean. Except in regions of upwelling or in the vicinity of the Congo River outflow, CDOM absorption coefficients and visible emission intensity were far smaller for surface waters ($a_{CDOM}(355)$: 0.057 - 0.162 m^{-1}; $\lambda_{exc}/\lambda_{em}$ = 350/450 nm: 0.396 - 1.431 QSE) than for waters below the mixed layer ($a_{CDOM}(355)$ 0.084-0.344 m^{-1}; $\lambda_{exc}/\lambda_{em}$ = 350/450 nm: 0.903 - 3.226 QSE), while spectral slopes were higher (surface: 0.019 to 0.025 nm^{-1}; deep: 0.013 to 0.019 nm^{-1}), consistent with photobleaching of CDOM in surface waters. Distinct emission bands were observed in the ultraviolet, primarily at excitation/emission wavelengths ($\lambda_{exc}/\lambda_{em}$) = 280/320 nm, but also at $\lambda_{exc}/\lambda_{em}$ = 300/340, 300/405 and 320/380 nm for some stations and depths. In contrast, visible emission exhibited maxima that continuously red-shifted with increasing λ_{exc} (> 330 nm), a property characteristic of CDOM from estuarine and coastal environments. Further evidence that CDOM in the offshore waters of this region is composed of a major terrestrial component includes: 1) similar spectral dependencies of the emission maxima and fluorescence quantum yields; 2) a large Stokes shift in the emission maxima with

short-wavelength excitation (λ_{exc} = 280 nm); 3) correlation of visible emission intensities with absorption at λ_{exc} = 280, 320 and 450 nm, with absorption to fluorescence ratios comparable to those found in estuarine and coastal environments; 4) affinity of C18 cartridges for the long wavelength (visible) absorbing and emitting material, but not the UV emitting material; 5) preferential loss of visible absorption and substantially enhanced blue-shifted emission in the visible following borohydride reduction of both the Equatorial Atlantic waters and the C18-OM of these waters. These results support the occurrence in offshore waters of a major terrestrial CDOM component that absorbs in the UV and visible and emits in the visible, as well as marine CDOM components that absorb and emit in the UV. The results further demonstrate that the simultaneous acquisition of complete spectral absorption and emission properties, combined with chemical tests (C-18 extractions, borohydride reduction) can provide a far clearer picture of the sources and cycling of CDOM within the oceans.

2.2 Introduction

The importance of chromophoric dissolved organic matter (CDOM) to aquatic ecosystems has been well established for some time (Blough and Del Vecchio, 2002; Blough and Green, 1995; Coble, 2007; Del Castillo, 2005; Mopper and Kieber, 2002; Nelson and Siegel, 2002), with its optical properties extensively studied over the last several decades (Blough and Del Vecchio, 2002; Boyle et al., 2009; Coble, 2007; Del Vecchio and Blough, 2004a; Nelson and Siegel, 2002). CDOM absorbs UV and visible light and is a major determinant of the optical properties of both fresh and marine waters, directly affecting the spectral quality of the underwater light field (Blough and Del

Vecchio, 2002; Morris and Hargreaves, 1997; Nelson and Siegel, 2002; Siegel et al., 2002; Vodacek et al., 1997; Zepp et al., 2007). Its photo-reactivity plays a significant role in the biogeochemistry of natural waters through the formation of biologically available compounds that fuel the growth of microbes (Kieber et al., 1989; Mopper and Kieber, 2002; Moran and Zepp, 1997; Wetzel et al., 1995), and reactive oxygen species that can influence the bioavailability of trace metals and nutrients (Blough and Del Vecchio, 2002; Blough and Zepp, 1995; Coble, 2007; Mopper and Kieber, 2002; Zepp et al., 2007). CDOM has also been employed as a tracer of upper ocean biogeochemical processes and water mass mixing (Chen and Gardner, 2004; Del Vecchio et al., 2009; Nelson et al., 2007; Nelson et al., 2010; Stedmon et al., 2010; Swan et al., 2009; Vodacek et al., 1997).

Despite the importance of CDOM and the plethora of studies that have examined the spatial and temporal variability of its optical properties, there remain many unanswered questions regarding the structural origin of these optical properties as they relate to CDOM source, particularly for marine environments. While CDOM in rivers and estuaries is thought to result primarily from the degradation products of lignins (Boyle et al., 2009; Del Vecchio and Blough, 2004a; Spencer et al., 2009; Stenson et al., 2003; Stubbins et al., 2010) and possibly tannins (Coble, 2007; Maie et al., 2008; Sleighter and Hatcher, 2008), the source of CDOM in open oceans away from river-dominated margins remains controversial, particularly for the "humic-like" CDOM that absorbs in the UV-visible and emits in the visible. Some investigators have argued that this "humic-like" CDOM is produced in situ from marine source materials by as yet poorly understood

processes (Coble, 2007; Harvey et al., 1984; Nelson et al., 2004; Nelson and Siegel, 2002; Yamashita and Tanoue, 2004), while others suggest that it is in part a remnant of the terrestrial material that has been diluted and modified during transit to and within the ocean (Blough and Del Vecchio, 2002; Hernes and Benner, 2006; Murphy et al., 2008). Based on the correlation of absorption at 325 nm with apparent oxygen utilization (AOU), Nelson et al. (2010) and Swan et al. (2009) recently concluded that CDOM in the ocean basins is created in situ by the oxidation of marine particulate organic matter (POM). Similarly, Yamashita et al. (2010; 2008) and Yamashita and Tanoue (2008; 2009) concluded that CDOM in the Pacific Ocean is created in situ by the oxidation of marine dissolved organic matter (DOM), based on the correlation of AOU with fluorescence intensity observed at 420 nm for a single excitation wavelength in the ultraviolet (325 nm). In contrast to these studies, Murphy et al. (2008), employing parallel factor analysis (PARAFAC) of fluorescence excitation–emission spectra (EEMS) for waters across the Atlantic and Pacific oceans, concluded that terrestrial "humic-like" CDOM components can be traced to the open ocean at levels up to ~ 1.5 % of riverine signal, suggesting a significant contribution of (modified) terrestrial CDOM to the open oceans.

Nelson et al. (2010), Swan et al. (2009), Yamashita et al. (2010, 2008) and Yamashita and Tanoue (2009, 2008) based their conclusions solely on correlations with AOU using only a single absorption or excitation wavelength, primarily in the ultraviolet, and no structural or chemical information was provided to support their conclusions. These correlations may not be valid for other spectral regimes, particularly for the visible

wavelengths where terrestrial CDOM can exhibit significant absorption and emission. Moreover, the complete spectral dependence of absorption and fluorescence emission, as well as the wavelength dependence of fluorescence quantum yields, have not been obtained for offshore marine waters, or extracts of these waters, thus precluding the acquisition of important complementary information that can be obtained by the combined use of these optical measurements and isolation techniques (Boyle et al., 2009; Del Vecchio and Blough, 2004a).

Here, we address these issues by acquiring the complete spectral dependence of absorption and fluorescence emission, as well as the wavelength dependence of the apparent fluorescence quantum yields, for both natural waters and C18-OM from the Equatorial Atlantic Ocean (Figure 2 - 1). Emission spectra were acquired across the entire UV-visible spectral range (excitation wavelength λ_{exc} 280-600 nm) and compared with absorption properties. Results showed a striking similarity between the optical absorption and emission behavior of these ocean samples (both natural waters and C18-OM) and terrestrially-derived CDOM and humic substances in the visible wavelength regime (Boyle et al., 2009). However, unlike terrestrially-derived CDOM, offshore waters also displayed distinct emission bands in the UV region.

We further employed a selective chemical reductant, $NaBH_4$ (Golanoski et al., 2012; Ma et al., 2010; Tinnacher and Honeyman, 2007), to examine changes in the optical properties produced by the reduction of carbonyl–containing moieties within both the natural waters and C-18 extracts (Golanoski et al., 2012; Ma et al., 2010). Past studies

have shown that the selective reduction of carbonyl–containing structures results in the preferential loss of visible absorption and enhanced blue-shifted emission for terrestrially-derived CDOM, aquatic humic substances and lignin (Golanoski et al., 2012; Ma et al., 2010; Sharpless, 2012). The similar response of the photophysical properties to reduction suggests a common structural basis consistent with an electronic interaction model for this source of material (Boyle et al., 2009; Del Vecchio and Blough, 2004a; Ma et al., 2010; Mignone et al., 2012). This model proposes that the optical properties in part result from intramolecular charge transfer interactions between electron donors and acceptors formed through the partial oxidation of lignin and other hydroxy- or polyhydroxy–aromatic polymeric precursors of terrestrial origin (Del Vecchio and Blough, 2004a). Past work indicates that redox–dependent changes in the optical properties can thus provide evidence of terrestrial material within a CDOM sample (Boyle et al., 2009; Del Vecchio and Blough, 2004a; Ma et al., 2010; Maurer et al., 2010). We find that $NaBH_4$ reduction of both C18-OM and natural waters from the Equatorial Atlantic produce a loss of visible absorption and enhanced blue–shifted emission, characteristic of terrestrial CDOM. In contrast, UV emission observed for these samples was unaffected by $NaBH_4$ reduction, suggesting that the UV emission is distinct, and most likely produced in situ.

These combined observations are consistent with the presence in marine samples from the Equatorial Atlantic of a major terrestrial component that absorbs in the UV and visible but emits in the visible, along with marine CDOM components that absorb and emit in the UV.

2.3 Materials and methods

2.3.1 Sample description

Samples were collected onboard the R/V Endeavor in the Equatorial Atlantic Ocean in May-June 2009 over a 5 week period (May 21st to June 29th). The transect encompassed three zonal sections (4°N, 0° and 5°S) and four meridional sections between 23°W and 5°E, (namely 23°W, 10°W, 0 and 5°E) (Figure 2 - 1).

Natural waters for optical measurements of chromophoric dissolved organic matter (CDOM) were collected from the surface (5 - 10 m) and at a depth below the mixed layer, and treated as previously reported by (Del Vecchio and Blough, 2004b). Briefly, samples were collected employing a CTD rosette, equipped with Niskin bottles and were immediately filtered through 0.2-μm millipore sterile filters. Filtered natural water samples were stored in the dark at 4°C until further analysis.

Water samples for extracting dissolved organic matter (DOM) were collected from the vessel's surface water pumping system (5 m) and CTD rosette (1000 m) and were then filtered through an in-line Gelman fluted capsule filter (0.2 μm pore size). Water samples (20 L) were acidified to pH 2 with HCl (16.5 ml of 12.1 N) and the organic matter was extracted with C18 extraction columns (United Chemical Technologies, Inc.) at the flow rate of 50 mL min^{-1} following a slightly modified method by Louchouarn et al. (2000) as previously described in Boyle et al. (2009). Prior to extraction the cartridges were pretreated with 100 mL of high purity methanol (Andwin Scientific) followed by 50

mL of acidified (pH 2) Milli-Q water. Following extraction, cartridges were rinsed with 1 L of acidified (pH 2) Milli-Q water to remove salts and were stored in the refrigerator (4 °C) until further processing.

The DOM was extracted from the C18 cartridges with 50 mL of high purity methanol (Burdick & Jackson); the first fraction (~8 mL), containing some aqueous residue was separated from the second fraction and discarded. The second fraction (~38 mL) was collected into a 100 mL round bottom flask and evaporated to dryness at 30-35° C using a rotary evaporator. The dried material was re-dissolved with Milli-Q water, pH adjusted to ~7, and stored frozen (-20°C) until further analysis. Hereafter, these samples are referred to as C18 extracted organic matter (C18-OM).

2.3.2 Optical measurements

Absorption spectra of natural waters were acquired employing a Shimadzu 2401-PC spectrophotometer using a 10 cm optical cell and an Ultrapath 200 cm liquid waveguide cell (World Precision Instruments)(Miller et al., 2002) with a Tidas 1 photodiode array spectrometer (J&M Analytische Messund Regeltechnik GmbH). The effective path-length (197.5 cm ±1.0 cm) was determined by WPI (Oct 11, 2007) following procedure of Belz et al. (1999). This liquid waveguide absorption cell has the advantage of greater sensitivity (dynamic range 0.002 - 230 m^{-1}) (Miller et al., 2002) allowing more accurate determination of absorption coefficients for the very low CDOM observed in open ocean surface waters (Nelson and Siegel, 2002). Absorption spectra of C18-OM were acquired

similarly employing the Shimadzu 2401PC spectrophotometer with a 1 cm or a 1 mm optical cell when sample volume was limited.

Absorption spectra were recorded over the range 200–800 nm against air, blank subtracted and corrected for baseline drifts by subtracting the average absorption over the 650-700 nm range from the entire spectrum. Milli-Q water (from a Milli-Q Academic water purification system) was used as the blank when using the Shimadzu spectrometer while a 35 ppt solution of high purity NaCl (99.99%, Sigma Aldrich) (average salinity of samples - 35.426 PSU) was used as the reference when employing the WPI spectrometer (Miller et al., 2002; Nelson et al., 2007).

CDOM absorption coefficients ($a_{CDOM}(\lambda)$) were calculated using the following equation

$$a_{CDOM}(\lambda) = 2.303 * A(\lambda) / L \qquad \text{Eq. (1)}$$

Here, $A(\lambda)$ is the absorbance at the wavelength λ and L is the pathlength. The spectra were then fit to equation 2 using a nonlinear least squares fitting routine over the range from 300 to 700 nm (Blough and Del Vecchio, 2002).

$$a_{CDOM}(\lambda) = a_{CDOM}(\lambda_o) \exp(-S(\lambda-\lambda_o)) \qquad \text{Eq. (2)}$$

Here λ_o is a reference wavelength and S is the spectral slope parameter.

Fluorescence spectra were acquired with an Aminco–Bowman AB2 luminescence spectrometer. Both the excitation and emission monochromator bandpasses were set to 8 nm when collecting measurements for natural water samples and 4 nm for C18-OM, employing milli-Q as the blank. Spectra were corrected for the instrument response

using factors supplied by the manufacturer. Emission spectra were recorded at excitation wavelengths (λ_{exc}) from 280 to 600 nm at every 10 nm; the emission spectra were recorded from 10 nm greater than λ_{exc} to 700 nm (Del Vecchio and Blough, 2004a). Samples were always optically thin (absorbance < 0.05 – 0.1 OD) at λ_{exc}. Fluorescence quantum yields (ϕ) were obtained as described in (Del Vecchio and Blough, 2004a). Absorption and fluorescence spectra were recorded repeatedly over a 2 yr period (Oct. 2009 & Feb. 2011), and measurement replicates showed no appreciable change (< 10 %), indicating sample stability under the conditions stored (4 °C in the dark) (Stedmon and Markager, 2001; Swan, 2009).

2.3.3 $NaBH_4$ Reduction

Reduction with $NaBH_4$ (Fisher) followed a modified version of Ma et al. (2010). Natural waters (27.0 mL) were placed in a glass vial, capped and sparged with ultrapure N_2 for 35 minutes. Solid $NaBH_4$ (27.0 mg) was added to the vial under continuous N_2 flow. C-18 extracts were reduced similarly employing a 1 cm quartz cuvette using ~ 3.0 mL of sample and 3.0 mg of $NaBH_4$. The reduction was considered complete when no further changes in absorption spectra were observed (~ 24 hrs). Because the sample pH increased to 10 during the reduction due to the reaction of excess $NaBH_4$ with water (Ma et al., 2010; Tinnacher and Honeyman, 2007), the sample pH was readjusted to its original value for comparison with the original sample. Reversibility of the reduction was also monitored following air exposure over a 24 hr period (Golanoski et al., 2012; Ma et al., 2010).

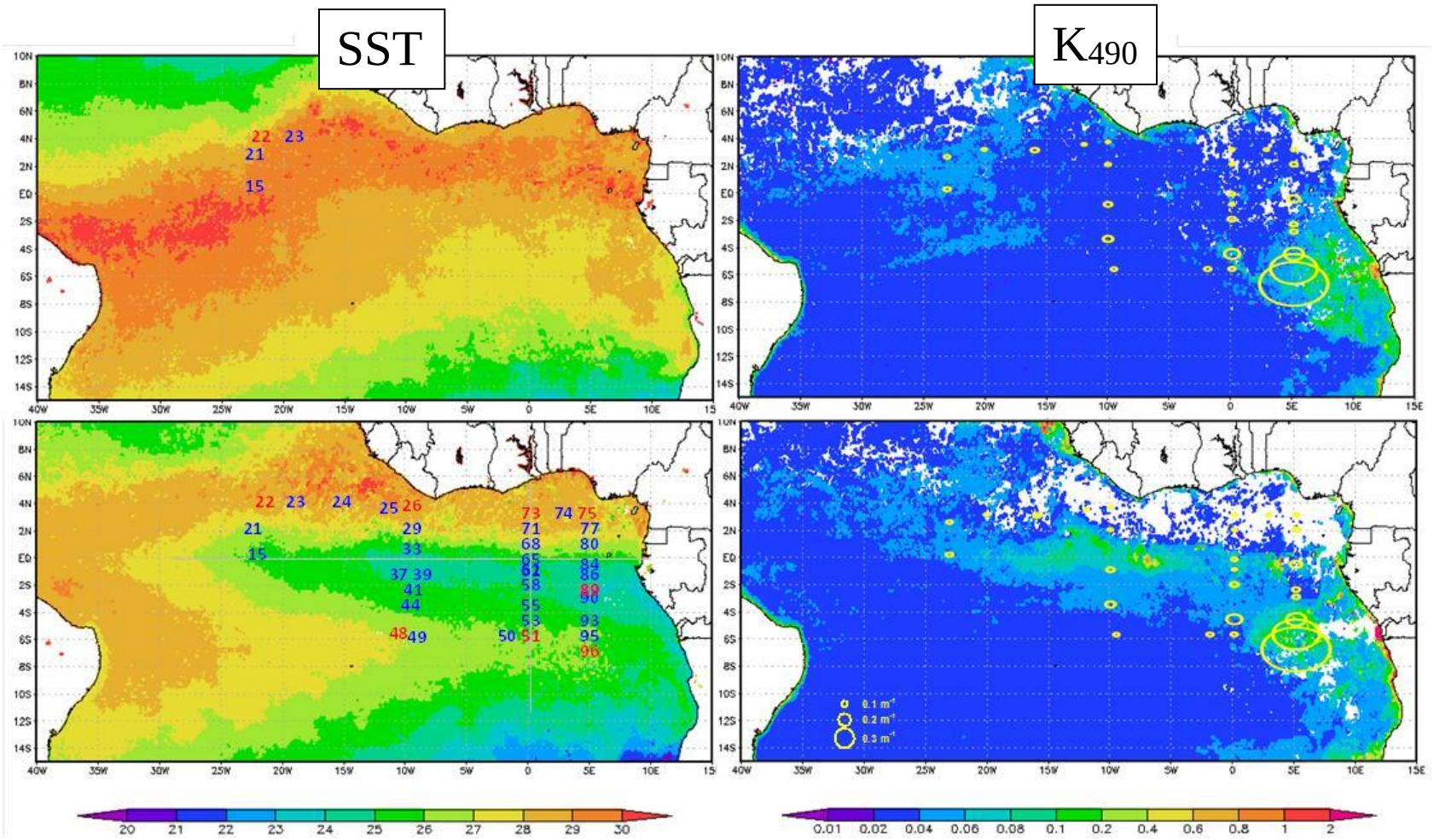

Figure 2 - 1: MODIS Aqua monthly averages satellite images of SST (left) and diffuse attenuation coefficient at 490 nm (K_{490}) (right) during May 2009 (top) and June 2009 (bottom) obtained employing the Giovanni online data system, developed and maintained by the NASA GES DISC. The Equatorial Atlantic Ocean cruise track is reported on the left panels (natural water samples, blue stations; and C18-OM samples, red stations). The $a_{CDOM}(355)$ (m^{-1}) for surface waters is reported on the right panels (yellow symbols).

2.4 Results and discussion

2.4.1 Description of study area

MODIS Aqua monthly composites of sea surface temperature (SST) (Figure 2 - 1), left panels) and diffuse attenuation coefficient at 490 nm (K_{490}) (Figure 2 - 1, right panels) were employed to provide a synoptic view of the region of study during May and June 2009 (Figure 2 - 1, top and bottom panels, respectively). During May (2009), warm (27-30 °C) and clear ($K_{490} < 0.05$ m^{-1}) waters were uniformly distributed across the entire region except in proximity to the Congo River outflow (5-10˚ E and 4-10˚ S) where waters exhibited greater K_{490} values (Figure 2 - 1, top panels). During June (2009), equatorial upwelling developed westward off the African coastline, at and south of the equator bringing colder (T ~ 23 °C) and more colored (K_{490} as high as 0.2 m^{-1}) waters to the surface (Fig. 1, bottom panels). Due to this phenomenon, waters north of the equator (approximately along 4˚ N) showed quite different physical and optical properties compared to waters affected by equatorial upwelling. Overall, waters across the region differed in physical properties (as salinity and temperature) as well as location (offshore distance and proximity to surface) thus displaying optical properties representative of open oceans as well as coastal regions impacted by terrestrial input.

2.4.2 CDOM optical properties and distribution - Absorption

Absorption coefficients at 355 nm ($a_{CDOM}(355)$), recorded with either instrument (Shimadzu 2401-PC spectrophotometer using a 10 cm optical cell or the Ultrapath 200 cm liquid waveguide cell) were highly correlated with each other (r^2=0.96) (Figure 2 - 2, A). As expected, the use of Ultrapath 200 cm liquid waveguide cell significantly

improved the signal-to-noise ratio at longer visible wavelengths (not shown) consistent with previous work by (Nelson et al., 2007) and (Miller et al., 2002). This result is significant because the overall absorption values in the visible regime for surface samples were extremely low, often very close to the detection limit of the Shimadzu 2401PC spectrophotometer (± 0.05 m^{-1}). Spectral slopes however, displayed a lower correlation (r^2= 0.46) (Figure 2 - 2) primarily as a result of the poorer fit to an exponential form obtained for the 200 cm data. Spectral slopes of samples below the mixed layer were closer to the one-to-one line, due to the higher absorption at depth, and thus better signal to noise, compared with those for surface samples. Overall, good agreement was observed between the two measurements (Figure 2 - 2).

At most sampling sites, CDOM absorption increased with decreasing wavelength in an approximately exponential fashion (Figure 2 - 3), similarly to that previously observed for both open oceans (Nelson and Siegel, 2002) and coastal environments (Blough and Del Vecchio, 2002) . However, a sharper increase in absorbance at wavelengths ≤ 300 nm was observed at open ocean sites (e. g. stations 15, 23 & 49) as compared with those sites likely influenced by the outflow of the Congo River (specifically station 96, 4m) (Figure 2 - 3). Occasionally, a small absorption shoulder at ~ 420 nm was also observed (Figure 2 - 3, C, red line), similar to that reported by Rottgers and Koch (2012). However, unlike their study, this shoulder was only observed in a small percentage (<11%) of samples, and exhibited no obvious dependence on depth or location, nor any related fluorescence emission at 650 nm. Thus we cannot exclude that this shoulder arises from a filtration artifact in a limited number of our samples.

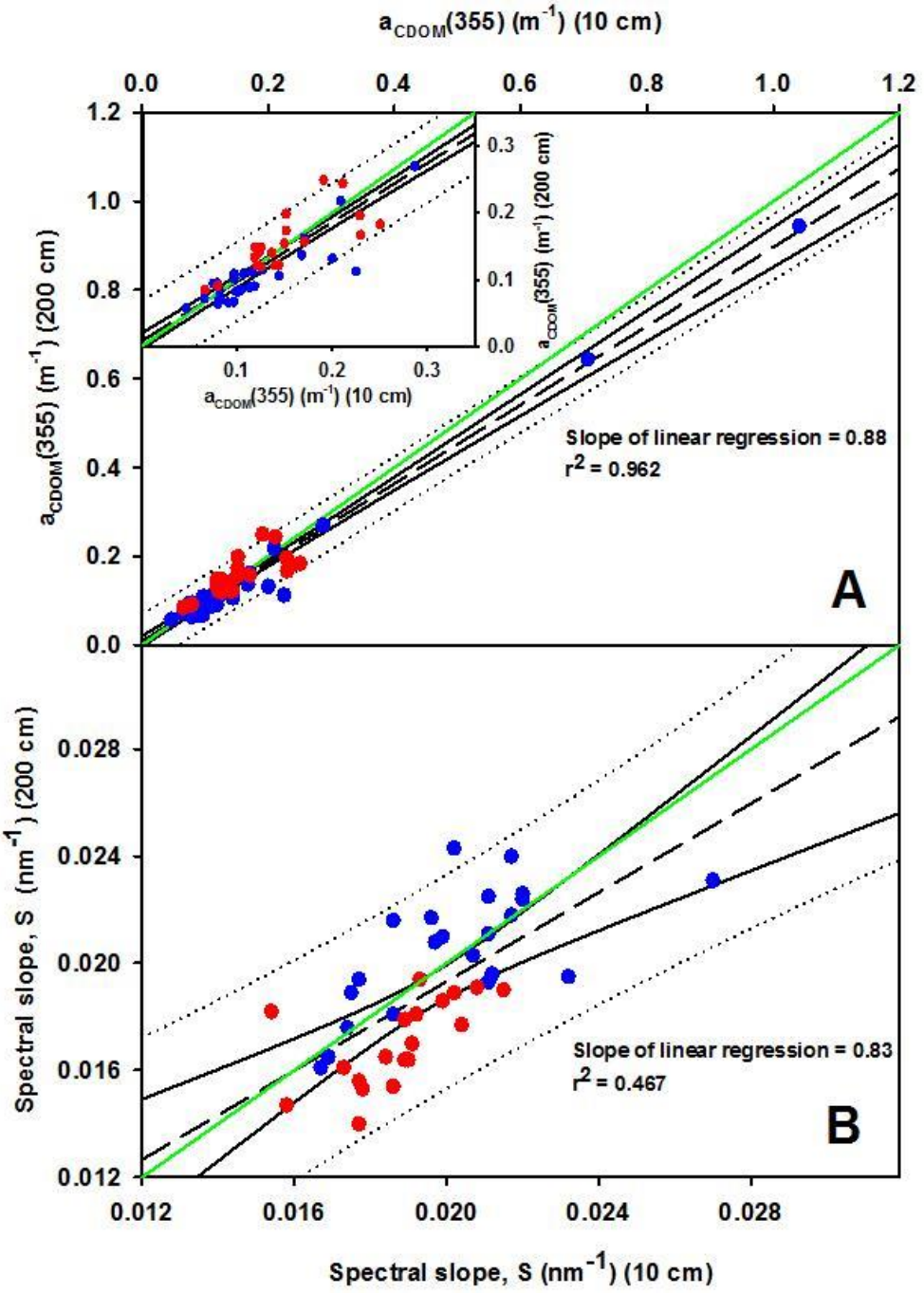

Figure 2 - 2: Comparison of optical measurements [(A) $a_{CDOM}(355)$ and (B) Spectral slope, S] collected with a long (200 cm) versus a short (10 cm) pathlength; ● represents surface samples and ● samples below the mixed layer (30 - 60m). (— — —) represents linear regression; (——) represents the 1:1, while (——) and (·····) represent the 95% confidence intervals and prediction band respectively.

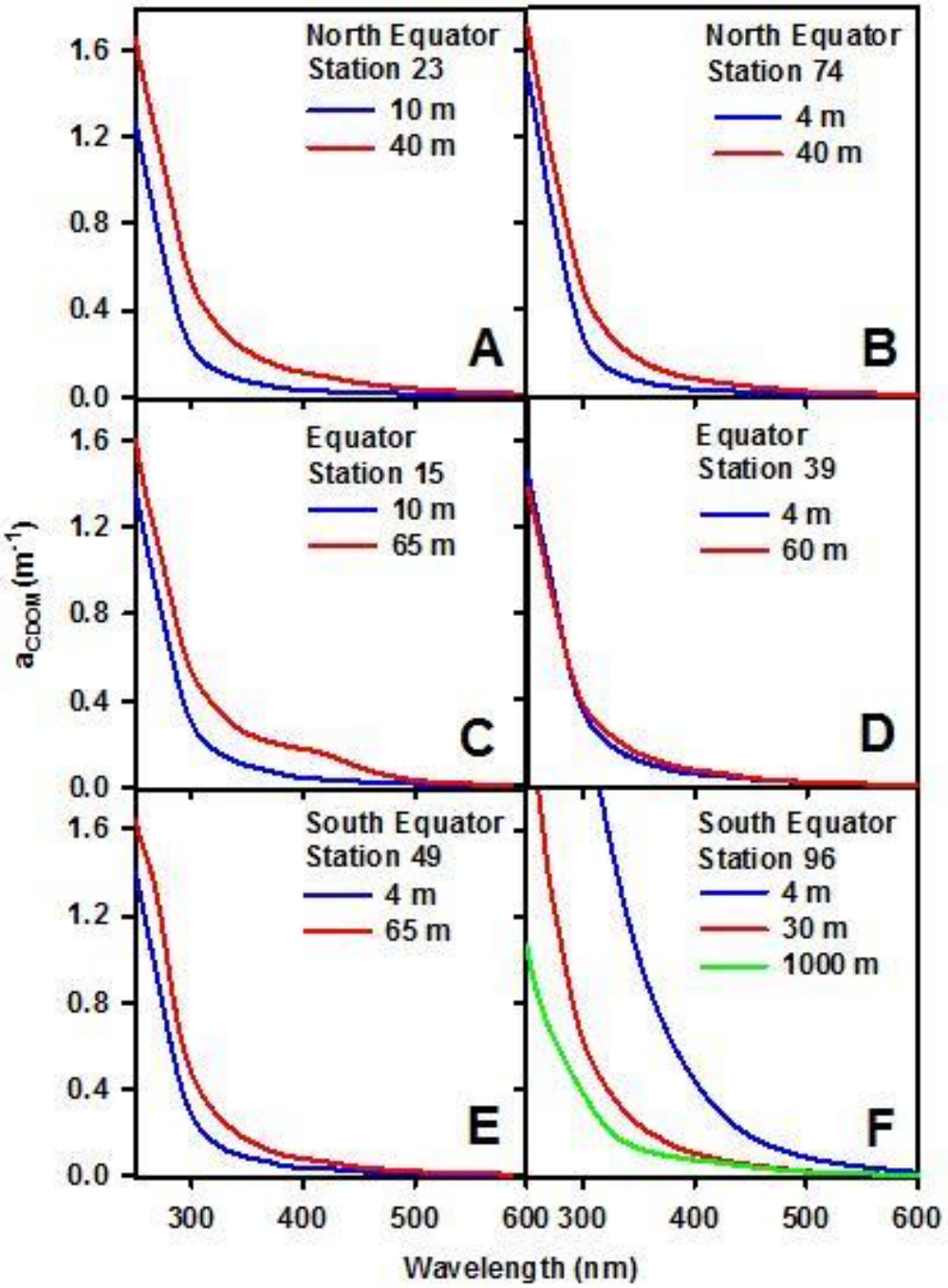

Figure 2 - 3: Absorption spectra (m^{-1}) of natural waters (—— surface, —— depth below the mixed layer (30 - 60 m) & —— 1000 m) for representative stations throughout the region. A: open ocean, north of the Equator, station 23 (3.0° N, 20.13° W); B: Gulf of Guinea, station 74 (2.98° N, 2.77° E). C: open ocean, Equator, station 15 (0.33° N, 23.0° W); D: equatorial upwelling, station 39 (0.67° S, 10.0° W). E: open ocean, south of the Equator: station 49 (5.0° S, 9.52° W); F: Congo River plume station 96 (6.0° S, 4.98° E).

Overall, absorption values for surface waters were extremely low across the entire spectrum but increased with depth (Figure 2 - 3, A-B-C-E), except for stations near the Congo River outflow, where absorption was higher at the surface (Figure 2 - 3, F), and in June for stations along the equator where absorption showed little variation with depth due to upwelling (Figure 2 - 3, D). The mixing of deep cold waters (enriched in CDOM) with warmer surface waters (depleted in CDOM) as a result of equatorial upwelling that occurred in June accounts for the observed $a_{CDOM}(355)$ vertical distribution for June sampling stations along the equator. However, $a_{CDOM}(355)$ values for surface waters and waters below the mixed layer for equatorial stations sampled in May were more typical of open ocean (Figure 2 - 3, compare C to D; Figure 2 - 4, compare stations sampled before and after upwelling).

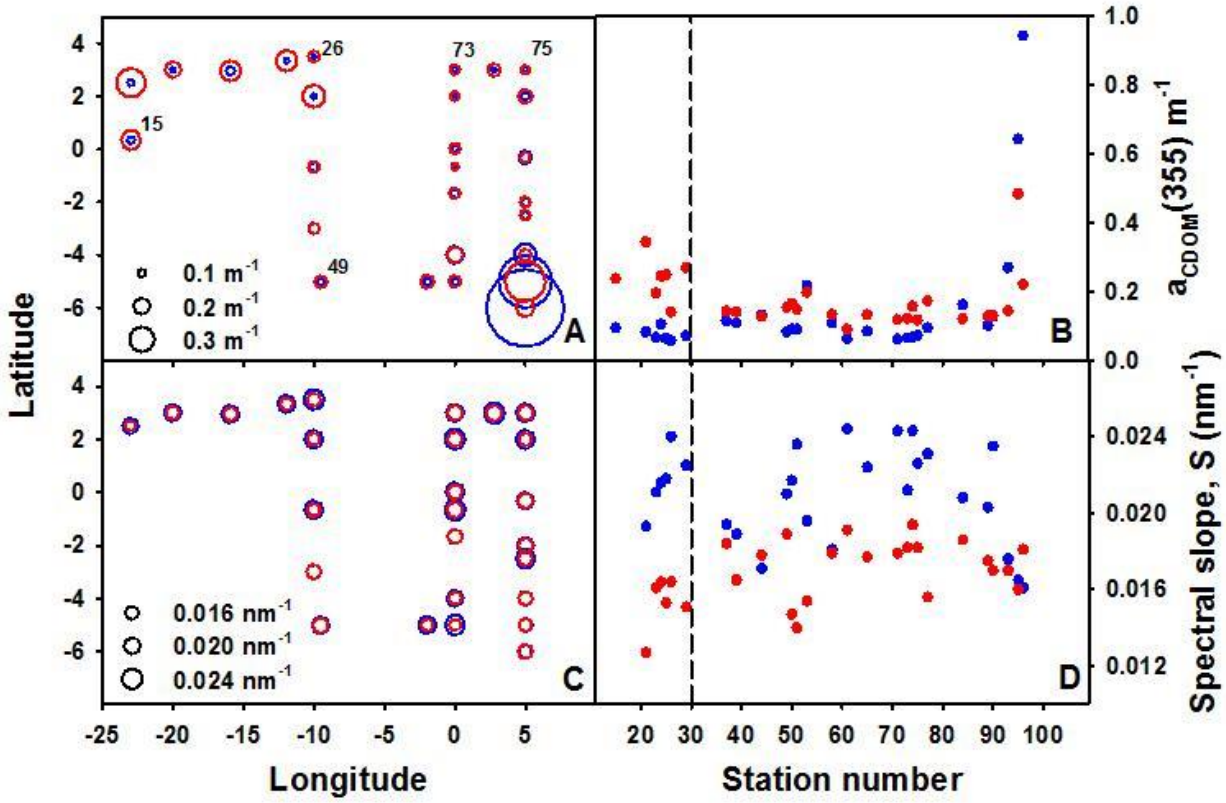

Figure 2 - 4: Spatial distribution of $a_{CDOM}(355)$ (m^{-1}) (A, B) and spectral slope, S (nm^{-1}) (C, D) for surface waters (●,○) and waters just below the mixed layer (●,○) from the Equatorial Atlantic Ocean. In A and C, diameter of open circles corresponds to magnitude of a_{CDOM} and spectral slope. Stations to the left of the dashed line (— — —) in B and D represent samples prior to upwelling; while those to the right, samples following upwelling.

CDOM absorption at a single wavelength ($a_{CDOM}(355)$) was employed to examine the spatial variability of CDOM within this region (Figure 2 - 4). Generally $a_{CDOM}(355)$ was small (range 0.057 - 0.943 m^{-1}, mean 0.155 m^{-1}, S.D. 0.190 m^{-1}) and much lower in surface waters relative to those below the mixed layer (Figure 2 - 4, top panels), indicating depletion through photobleaching (Del Vecchio and Blough, 2002) consistent with CDOM seasonal dynamics observed in the Middle Atlantic Bight (MAB) (DeGrandpre et al., 1996; Del Vecchio and Blough, 2004b; Vodacek et al., 1997), as well as other pen ocean regions (Bricaud et al., 2010; Matsuoka et al., 2011; Vodacek et al.,

1997). The lowest surface $a_{CDOM}(355)$ values (< 0.3 m^{-1}) were generally observed in the central Equatorial Atlantic away from the coastal margin. In contrast, $a_{CDOM}(355)$ for surface waters near the coast of Africa were as much as 3 times higher (0.94 m^{-1}) and decreased with offshore distance and depth, indicative of a significant contribution of terrestrial CDOM from the Congo River outflow to this region (Figure 2 - 3F; Figure 2 - 4, St. 95-96). Satellite composites of K_{490} clearly support this conclusion (Figure 2 - 1). This spatial variation in surface $a_{CDOM}(355)$ observed for the Equatorial Atlantic is similar to that reported by Nelson et al. (2007) for waters in the North Atlantic. They observed lowest surface $a_{CDOM}(325)$ values of < 0.1 m^{-1} in the central subtropical gyre and highest values (as much as ~ 0.7 m^{-1}) in coastal areas influenced by terrestrial input from rivers such as the Orinoco and Amazon in agreement with prior work (Blough et al., 1993; Del Castillo et al., 1999; Del Vecchio and Subramaniam, 2004; Green and Blough, 1994).

Unlike the variability in $a_{CDOM}(355)$ observed for surface waters, waters below the mixed layer exhibited relatively uniform $a_{CDOM}(355)$ (range 0.084-0.344 m^{-1}, mean = 0.156 m^{-1}, S.D. = 0.043), implying a fairly constant background at depth within the Equatorial Atlantic Ocean (Figure 2 - 4B).

In contrast to the absorption coefficients, the spectral slope (S) was high in surface waters and decreased with depth (ranging from 0.019 to 0.025 nm^{-1} and 0.013 to 0.019 nm^{-1}, respectively) (Figure 2 - 4, bottom panels). This result agrees with other observations of most surface waters over the summertime, where high spectral slope is coupled with low surface absorption due to photobleaching (Del Vecchio and Blough, 2002; Matsuoka et

al., 2011; Moran et al., 2000; Vodacek et al., 1997). However, towards the coast of Africa, surface values of S were lower (stations 93-96) while absorption was higher, and comparable to the values reported for CDOM in coastal regions dominated by terrestrial input (Del Vecchio and Blough, 2004b; Stedmon et al., 2000), consistent with significant terrestrial contribution from the Congo River to the surface waters of this region. Spectral slope values for waters impacted by equatorial upwelling were more uniform with depth, similar to the absorption coefficients. As with absorption coefficients, the spectral slopes were uniform below the mixed layer (0.017 nm^{-1} S.D. = 0.001) for the entire study area, and similar to that measured near the Congo River (Figure 2 - 4) and across the MAB (0.018 nm^{-1}) (Del Vecchio and Blough, 2004b). Greater variation in spectral slope was observed for surface waters relative to waters below the mixed layer reflecting the greater number of factors influencing the nature and diversity of CDOM in surface waters including upwelling, the degree of photobleaching and riverine input.

2.4.3 CDOM optical properties and distribution - Fluorescence

Fluorescence emission was observed across the ultraviolet and visible wavelengths for all natural water samples (Figure 2 - 5). Emission in the visible was broad and unstructured and exhibited a continuous red-shift in emission maximum with increasing excitation wavelength ($\lambda_{exc} \geq 330$ nm), characteristic of the behavior of CDOM from rivers and coastal margins receiving terrestrial input (Boyle et al., 2009; Del Vecchio and Blough, 2004a; Green and Blough, 1994). The intensity of the visible emission varied depending on depth and location. Highest intensities were observed in the region of the Congo River

outflow (Figure 2 - 5 G), and decreased with increasing offshore distance, with much lower levels observed for surface waters than for waters below the mixed layer (Figure 2 - 5, compare A to B). Consistent with the absorption measurements, visible emission intensity in the upwelling region showed little variation with depth (Figure 2 - 5, compare D to E).

Unlike the continuously red–shifting emission bands observed in the visible, a distinct emission band of varying intensity was observed for most samples in the ultraviolet ($\lambda_{exc}/\lambda_{em}$ = 280 - 300/~320 nm) (Figure 2 - 5 A-B-D-E-H). Three other distinct emission bands were also observed in the ultraviolet, but only at a limited number of stations and depths (Figure 2 - 6, $\lambda_{exc}/\lambda_{em}$ = 300/340, 300/405 and 320/380 nm). The bands at $\lambda_{exc}/\lambda_{em}$ = 320/380 nm and 300/405 nm were observed at stations along the 0° and 5° E line of longitude primarily in the Gulf of Guinea region. While $\lambda_{exc}/\lambda_{em}$ = 300/405 nm was present in surface waters as well as waters at 1000 m, $\lambda_{exc}/\lambda_{em}$ = 320/380 was only observed in waters just below the mixed layer (~40 m). The $\lambda_{exc}/\lambda_{em}$ = 300/340 nm band showed no obvious dependence on location or depth. Although these bands contributed substantially to the total fluorescence, visible emission was still present, albeit at much lower intensity (Figure 2 - 5, A-B-D-E-H).

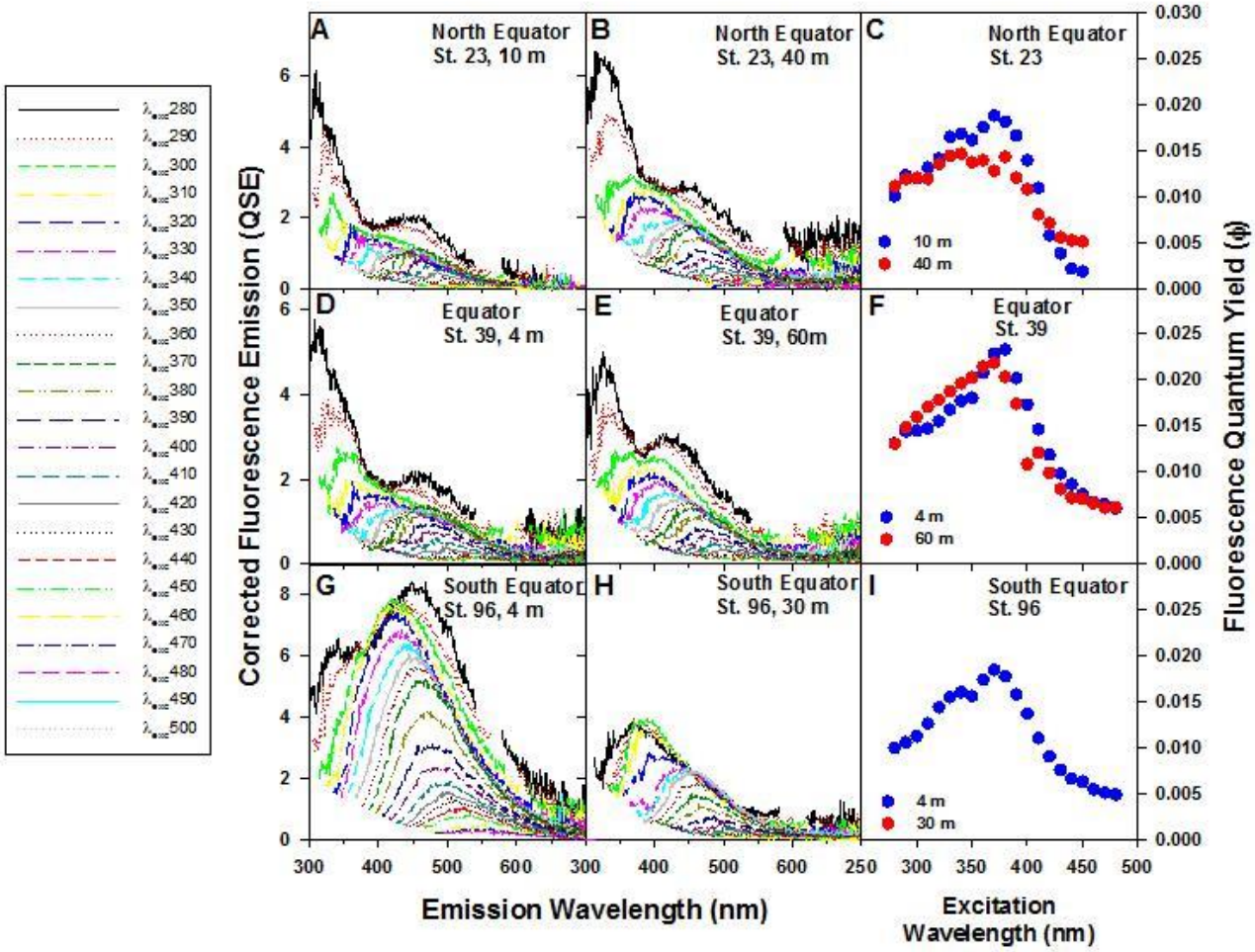

Figure 2 - 5: EEM spectra and corresponding fluorescence quantum yields (ϕ) (●surface & ●depth below mixed layer) for representative stations throughout the region. North of the Equator (open ocean) (A-B-C) (Station 23: 3.0° N, 20.13° W); Equator (equatorial upwelling) (D-E-F) (Station 39: 0.67° S, 10.0° W); South of the equator (Congo River Plume) (G-H-I) (Station 96: 6.0° S, 4.98° E).

Except in cases where distinct UV emission bands were observed, the spectral dependence of fluorescence quantum yields showed a very similar trend to that observed for coastal and terrestrial CDOM samples (Figure 2 - 5, C-F-I) (Boyle et al., 2009; Green and Blough, 1994; Hoge et al., 1993; Ma et al., 2010; Vodacek et al., 1995). Fluorescence quantum yields (Φ) increased from λ_{exc} = 280 nm to a maximum at λ_{exc} ~ 370/380 nm, ranging from 1.8 to 2.5 % (Figure 2 - 5, C-F-I), and decreased

monotonically thereafter. However, when present, quantum yields for the distinct emission bands (Figure 2 - 6) were much higher (5 to 7 %). No obvious concomitant increase in absorption was observed at excitation wavelengths corresponding to these more highly fluorescent bands (Figure 2 - 6), implying that they contribute little to the total absorption at these wavelengths.

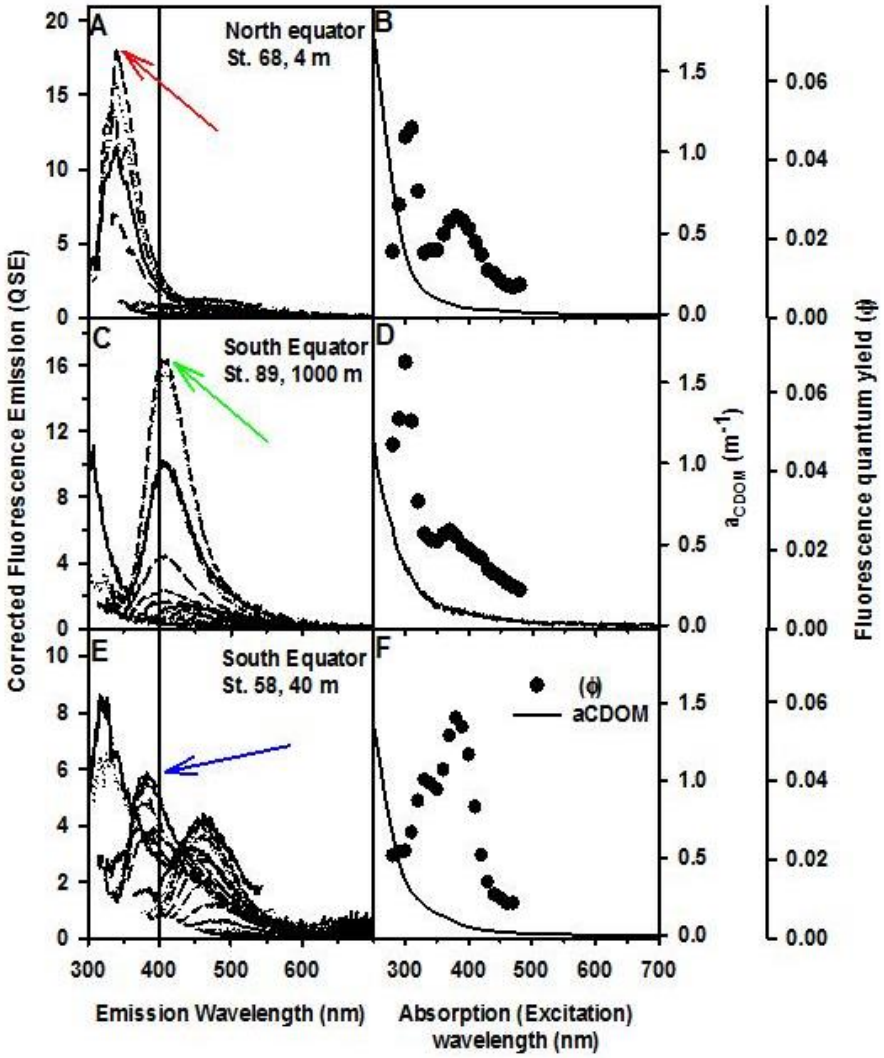

Figure 2 - 6: EEM spectra, fluorescence quantum yields (ϕ) and absorption spectra for selected stations exhibiting major, distinct UV emission bands ($\lambda_{exc}/\lambda_{em}$ = 300/340 nm ↓ (A); 300/405 nm ↓ (C); 320/380 nm ↓ (E)). The a_{CDOM} data for station 89 (D) was collected employing the 10 cm instead of the 200 cm pathlength as for stations 68 (B) and 58 (F). (A, B) (Station 68: 1.0° N, 0.0° W); (C, D) (Station 89: 2.0° S, 5.0° E); (E, F) (Station 58: 1.65° S, 0.0° E).

2.4.4 Fluorescence and relation to absorption

The above data indicate that short (UV) and long wavelength (visible) emission bands vary independently of each other. Further, while the UV bands exhibit distinct emission maxima, the visible emission bands continuously red-shift with increasing λ_{exc}. Moreover, the magnitude and spectral dependence of the fluorescence quantum yields mirror those observed for terrestrial materials (Figure 2 - 5, C-F-I) (Boyle et al., 2009). These results argue that the visible emission arises from a terrestrial source and that this visible emission is directly related to the absorption at the excitation wavelength. To test this idea further, the relationship between fluorescence emission intensity and absorption coefficient at selected λ_{exc} was examined (Del Vecchio and Blough, 2004b; Hoge et al., 1993; Vodacek et al., 1995).

Four pairs of $\lambda_{exc}/\lambda_{em}$ were chosen (specifically 280/320, 280/450, 320/420 and 350/450 nm) to examine this relationship. The UV emission at $\lambda_{exc}/\lambda_{em}$ =280/320 nm varied widely throughout the region (Figure 2 - 7A), and exhibited no apparent correlation between fluorescence emission and the absorption coefficient at λ_{exc} (Figure 2 - 7 B). This result implies that this species contributes very little to the total absorption at λ_{exc} = 280 nm. In contrast, the emission observed for $\lambda_{exc}/\lambda_{em}$ = 280/450 nm, was highly correlated to absorption at 280 nm (Figure 2 - 7D) indicating that absorption at 280 nm primarily gives rise to the visible emission at 450 nm. Similar to $\lambda_{exc}/\lambda_{em}$ = 280/450 nm, visible emission observed at $\lambda_{exc}/\lambda_{em}$ = 320/420 nm (Figure 2 - 7E) and 350/450 nm (Figure 2 - 7F) were also correlated with absorption at the λ_{exc} (Figure 2 - 7E & F), with a

dependence similar to that observed for CDOM from other coastal areas (Del Vecchio and Blough, 2004b; Vodacek et al., 1997; Vodacek et al., 1995).

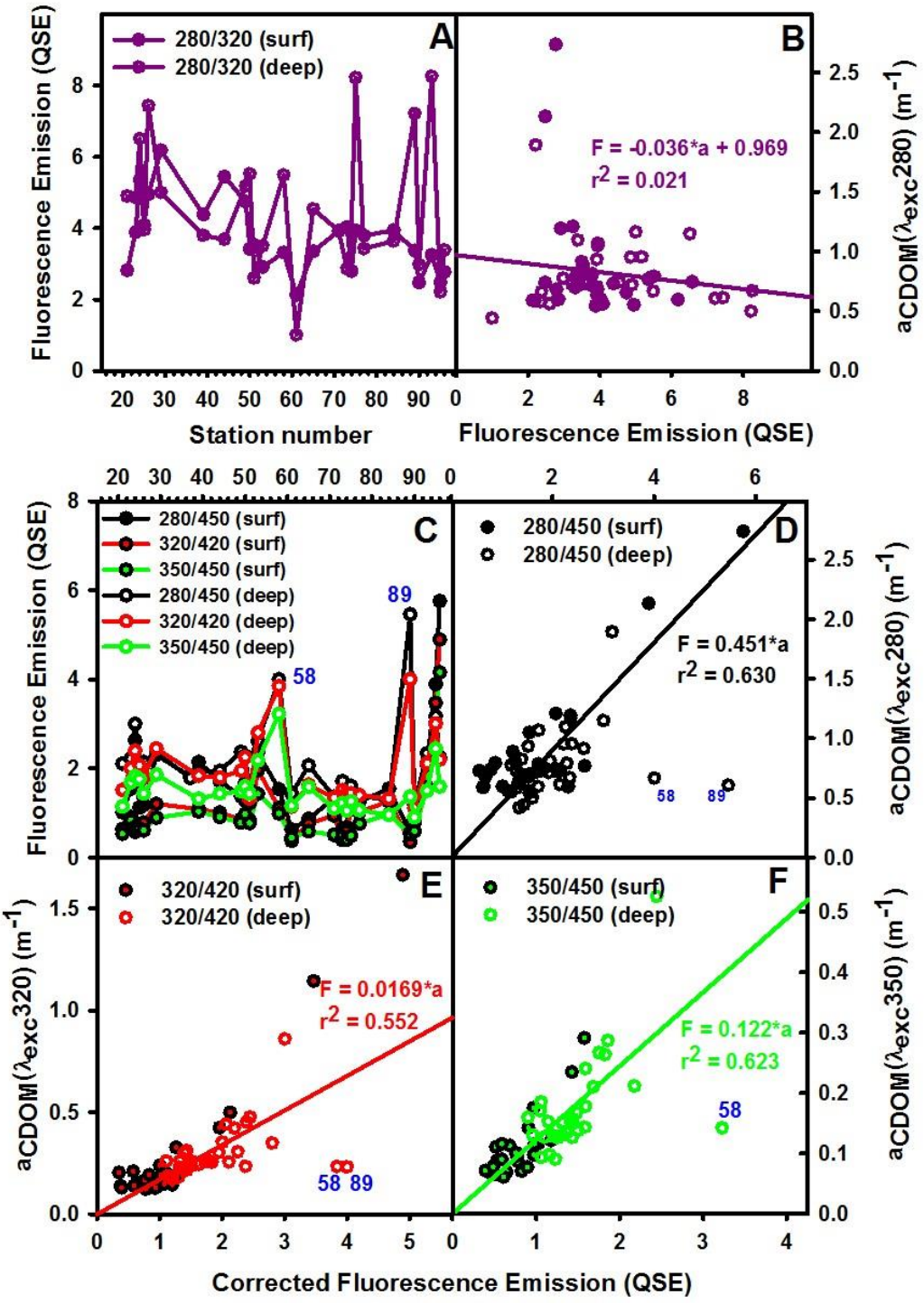

Figure 2 - 7: Spatial distribution of fluorescence emission (A & C) and dependence of fluorescence emission on absorption at the λ_{exc} (B- D- E- F) for the 'marine' (B: $\lambda_{exc}/\lambda_{em}$ = 280/320 nm) and the 'terrestrial' pools (D: $\lambda_{exc}/\lambda_{em}$ = 280/450 nm, E & F: $\lambda_{exc}/\lambda_{em}$ = 320/420 and 350/450 nm). Surface waters (open symbols); waters below the mixed layer (solid symbols). Station numbers in blue are waters where discrete emission bands were observed (see Figure 2 - 6).

Further, the substantial Stokes shift observed between the excitation wavelength and emission maximum when λ_{exc} = 280 nm is characteristic of samples from terrestrial environments (Boyle et al., 2009; Del Vecchio and Blough, 2004a). These results provide evidence that the UV emission at $\lambda_{exc}/\lambda_{em}$ = 280/320 nm represents material of a possible autochthonous/marine source, while those at $\lambda_{exc}/\lambda_{em}$ 280/450, 320/420 and 350/450 nm, are all components from an allochthonous/terrestrial source.

The ratio of a_{CDOM} (350) to fluorescence at $\lambda_{exc}/\lambda_{em}$ = 350/450 nm for offshore waters away from the influence of the Congo River, was 0.122 (m^{-1} QSE^{-1}), while a larger value of 0.227 (m^{-1} QSE^{-1}) was observed for waters in the region of the Congo River outflow. These values are similar to values recorded for waters in the Delaware Bay and the mid-Atlantic Bight (0.125 - 0.227 based on a_{CDOM} (355) at $\lambda_{ex}/\lambda_{em}$ = 355/450 nm) consistent with photochemically modified terrestrial material, although they fall at the upper and lower limit of that range (Del Vecchio and Blough, 2004b; Vodacek et al., 1997). The lower absorption to fluorescence ratio observed for offshore waters agrees with the higher quantum efficiency observed for these waters relative to waters of the Congo River outflow. This result is consistent with CDOM in these waters being modified (lower molecular weight) relative to the waters of the Congo River outflow (Boyle et al., 2009).

A few samples did not fit these trends and appear as outliers in Figure 2 - 7 (blue labeled station numbers 58 & 89). However, these are the same samples that exhibited distinct emission bands at the wavelengths explored (Figure 2 - 6) supporting the conclusion that the UV bands arise from a different source.

2.4.5 Comparison of optical properties of natural waters to C18-OM

The optical properties of C18-OM were compared with those of CDOM from natural waters (Figure 2 - 8). Consistent with past work (Boyle et al., 2009; Green and Blough, 1994), C18 preferentially extracted the long-wavelength absorbing and emitting material (Figure 2 - 8, A vs. B and D vs. E) leading to lower spectral slopes (S) for the C18-OM. However, the spectral dependencies of the optical absorption, fluorescence emission maxima and quantum yields were not only very similar for CDOM and C18-OM (Figure 2 - 8, C-F), but were also very similar to these obtained for terrestrial humic substances (Boyle et al., 2009), and CDOM and C18-OM from coastal waters (Boyle et al., 2009; Green and Blough, 1994). Interestingly, the emission bands at $\lambda_{exc}/\lambda_{em}$ = 280/~320 nm and $\lambda_{exc}/\lambda_{em}$ = 300/405 nm were not extracted, while that at $\lambda_{exc}/\lambda_{em}$ = 300/340 nm was only partially extracted (Figure 2 - 9). The effect of extraction on the band at $\lambda_{exc}/\lambda_{em}$ = 300/380 is not known, because no extracts were collected for any of the natural water samples where this band was observed. Failure of the C18 cartridges to extract these species suggests that they are either highly polar or charged at low pH, further showing that these UV emitting species are distinct from that emitting in the visible.

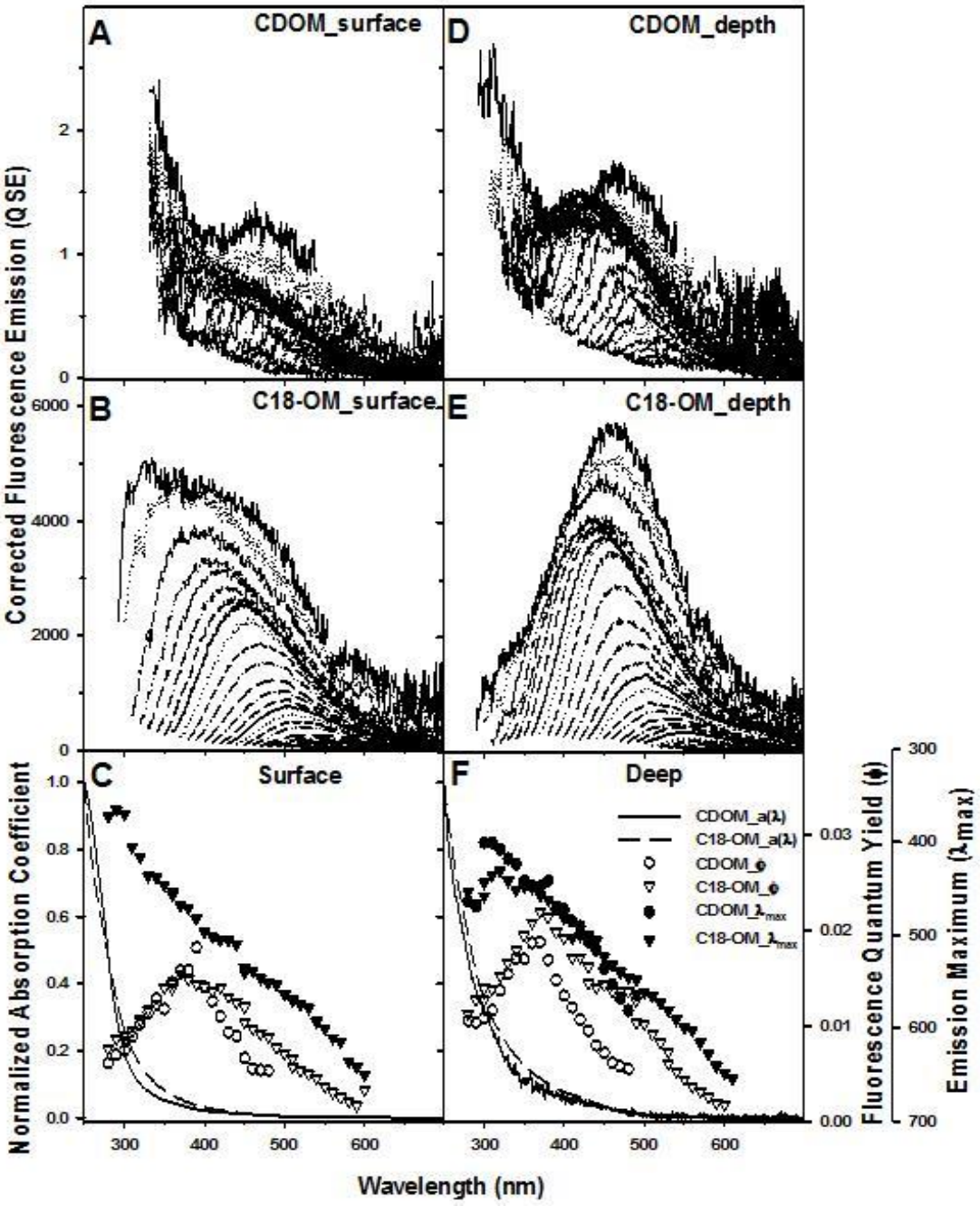

Figure 2 - 8: Comparison of the optical properties of CDOM with that of C18-OM for surface (A-B-C) and deep water samples (D-E-F) at station 51(4.98º S, 0.0º E). Comparison of CDOM and C18-OM fluorescence emission (A vs. B and D vs. E), absorption spectra normalized at 250 nm (C-F, lines), emission maxima, λ_{max} (C-F, solid symbols ▼, ●) and fluorescence quantum yield (Φ) (C-F, open symbols ▽, ○). CDOM absorption spectra were obtained using the 200 cm pathlength, while C18-OM absorption spectra were obtained using the 10 cm cuvette.

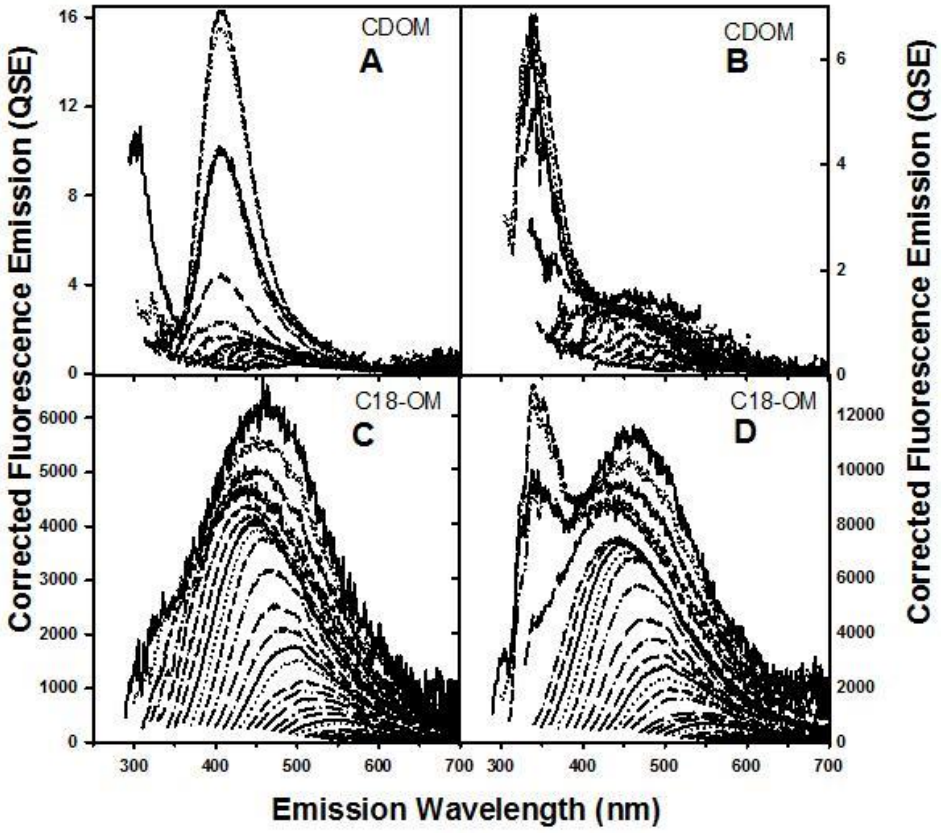

Figure 2 - 9: Affinity of the short wavelength discrete emission bands for the C18 cartridges. A vs. C Station 89, 1000 m (2.0° S, 5.0° E) ($\lambda_{exc}/\lambda_{em}$ = 300/405 nm not extracted by C18 cartridge). B vs. D Station 75, 1000 m (2.98° N, 5.0° E) ($\lambda_{exc}/\lambda_{em}$ = 300/340 nm, only partially extracted).

2.4.6 Comparison of the effects of borohydride reduction on C18-OM and natural waters

Following reduction with $NaBH_4$, all samples (both C18-OM and CDOM) exhibited a significant loss of absorption across the visible and ultraviolet wavelengths, but preferentially across the visible (> 50 %) (Figure 2 - 10, Figure 2 - 11, left panels; Figure 2 - 12, insets; Figure 2 - 13, right panels), consistent with past observations of lignin, terrestrial humic substances and C-18 extracts from coastal waters (Golanoski et al., 2012; Ma et al., 2010; Sharpless, 2012).

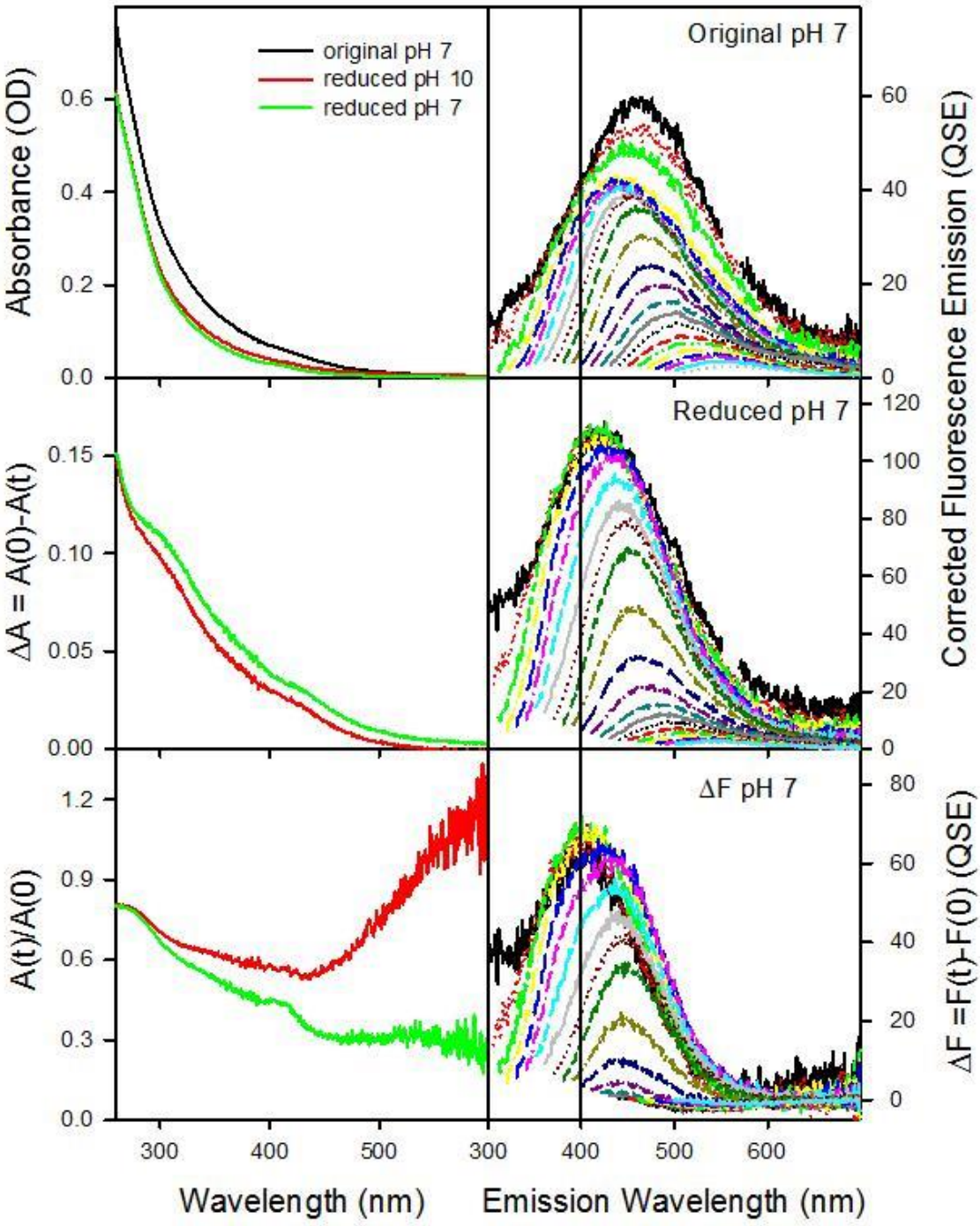

Figure 2 - 10: Changes in the optical properties (absorbance and fluorescence emission) for C18-OM sample at station 51, 1000 m (4.98° S, 0.0° E), following $NaBH_4$ reduction. Note that ΔA>0 indicates loss of absorbance while ΔF>0 represents gain of fluorescence signal. Colored lines represent excitation wavelengths as shown in Figure 2 - 5.

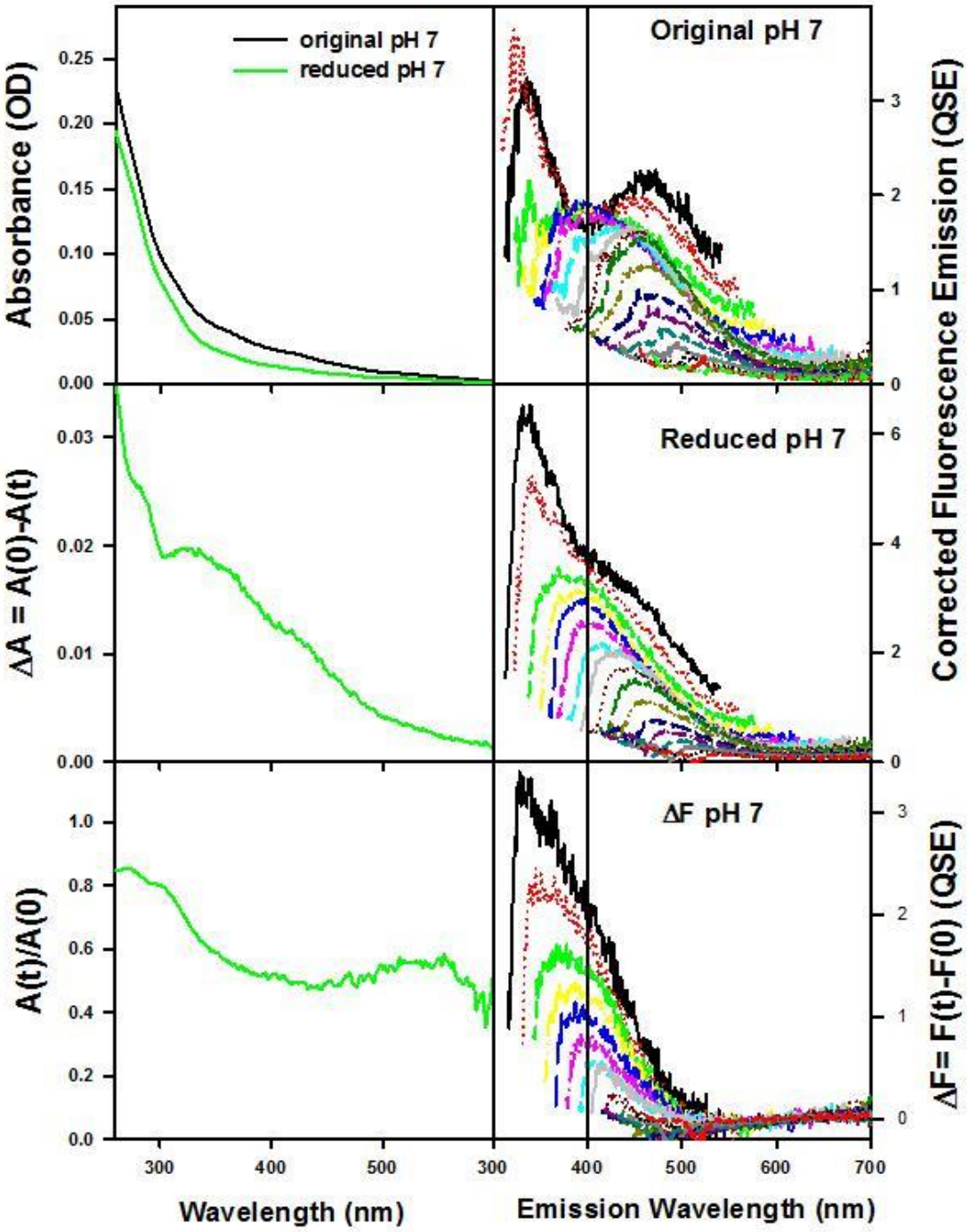

Figure 2 - 11: Changes in optical properties (absorbance and fluorescence emission) for CDOM sample at station 51, 1000 m (4.98° S, 0.0° E) following $NaBH_4$ reduction. Note that ΔA>0 indicates loss of absorbance while ΔF>0 represents gain of fluorescence signal. Absorbance spectra obtained using a 50 cm optical pathlength. Colored lines represent excitation wavelengths as shown in Figure 2 - 5.

A substantial enhancement (~ 2 fold) of fluorescence emission intensity in the blue portion of the visible spectrum was also observed, with peak maxima blue-shifted by as much as ~ 35 nm (Figure 2 - 10- Figure 2 - 11, right panels; Figure 2 - 12; Figure 2 - 13, middle panels). Exposing the reduced samples to O_2 following reduction did not significantly alter the optical properties (< 5 %). Adjusting the pH of the reduced samples back to its original value (from pH 10 to 7) further enhanced the loss of absorption in the visible, and slightly reduced the fluorescence emission gain (no more than ~ 15 %). The further loss in absorbance was most noticeable for the extracted samples, due to their much higher absorption relative to the natural waters. Importantly, reduction with $NaBH_4$ did not impact the spectral dependence of UV emission of the distinct bands at $\lambda_{exc}/\lambda_{em}$ = 280/320 (Figure 2 - 11, Figure 2 - 13) nor those at $\lambda_{exc}/\lambda_{em}$ = 300/340, 300/405 and 320/380 nm (Figure 2 - 14). Although the spectral dependence was unaffected, an increase in the fluorescence intensity was observed following reduction, due to the intensity enhancement of the blue-shifted emission.

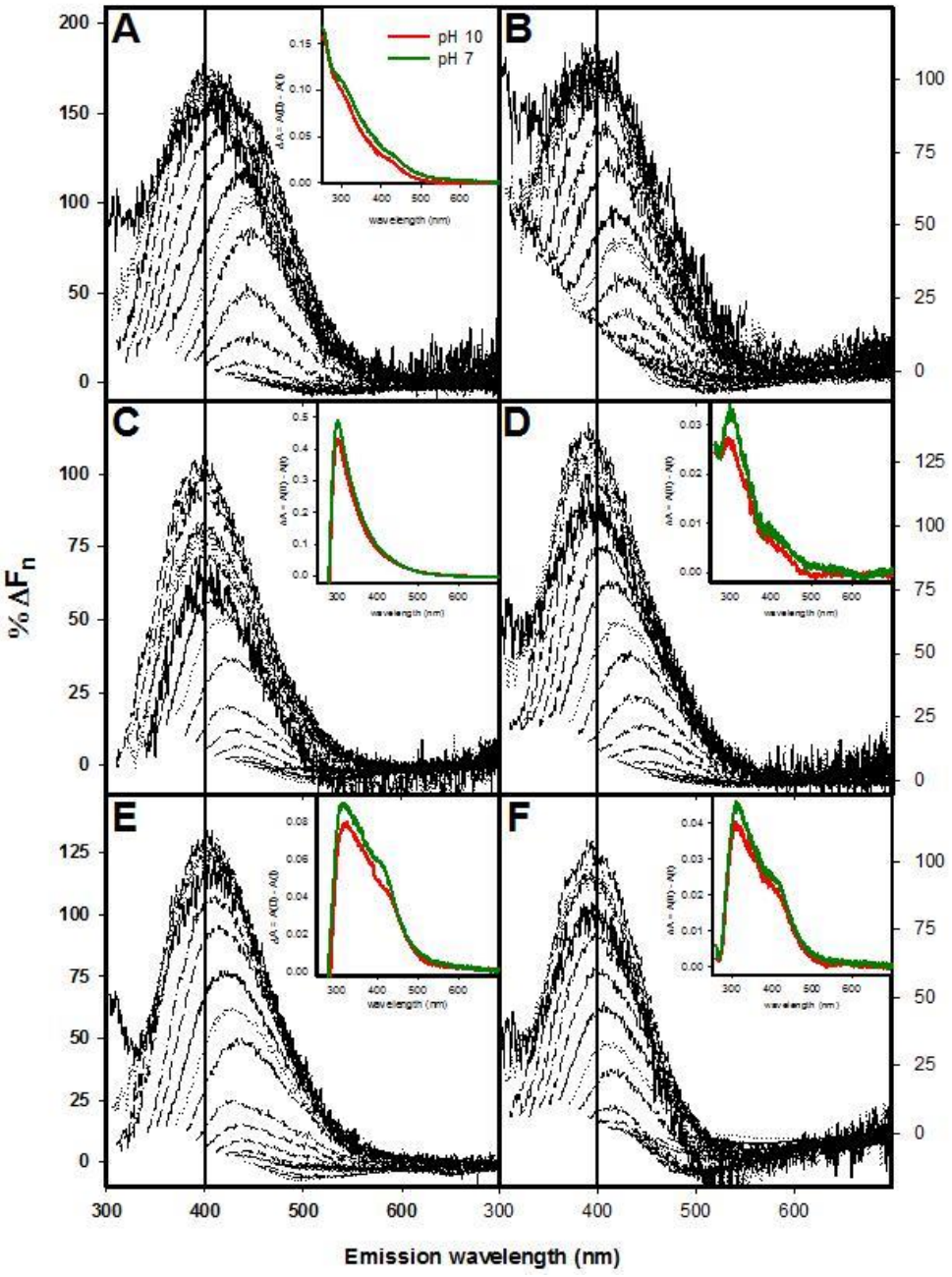

Figure 2 - 12: Wavelength dependence of the % fluorescence increase (%ΔF_n) and ΔA (inset) following $NaBH_4$ reduction of C18-OM at selected stations (A) St. 51, 1000 m (4.98° S, 0.0° E); (B): St. 26, 1000 m (3.48° N, 9.98° W); (C&E): St. 75, 5 m & 1000 m (2.98° N, 5.0° E); (D&F): St. 89, 5 m & 1000 m (2.0° S, 5.0° E). Note %ΔF_n > 0 indicates a gain in fluorescence (F), while ΔA > 0 corresponds to a loss of absorption (A). ($\%\Delta F_n = \frac{F(t) - F(0)}{F(0) at\ \lambda\ of\ \Delta Fmax}\ x\ 100$ **).**

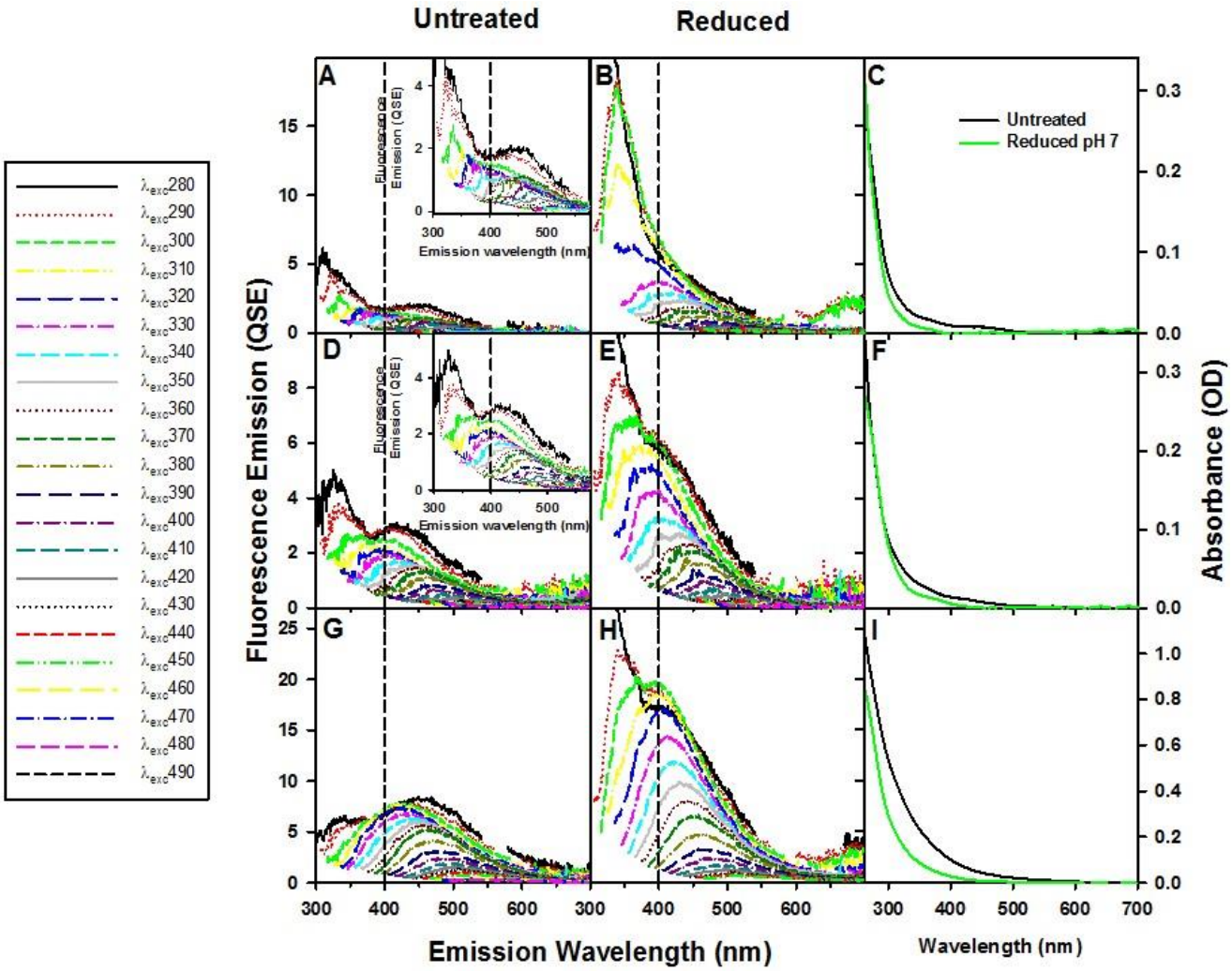

Figure 2 - 13: Changes in optical properties following $NaBH_4$ reduction of the natural waters from selected stations(A-C) Station 23, 10 m (3.0° N, 20.13° W); (D-F) Station 39, 60 m (0.67° S, 10.0° W); (G-I) Station 96, 4 m (6.0° S, 4.98° E).

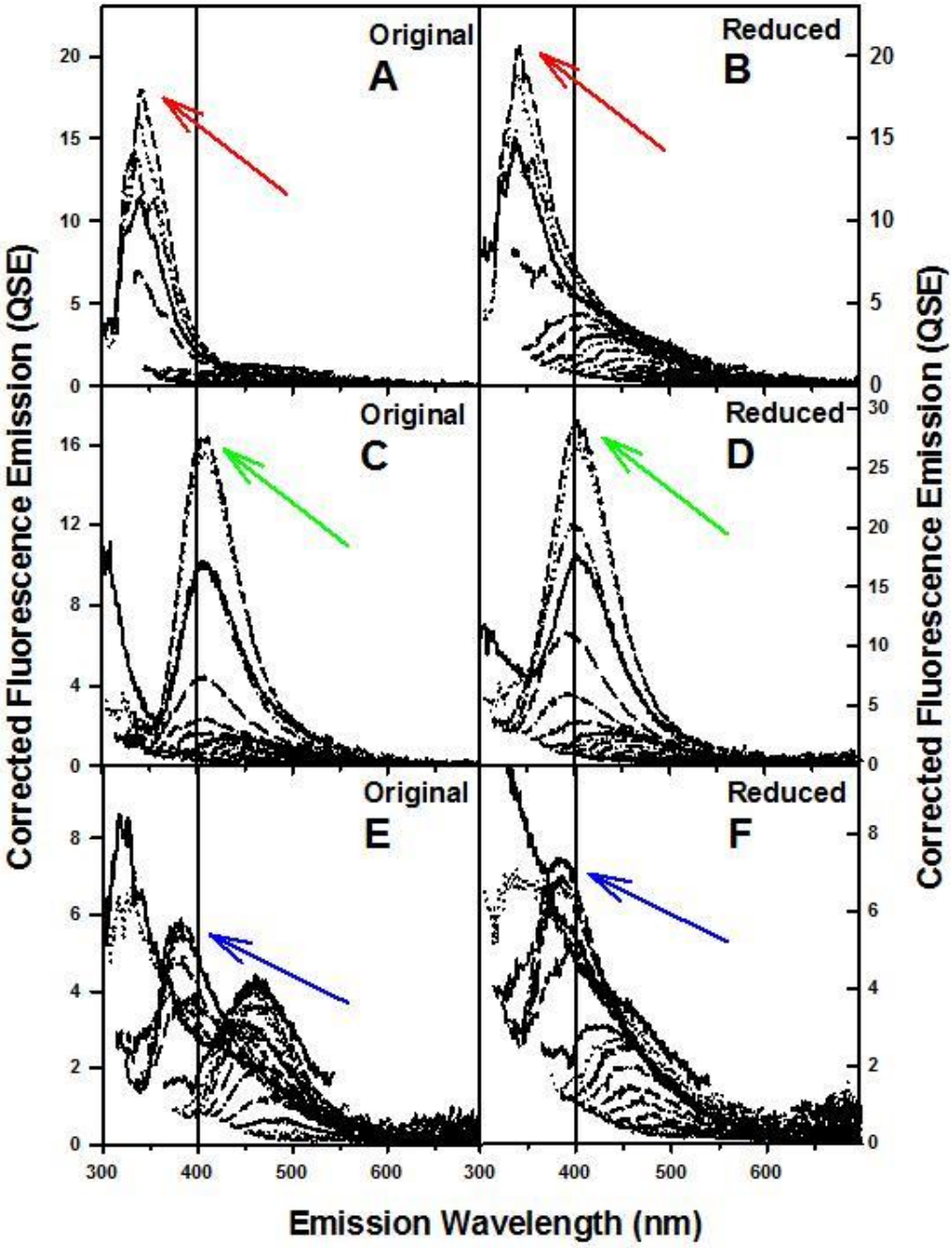

Figure 2 - 14: Spectral dependence of fluorescence emission of discrete emission bands ($\lambda_{exc}/\lambda_{em}$ = 300/340 nm ↓, 300/405 nm ↓ and 320/380 nm ↓) before (left A-C-E) and after (right B-D-F) reduction with $NaBH_4$. (A, B) Station 68, 4 m (1.0° N, 0.0° W); (C, D) Station 58, 40 m (1.65ºS, 0.0º W); (E, F) station 89, 1000 m (2.05° S, 5.0° E). The vertical line represents the 400 nm line.

2.5 Conclusions

This work has provided multiple lines of evidence that CDOM in Equatorial Atlantic waters is composed of a major terrestrial component. This evidence includes: (1) emission maxima in the visible that continuously red-shifts with increasing λ_{exc} (Figure 2 - 5) ((Boyle et al., 2009; Del Vecchio and Blough, 2004a); (2) spectral dependencies of the emission maximum and fluorescence quantum yields that are very similar to terrestrial material and CDOM from coastal margins receiving terrestrial input (Figure 2 - 5 C-F-I; Figure 2 - 8 C-F) (Boyle et al., 2009; Green and Blough, 1994; Hoge et al., 1993); (3) a large Stokes shift in the emission maxima with short wavelength excitation (λ_{exc} = 280 nm) (Boyle et al., 2009); 4) correlation of emission intensities with absorption coefficients at λ_{exc} (Figure 2 - 7), with absorption to fluorescence ratios comparable to those found in estuarine and coastal environments (Del Vecchio and Blough, 2004b; Hoge et al., 1993; Vodacek et al., 1997); 5) affinity of the C18 cartridges for the long wavelength (visible) absorbing and emitting material, but not for the UV emitting material (Figure 2 - 8 A-B-D-E) (Boyle et al., 2009; Green and Blough, 1994) ; 6) preferential loss of visible absorption and substantially enhanced blue-shifted emission in the visible following borohydride reduction, for both the Equatorial Atlantic waters and the C18-OM of these waters (Figure 2 - 10 - Figure 2 - 11, Figure 2 - 12, insets; Figure 2 - 13, right panels) (Ma et al., 2010). All of these properties have previously been shown to be characteristic of terrestrially-derived materials originating from vascular plant precursors (lignin, possibly tannins and other hydroxy- (methoxy) and polyhydroxy-aromatic compounds) (Boyle et al., 2009; Del Vecchio and Blough, 2004a), and can be explained within an electronic interaction model (Boyle et al., 2009; Ma et

al., 2010; Mignone et al., 2012). Existing ultra-high resolution mass spectral data of marine waters provide further evidence of the presence of lignins in marine samples (Kujawinski et al., 2009; Liu et al., 2011). To assign this "humic-like" material to a marine source, one would need to invoke diagenetic pathways for the marine source materials that would produce functionally similar types of structures, which to our knowledge has never been demonstrated. Further, past evidence for the in situ production of CDOM has primarily relied upon correlations of a single optical parameter, such as absorption or fluorescence, with AOU (Nelson et al., 2010; Swan et al., 2009). These increases in these single optical parameters with AOU have usually been interpreted to result from either the release, alteration, or the de nova formation of absorbing or emitting species through the microbial processing of marine source materials. While this may well be true for the UV-emitting species, our results from the Equatorial Atlantic indicate that this is not the case for the so-called "humic-like" materials. What most prior studies have uniformly failed to consider is that these optical changes could also result from chemical or microbial modification of an existing terrestrial source material through, for example, redox processes (Figure 2 - 10 - Figure 2 - 13) (Golanoski et al., 2012; Ma et al., 2010; Maurer et al., 2010).

This work shows that the simultaneous acquisition of complete spectral absorption and emission properties, combined with chemical tests (borohydride reduction, C18 extractions) can provide a far clearer understanding of the sources and cycling of marine CDOM. Unequivocal confirmation of sources (and structure) may ultimately be achieved by further combining this approach with ultra-high resolution mass spectrometry

(Kujawinski et al., 2009; Schmidt et al., 2009; Sleighter et al., 2010) and other (photo) chemical tests (Golanoski et al., 2012; Sharpless, 2012).

Chapter 3: Impact of C18 extraction on CDOM optical properties

3.1 Overview

Some properties of CDOM (such as the optical) can be easily measured on whole waters but others require sample concentration and removal of natural salts, particularly for marine samples. To increase CDOM content and eliminate naturally occurring salts, solid phase extraction is often employed. Biases following extraction and elution are inevitable, thus raising the question of how truly representative the extracted material is of the original. In this context, we investigated the wavelength dependence of extraction and elution for C18 cartridges in relation to CDOM optical properties. Samples were obtained from the Middle Atlantic Bight (MAB) and the Equatorial Atlantic Ocean (EAO) thus encompassing riverine impacted waters as well as oceanic waters. Further, we compared the optical changes of C18 extracts and the corresponding whole water following chemical reduction with sodium borohydride ($NaBH_4$).

For inshore MAB samples, C18 cartridges preferentially extract higher molecular weight, long-wavelength absorbing material. Extraction efficiency decreases with offshore distance and becomes more uniform with wavelength. Absorption and fluorescence are changed in a similar fashion by the extraction process thus leading to essentially identical fluorescence quantum yields. Overall, the optical properties of the original water samples and the corresponding extracted material did not vary significantly. Moreover, C18 extracts and corresponding water samples exhibited very

similar changes in optical properties following $NaBH_4$ reduction suggesting a common structural basis for the optical properties of these materials.

Overall, CDOM optical properties and the changes upon chemical reduction are very similar to that of the C18 extracted material for the majority of the samples studied, indicating that the extracted material is largely representative of the original CDOM.

3.2 Introduction

The optical properties of chromophoric dissolved organic matter (CDOM) (and humic substances, HS) have been intensively studied during the last several decades. However, inter-laboratory data are often not comparable due to various methods employed to collect, extract and analyze DOM and CDOM. Despite a few very sensitive analytical techniques such as UV/Vis absorption and fluorescence which allow direct measures of bulk CDOM in natural waters, the majority of the available techniques require prior extraction and/or concentration of DOM/CDOM.

Many solid phase extraction (SPE) techniques for DOM isolation from fresh to salt waters have thus been widely used including cartridges pre-packed with XAD resins (Daignault et al., 1988), C18-bonded silica sorbents (Benner, 2002) and references therein), and more recently, modified styrene-divinylbenzene copolymer type sorbents (PPL - (Priority PolLutant) (Dittmar et al., 2008). Reverse osmosis (RO) has also been used for retention and concentration of DOM from fresh waters (Serkiz and Perdue, 1990). Most recently, a new technique for more efficient isolation of DOM from

seawater was developed by combining reverse osmosis with electrodialysis (RO/ED) (Vetter et al., 2007). Extraction efficiencies vary among these techniques and are routinely expressed relative to dissolved organic carbon (DOC).

XAD resins have been widely used to remove hydrophobic compounds of various molecular sizes. International Humic Substances Society (IHSS) has used XAD to extract standard reference materials (Suwannee River Fulvic and Humic Acids, SRFA and SRHA) from natural waters. However, XAD resins used for the extraction of marine DOM are no longer available (Dittmar et al., 2008). Silica-C18 sorbents have been widely employed for reversed phase extraction of nonpolar to moderately polar compounds from water. Retention is based on the partitioning of the nonpolar organic analyte between the nonpolar alkyl functional groups. Thus, charged compounds are usually not retained and require ion exchange SPE for their extraction. Sequential solid phase extraction through two different XAD resins has been shown to recover comparable DOC as silica-C18, with percent DOC recovery ranging from 23% to 40% (Amador et al., 1990; Druffel et al., 1992). More recently, PPL sorbents have been employed for extracting DOM. As with XAD and silica-C18, PPL retains moderately polar to nonpolar substances from large volumes of water. Recent work by Dittmar et al. (2008) showed PPL to be more efficient in terms of percent DOC extracted relative to the C18. Vetter et al. (2007) showed that DOC recoveries from waters in the Atlantic ocean using PPL exceeded 60%.

These extraction processes facilitate the elimination of the high concentrations of inorganic salts occurring in marine waters. Thus, highly concentrated organic samples with relatively low salt content can be generated and different analytical techniques can be performed on the extracts. However, biases of DOM properties following extraction are inevitable, raising the question as to how representative the extracts reflect the properties of the original samples. Moreover, the fraction of organic carbon retained during solid phase extraction is most often reported, rather than the fraction recovered after elution. Given the selective mechanisms of DOM sorption, whether the material eluted from the sorbent is a true representation of the material initially adsorbed, is another question for consideration.

Some earlier studies have made attempts to address this question by comparing the optical properties of natural water samples (CDOM) collected from different environments to their corresponding C18 extracts (C18-OM). Green and Blough (1994) employed water samples from southern and western coast of Florida to the eastern Gulf of Mexico, and compared spectral slopes, absorption coefficient at 355 nm and quantum yields for CDOM and C18-OM. They also examined the efficiency of extraction of the various water types. Boyle et al (2009) investigated the optical properties of CDOM and C18-OM, using samples from the Middle Atlantic Bight (MAB), but only compared $a_{CDOM}(355)$ and spectral slopes.

In this study, we present a more detailed and extensive comparison of the optical properties of CDOM and C18-OM. To our knowledge no study has done such a detailed

characterization of these optical properties. Samples were collected from very different geographic locales to span riverine, estuarine and marine type environments: (a) along a transect from the Delaware River to the Sargasso Sea (Middle Atlantic Bight, MAB); and (b) across the Equatorial Atlantic Ocean (EAO) from the open ocean gyre to the Congo River Plume. The extraction efficiency of C18 cartridges was examined (for MAB samples) as well as the relative wavelength dependence of elution of the sorbed organic matter in relation to the optical properties (MAB and EAO). Absorption and fluorescence were measured directly for natural waters and compared to those of C18 extracts (C18-OM). This comparison was extended further by examining the changes in the optical properties of CDOM and C18-OM following chemical reduction with sodium borohydride. A representative group of samples characteristic of the different water types was reduced, and optical changes were compared.

3.3 Material and Procedures

3.3.1 Samples

Samples from the Mid Atlantic Bight (MAB) were collected onboard the R/V Cape Henlopen and R/V Cape Hugh Sharp from April to December during five cruises from 2005 to 2006: April 9-15, 2006; August 24-28, 2006; September 20-24, 2005; October 12-20, 2006 and November 30-December 4, 2006. A typical transect from the Delaware River (~ 40 N; -75W) to the western boundary of the Gulf Stream (~ 36N; -72W) was visited during all cruises (Figure 3 - 1 D). The water column was thermally- and density-stratified during the summertime, typical of coastal waters on the shelf of the MAB,

while stratification was absent or not fully developed during the spring, fall and winter surveys (Del Vecchio and Blough, 2004b). Ocean samples were collected onboard the R/V Endeavor in the Equatorial Atlantic Ocean (EAO) in May-June 2009 over a 5 week period, encompassing three zonal and meridional sections between 23°W and 5°E, and 3°N and 3°S, respectively (Andrew et al., 2013). Comparison of optical properties of CDOM and C18-OM are based on measurements obtained in 2006 and 2009 for the MAB and EAO, respectively. Optical measurements were collected for all EAO samples (18). Optical measurements for C18-OM from the MAB are presented for 23 of the 43 samples collected, and are representative of the various water types characteristic of that region.

Water samples for the optical measurements were collected as previously reported (Del Vecchio and Blough, 2004b). Briefly, samples were collected employing a CTD (conductivity–temperature–depth) rosette equipped with Niskin bottles and were immediately filtered using GF/F filters (0.7-μm pore size). Samples for optical measurements were stored in the dark at 4 ºC until measurement (about 2 weeks for coastal samples and 3 months for ocean samples). Before measurement, samples were re-filtered through 0.2-μm pore-size nylon syringe filters to ensure removal of all particles.

Water samples for optical measurements of extracted material were collected from the vessel's surface water pumping system (2 m and 5 m) and CTD rosette after filtration through an in-line Gelman fluted capsule filter (0.2 μm pore size). A clean Teflon line for the pumping system was supplied at the beginning of each cruise to prevent contamination by material accumulating in the line. Water samples (20 L) were acidified

to pH 2 and then pumped through the SPE cartridge (C18 extraction column, UCT) at the flow rate of 50 ml min^{-1} as described by Boyle et al. (2009). The cartridges were pretreated with 100 ml of high purity methanol followed by 50 ml of acidified (pH 2) Milli-Q water prior to extraction. After extraction each cartridge was rinsed with 1 L of acidified (pH 2) Milli-Q water to remove salts and stored in the refrigerator (4 ° C) until further processing.

DOM was extracted from the C18 cartridges with 50 mL of high purity methanol: the first fraction (5 ml) that contained some aqueous residue was separated from the second fraction (45 ml). The second fraction (C18-OM) was collected into a 100 ml round bottom flask and evaporated to dryness under vacuum using a rotary evaporator at 30-35 ° C. The dried material was re-dissolved with Milli-Q water, neutralized with diluted NaOH solution to pH 7 and stored frozen till further analysis. This material is here on referred to as C18-OM.

3.3.2 Optical measurements

CDOM absorption spectra were acquired with a Shimadzu 2401-PC spectrophotometer employing a 10 cm optical cell (1 cm cell for C18-OM) using Milli-Q water as the blank, as reported previously (Del Vecchio and Blough, 2004b; Vodacek et al., 1997). Absorption spectra for offshore CDOM samples (including samples from the EAO as well as samples further offshore in the MAB region) were obtained on a liquid core capillary waveguide long path spectrometer (WIP) using the 10 or 50 cm fiber optic cell. Salinity-matched solutions were used as reference to avoid absorbance baseline offsets

caused by refractive index differences between reference and sample. Absorption spectra were recorded over the range 200–800 nm. Absorption coefficients, $a(\lambda)$, were calculated using the following equation,

$$a(\lambda) = 2.303A(\lambda)/L \quad \text{Eq. (1)}$$

where $A(\lambda)$ is the absorbance over pathlength L . The spectra were then fit to an exponential function,

$$a(\lambda) = a(\lambda_0)e^{-S(\lambda-\lambda_0)} \quad \text{Eq. (2)}$$

using a nonlinear least squares fitting routine (NLF) over the range 300–700 nm. Here λ_0 is a reference wavelength and S is the spectral slope parameter.

The C18 extraction efficiency was calculated using equation 3 below.

$$Extraction\ efficiency = 1 - \frac{Abs\ (post\ extraction\ acidified\ waters, pH\ 2)}{Abs\ (pre\ extraction\ acidified\ waters, pH\ 2)} \quad \text{Eq. (3)}$$

Here values of 0 and 1 indicate 0 % and 100 % extraction efficiency respectively. Absolute values of extraction efficiency for EAO samples were not calculated because the C18 post extraction waters were not collected at the time of extraction. The relative wavelength dependence of elution across the UV visible regime was obtained using equation 4.

$$Relative\ wavelength\ dependence\ of\ elution = \frac{Abs\ spectrum\ (C18-OM)}{Abs\ spectrum\ (CDOM)} \quad \text{Eq. (4)}$$

The resulting ratio as a function of wavelength does not provide information on absolute elution efficiency because it is not volume normalized. Accurate volumes of dilution were not recorded, hence the reason for examining wavelength dependence (spectral comparisons) and not absolute elution efficiency.

CDOM and C18-OM fluorescence measurements were acquired with an Aminco–Bowman AB2 luminescence spectrometer employing a 1-cm optical cell and Milli- Q water as blank. Both the excitation and emission monochromator bandpasses were set to 4 nm for extracts and 8 nm for the natural waters. The emission spectra were recorded from 10 nm greater than λ_{exc} to 700 nm, with λ_{exc} incremented every 10 nm over the range 290-600 nm. The spectra were corrected for the instrument response using factors supplied by the manufacturer. Fluorescence emission was normalized to the integrated emission of 1 ppb quinine sulfate with excitation at 350 nm and reported in quinine sulfate equivalents (QSE). The wavelength dependence of fluorescence emission maxima and quantum yields were measured as in Del Vecchio and Blough (2004a).

3.3.3 $NaBH_4$ Reduction

CDOM and the corresponding C18-OM sample was selected from four sites in the study region for the $NaBH_4$ reduction analysis based on geographic locale. The samples consisted of waters from inshore (river - 0 ppt), bay (intermediate salinity -17.6 ppt), shelf (32.5 ppt) and open ocean (2 m and 1000 m) region.

Reduction with $NaBH_4$ (Fisher) was performed as described by Andrew et al. (2013). Briefly, natural waters (20.0 - 30.0 mL) were placed in a glass vial, capped and sparged with ultrapure N_2 for 35 min. Solid $NaBH_4$ was added to the vial using a one-to-one ratio of $NaBH_4$ (mg) to sample volume (mL) (resulting in very large mass excess of $NaBH_4$ relative to CDOM), under continuous N_2 flow. C18-OM was reduced in a 1 cm quartz cuvette using 3.0 mL of sample. Mass excess of $NaBH_4$ (~50 fold) was added based on approximate organic matter content derived from matching absorbance spectra to that of known concentrations of SRFA. This was accomplished by adding ~85-95 μL of a concentrated $NaBH_4$ stock solution prepared in a pH 12 aqueous solution to the C18-OM sample. Optical properties were measured prior to and following reduction. The reduction was considered to be complete when no further changes in absorption spectra were observed (~24 hrs). Sample pH increased from pH 7-8 to pH 10-11 due to the reaction of excess $NaBH_4$ with water (Golanoski et al., 2012; Ma et al., 2010; Tinnacher and Honeyman, 2007). Thus sample pH was readjusted to the original pH to allow for comparison with the untreated natural water sample.

3.4 Results and discussion

3.4.1 Extraction efficiency and wavelength dependence of elution

The C18 extraction efficiency for inshore MAB waters (river and bay) was approximately 40 % at 250 nm and increased with wavelength to ~ 80 % at 500 nm, thus exhibiting a preferential retention of the long-wavelength absorbing material from the bulk CDOM (Figure 3 - 1, B&C), consistent with previous work (Green and Blough, 1994). Offshore

samples exhibited a lower (~ 20 % at 250 nm) extraction efficiency that was however relatively uniform across the entire wavelength range investigated (Figure 3 - 1, A&C). The overall extraction efficiency decreased from fresh to offshore marine waters (Figure 3 - 1C) but decreased more quickly over the longer wavelength regime.

The relative wavelength dependence of elution was relatively constant in the UV wavelength regime, but tailed upwards or downwards at longer wavelengths in areas of high or low CDOM absorption, respectively (Figure 3 - 2). The observed spectral dependence of elution mirrored the wavelength dependence of extraction efficiency in the MAB (compare Figure 3 - 1 , Figure 3 - 2). This result is significant, suggesting that the eluted material is qualitatively representative (at least in optical absorbance) of that retained on the sorbent, indicating that no significant biasing occurs during the elution process. Interestingly, the wavelength dependence of elution for EAO was comparable to that obtained for MAB shelf and shelf break samples (Figure 3 - 2). Elution was relatively constant over most of the UV regime (<360 nm) but slowly decreased at all longer wavelengths.

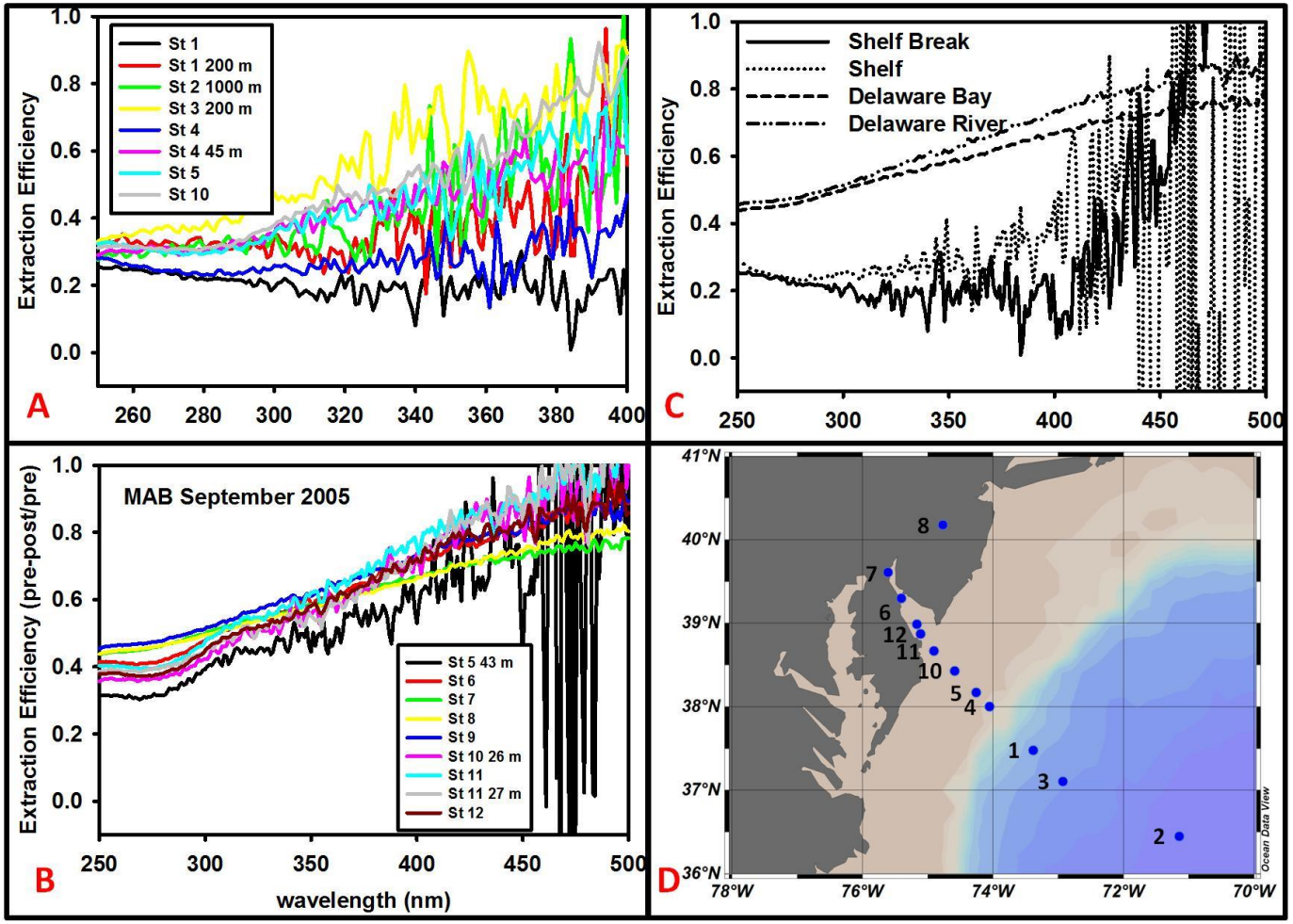

Figure 3 - 1: Extraction efficiency of C18 cartridges from a transect from the MAB shelf break to the Delaware River during September 2005. $Extraction\ efficiency = 1 - \frac{A\ (post\ extraction\ \text{acidified}\ waters, pH\ 2)}{A\ (pre\ extraction\ acidified\ waters)}$**. Values 1 and 0 correspond respectively to 100 and 0 % extraction efficiencies. The large noise at longer wavelengths (> 400 nm) is due to the small absorbance values.**

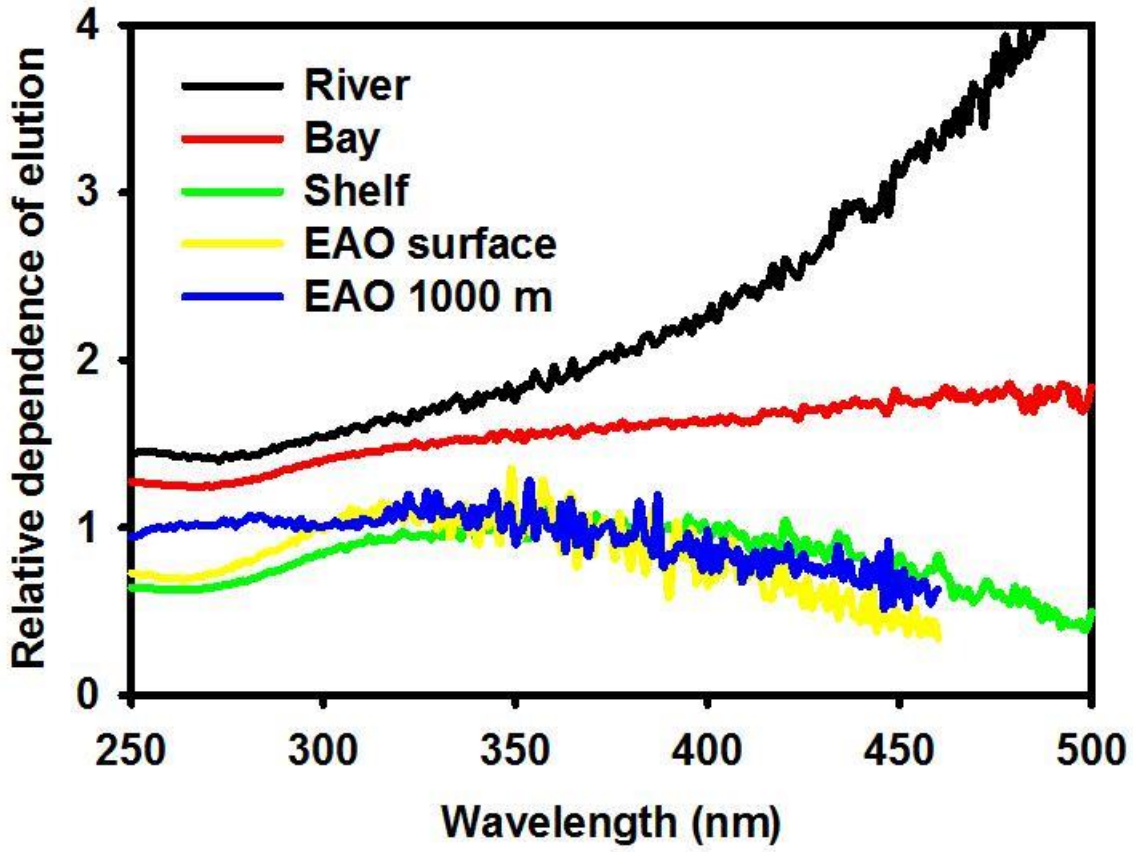

Figure 3 - 2: Wavelength dependence of relative elution off the C18 cartridges for river (black), bay (red) and shelf (green) samples from the MAB, and EAO surface (yellow) and deep (blue) samples. The ratio of the absorption spectra of C18-OM (1 cm) to CDOM (10 cm) is presented as the relative spectral dependence of elution. For comparison, spectra were scaled to fit on one plot.

Sample	Geographic locale	Position		Salinity (ppt)	S (nm^{-1})	
		Lat.	Long.			
MAB August					***CDOM***	***C18-OM***
St 1 2 m	bay mouth	38.9	-75.1	29.6	0.0184	0.0160
St 1 17 m	bay mouth	38.9	-75.1	31.5	0.0178	0.0152
St 4 2 m	shelf	38.0	-74.0	31.6	0.0219	0.0181
St 4 75 m	shelf	38.0	-74.0	35.1	0.0168	0.0143
St 7 1000 m	gulf stream	36.2	-71.8	35.1	0.0160	0.0133
St 10 2 m	mid shelf	38.2	-74.3	31.5	0.0240	0.0200
St 10 35 m	mid shelf	38.2	-74.3	33.1	0.0168	0.0151
St 12 2 m	lower bay	39.0	-75.1	28.4	0.0199	0.0160
St 14 2 m	mid bay	39.3	-75.4	17.6	0.0177	0.0161
St 19 2 m	river	40.1	-74.8	0.1	0.0173	0.0149
St 20 2 m	mid bay	39.3	-75.4	12.5	0.0177	0.0166
MAB December		**Lat.**	**Long.**	**Salinity**	***CDOM***	***C18-OM***
St 2 2 m	offshore	38.00	-74.05	33.7	0.0192	0.0162
St 2 50 m	offshore	38.00	-74.05	33.8	0.0192	0.0159
St 3 30m	shelf	38.18	-74.25	33.7	0.0192	0.0130
St 4 20 m	bay mouth	38.68	-74.89	31.8	0.0181	0.0104
St 6	bay nouth	38.88	-75.09	26.44	0.0180	0.0126
St 6 15m	bay mouth	38.88	-75.09	28.3	0.0180	0.0102
St 7	river	39.97	-75.13	0.08	0.0156	0.0107
St 8	upper bay	39.58	-75.55	0.09	0.0162	0.0147
St 9	shelf	-74.57	32.53	32.53	0.0185	0.0109
St 9 20 m	shelf	-74.57	32.53	32.5	0.0185	0.0122
St 11	Lower bay	-75.14	23.28	23.28	0.0180	0.0128
St 13	upper bay	-75.58	0.12	0.12	0.0162	0.0118
St 14	bay mouth	-75.09	28.66	28.66	0.0185	0.0126

Sample	Position		Salinity	S (nm^{-1})	
	Lat.	Long.			
EAO (5 m)				***CDOM***	***C18-OM***
St 22	3.0	-23.0	34.6	NA	NA
St 26	3.50	-10.00	34.4	0.0217	0.0229
St 48	-5.00	-10.00	35.3	0.0227	0.0207
St 51	-5.00	0.00	35.2	0.0319	0.0221
St 61	-0.67	0.00	35.4	0.0314	0.0209
St 73	3.00	0.00	34.7	0.0288	0.0232
St 75	3.00	5.00	35.1	0.0220	0.0221
St 89	-2.00	5.00	36.1	0.0207	0.0186
St 96	-6.00	5.00	34.1	0.0168	0.0153
EAO (1000m)	**Lat.**	**Long.**	**Salinity**	***CDOM***	***C18-OM***
St 22	3.0	-23.0	34.6	0.0179	0.0160
St 26	3.5	-10.0	34.7	0.0188	0.0158
St 48	-5.0	-10.0	34.6	0.0214	0.0164
St 51	-5.0	0.0	34.6	0.0175	0.0152
St 61	-0.7	0.0	34.6	0.0206	0.0151
St 73	3.0	0.0	34.6	0.0152	0.0153
St 75	3.0	5.0	34.6	0.0180	0.0153
St 89	-2.0	5.0	34.6	0.0173	0.0163
St 96	-6.0	5.0	34.6	0.0154	0.0157
MAB September	**Lat.**	**Long.**	**Salinity**	***CDOM***	***C18-OM***
St 2 2m	36.5	-71.2	36.0	0.0159	0.0208
St 2 1000m	36.5	-71.2	36.0	0.0198	0.0166
St 5	38.2	-74.3	32.5	0.0241	0.0208
St 5 41m	38.2	-74.3	32.5	0.0182	0.0163
St 7	39.3	-75.4	14.4	0.0178	0.0158

Table 3 - 1: Spectral slopes (S nm-1) obtained for August MAB, a small set from December MAB, and surface and deep samples from the equatorial Atlantic Ocean. S (Eq. 2) values have uncertainty ≈ 0.0001. NA, data not available

3.4.2 Absorbance and spectral slope

The values of spectral slope (S) obtained from the fits of absorbance spectra of selected CDOM and C18-OM samples from both environments are provided in Table 3 - 1. Overall, the spectral slopes for CDOM were higher relative to C18-OM (Figure 3 - 3). Higher values of S indicate that there is a more rapid decline in CDOM absorption with wavelength, thus a lower absorption contribution in the visible wavelengths (Figure 3 - 4, Figure 3 - 5, Figure 3 - 6). Numerous workers have found that S usually increases with decreasing molecular size (Boyle et al., 2009; Green and Blough, 1994; Sharpless and Blough, 2014; Yan et al., 2012). Thus, lower values of S for C18-OM is indicative of the presence of higher molecular weight material, suggesting the preferential extraction of this HMW material. This is a reasonable expectation, as higher molecular weight (HMW) material, generally considered to be more nonpolar, would be more easily adsorbed and thus extracted.

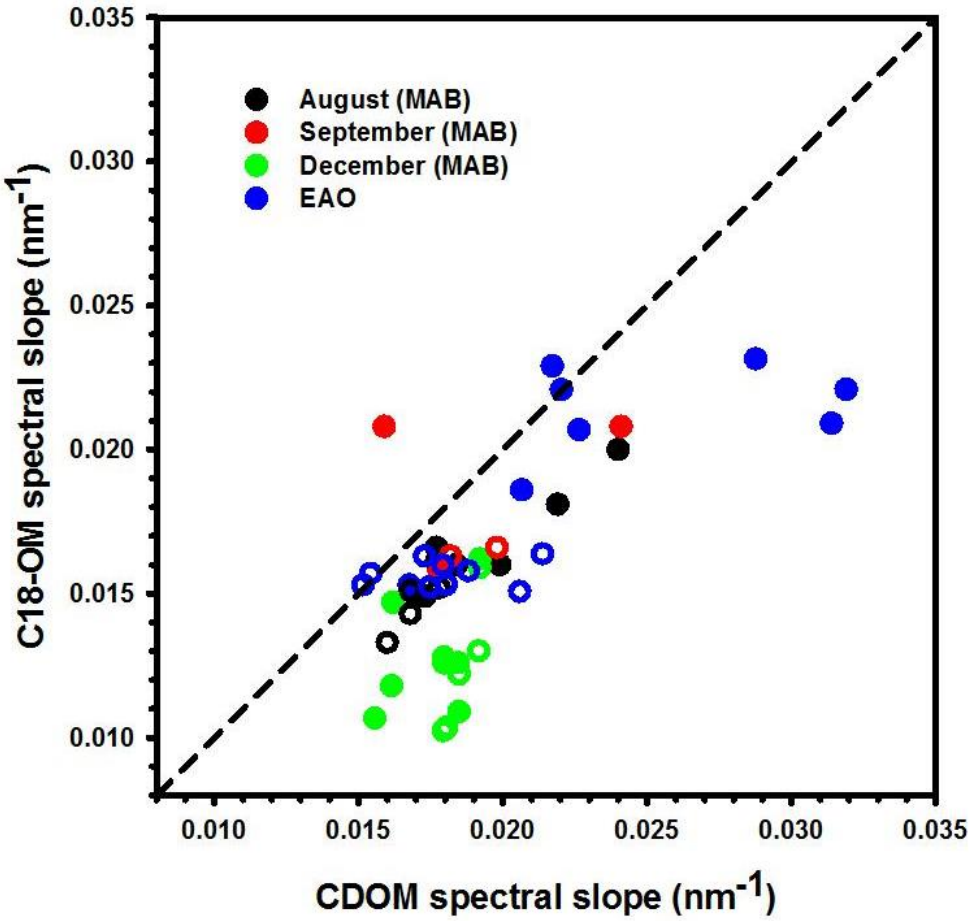

Figure 3 - 3: Comparison between the values of S acquired for CDOM and C18-OM for waters from the MAB August, September and December season, and for the Equatorial Atlantic Ocean. Open symbols represent surface samples. Solid symbols represent depths below the surface. 1:1 line is also shown.

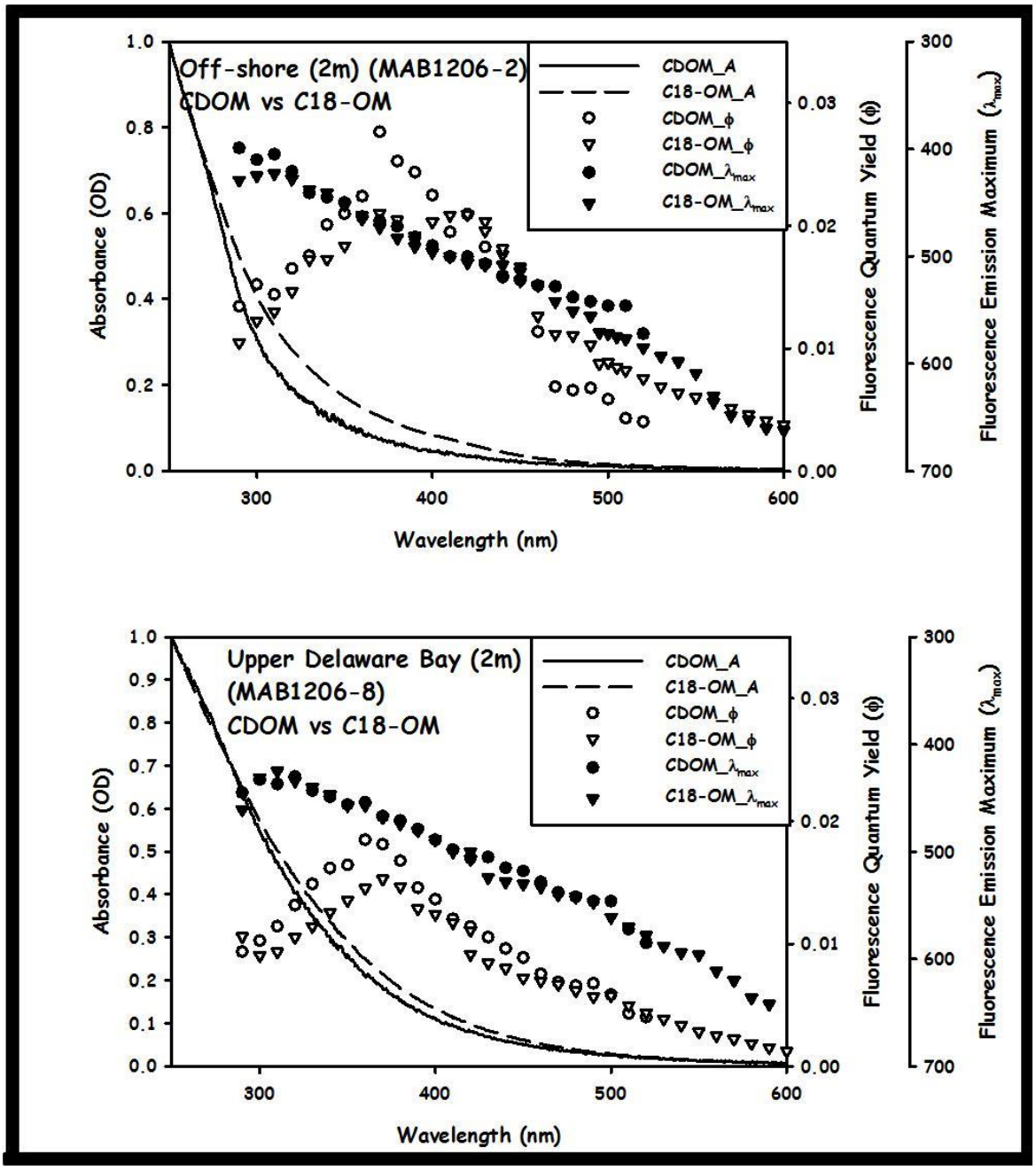

Figure 3 - 4: Comparison of CDOM and C18-OM optical properties for representative samples from the MAB offshore shelf waters (top) and upper Delaware Bay (bottom) during December 2006. 10 cm absorbance normalized to 250 nm (lines); fluorescence emission maxima, λ_{max} (solid symbols) and fluorescence quantum yield (ϕ) (λ_{exc} 280-600 nm) (empty symbols).

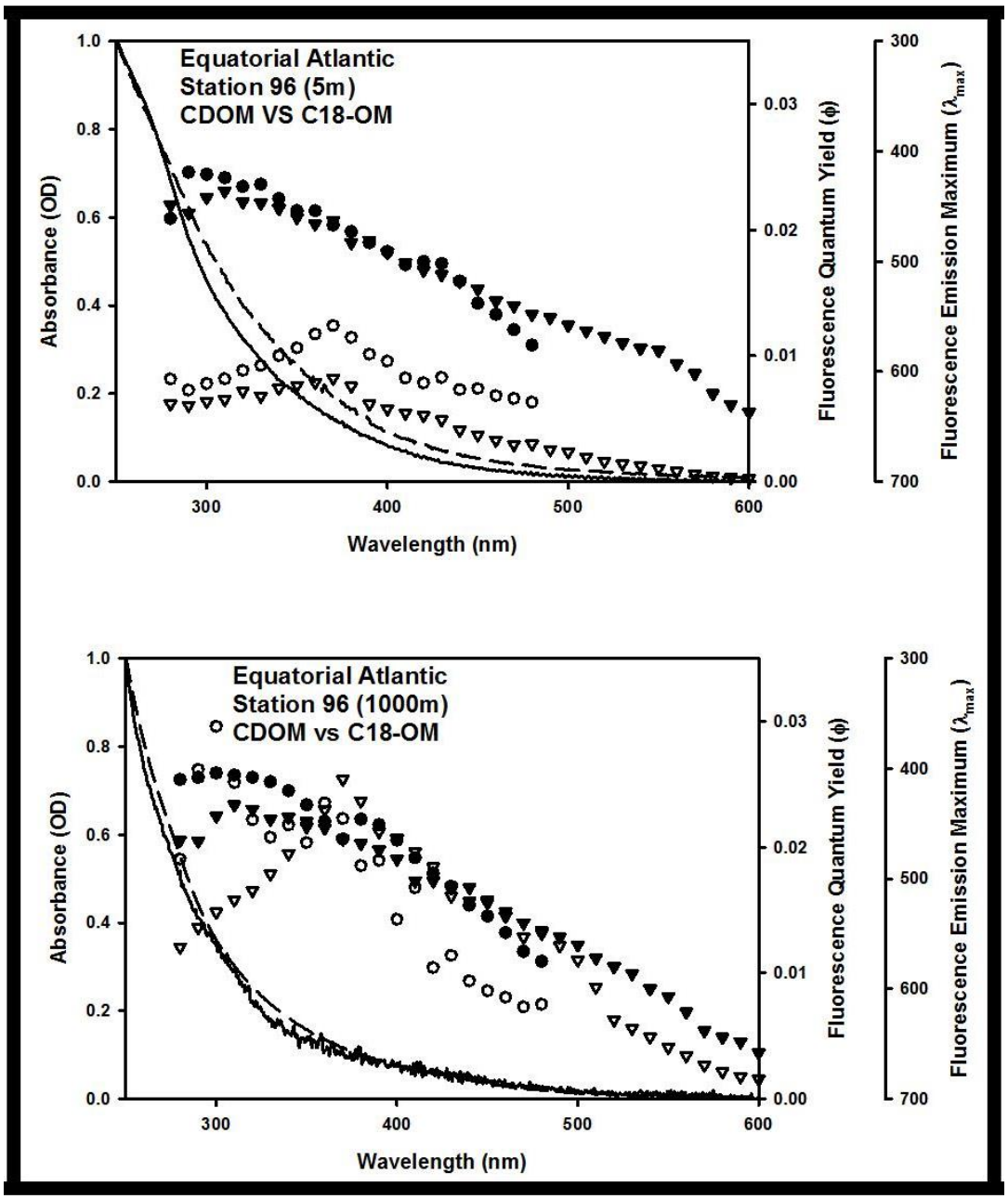

Figure 3 - 5: Comparison of CDOM and C18-OM optical properties for representative samples from EAO from a terrestrially influenced coastal margin, surface (top) and 1000 m (bottom). 10 cm absorbance normalized to 250 nm (lines); fluorescence emission maxima, λ_{max} (solid symbols) and fluorescence quantum yield (ϕ) (λ_{exc} 280-600 nm) (empty symbols).

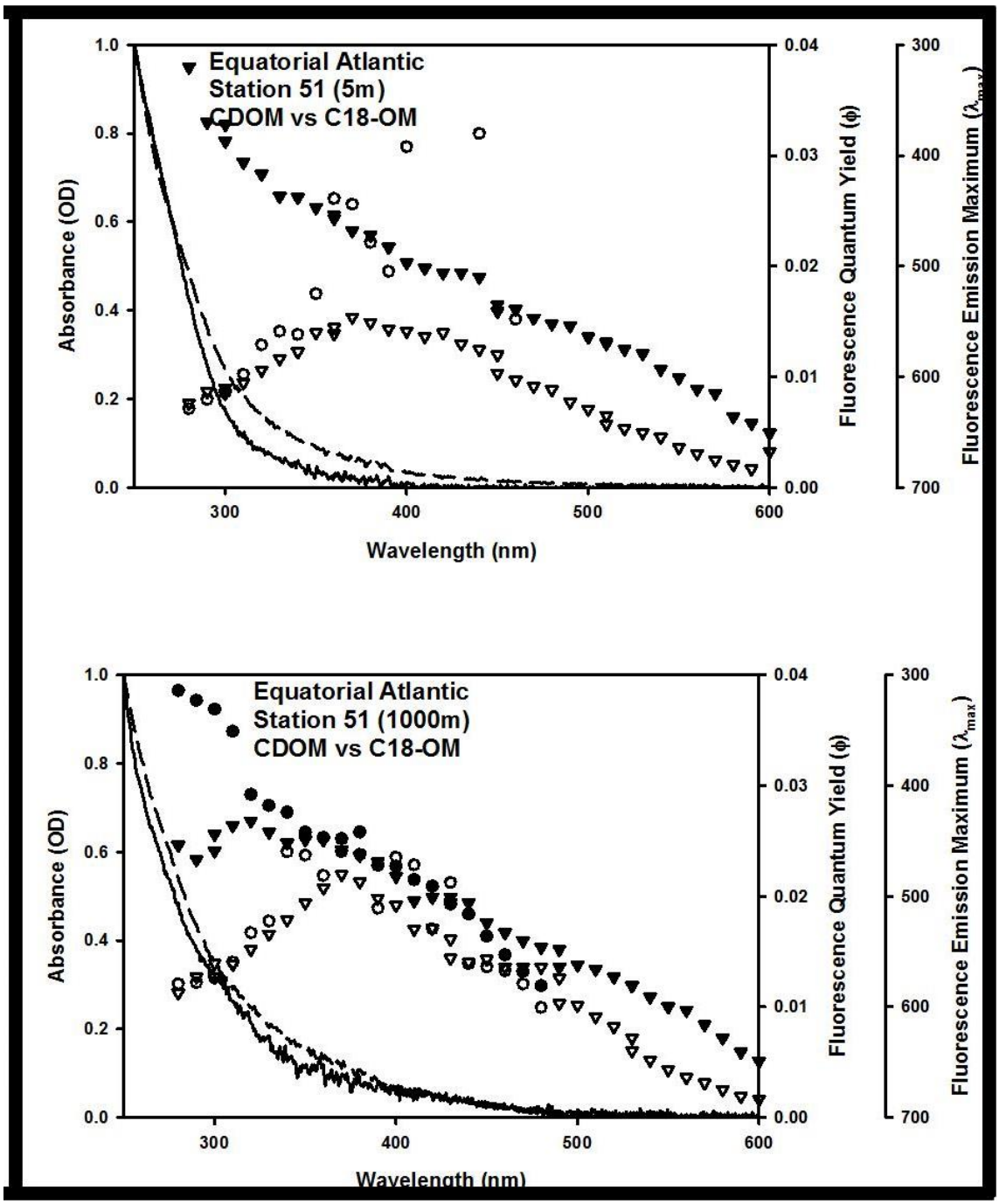

Figure 3 - 6: Comparison of CDOM and C18-OM optical properties for representative samples from the central EAO region. 10 cm absorbance normalized to 250 nm (lines); fluorescence emission maxima, λ_{max} (solid symbols) and fluorescence quantum yield (ϕ) (λ_{exc} 280-600 nm) (empty symbols).

It was also generally observed that C18-OM spectral slope values were smaller for inshore waters of the MAB (Table 3 - 1: compare August surface samples) and for deep waters of the EAO (Table 3 - 1: compare surface and deep EAO samples). This may be due to greater retention in relatively high CDOM waters (i.e. greater long wavelength absorption). CDOM undergoes transformations as it transits from the upper bay region out to the shelf and shelf break waters as a result of photobleaching or microbial degradation. Surface ocean waters are generally more highly photobleached (and oxidized) relative to deep waters. Photo-bleaching of CDOM (or other degradation processes) has been shown to result in an increase in S, due to the conversion of higher molecular weight species to lower molecular weight species (Nelson and Siegel, 2002). Boyle et al (2009) also concluded that S increases with lower molecular weight material, based on relative retention times obtained by gel permeation chromatography (GPC). These lower molecular weight species are generally expected to be relatively more polar and thus adsorb less strongly to the C18 resin, resulting in higher spectral slopes with degree of transformation and geographic locale. Therefore, increased long wavelength extraction efficiency of CDOM in the Delaware Bay and Bay mouth relative to the shelf, is attributed to the presence of higher molecular weight, more non polar organic material in these waters, which tend to adsorb more readily.

3.4.3 Fluorescence and quantum yield

The overall fluorescence emission for CDOM and C18-OM from the MAB and EAO exhibited very similar spectral dependencies, except in a few cases in the EAO (Chapter 2, Figure 2 - 6). Emission was broad and unstructured and emission maxima

continuously red-shifted with increasing excitation wavelength (λ_{exc} >~300 nm) (Figure 3 - 4, Figure 3 - 5 and Figure 3 - 6). Often emission maxima at short λ_{exc} <350nm was more red-shifted for C18-OM than for CDOM.

The wavelength dependence of apparent quantum yields for CDOM and C18-OM was very similar for coastal waters from the MAB and EAO samples (Figure 3 - 4, Figure 3 - 5 and Figure 3 - 6). QY values increased with increasing excitation wavelength up to ~370 m, and then decreased monotonically at longer excitation wavelengths. Interestingly, QY values for C18-OM relative to CDOM from the MAB were smaller only at λ_{exc} < 380 nm while they were more comparable at longer wavelengths. These results are fully consistent with the preferential retention and elution of the long-wavelength absorbing material and decrease in slope (S) of C18-OM. These results further indicate that the species excited at short wavelengths (<380 nm) were only partially extracted relative to those excited at longer wavelengths (>380 nm), and support the red-shift in the emission maxima. This difference diminished with increasing salinity and offshore distance (Figure 3 - 4, Figure 3 - 5 and Figure 3 - 6).

Apparent QY for CDOM and C18-OM from the EAO were comparable at λ_{exc} < ~370 nm. At longer wavelengths (~>370 nm), effective comparison of QY could not be made. This was due to very low absorption coefficients in some cases (close to detection limit) or very low (noisy) fluorescence emission for the CDOM samples resulting in large uncertainties.

C18 cartridges failed to extract discrete emission peaks observed in a few open ocean samples, as previously reported by Andrew (2013) (see Chapter 2, Figure 2 - 9). These discrete peaks were observed in the UV region (see Chapter 2, Figure 2 - 6, Figure 2 - 9) and exhibited very high efficiencies relative to the bulk CDOM (see Chapter 2, Figure 2 - 6), characteristics that were not observed in C18-OM. These observations suggest that these species are possibly different from that responsible for the long wavelength emission.

3.4.4 $NaBH_4$ Reduction

Reduction of both CDOM and C18-OM samples with $NaBH_4$ resulted in a significant loss in absorbance across the UV-visible wavelengths, with the largest fractional losses observed in the visible wavelength regime (Figure 3 - 7) consistent with past observations (Andrew et al., 2013; Golanoski et al., 2012; Ma et al., 2010; Sharpless and Blough, 2014; Tinnacher and Honeyman, 2007; Zhang et al., 2012). Absorption losses of ~50% were observed for CDOM in both the MAB and the EAO samples. However, much greater losses, as much as 80% over the longer wavelength visible regime, were reported for C18-OM due to the much higher absorbance values of C18-OM relative to CDOM. This supports the idea that C18 cartridges enrich the long wavelength material that is also more substantially affected by $NaBH_4$ reduction.

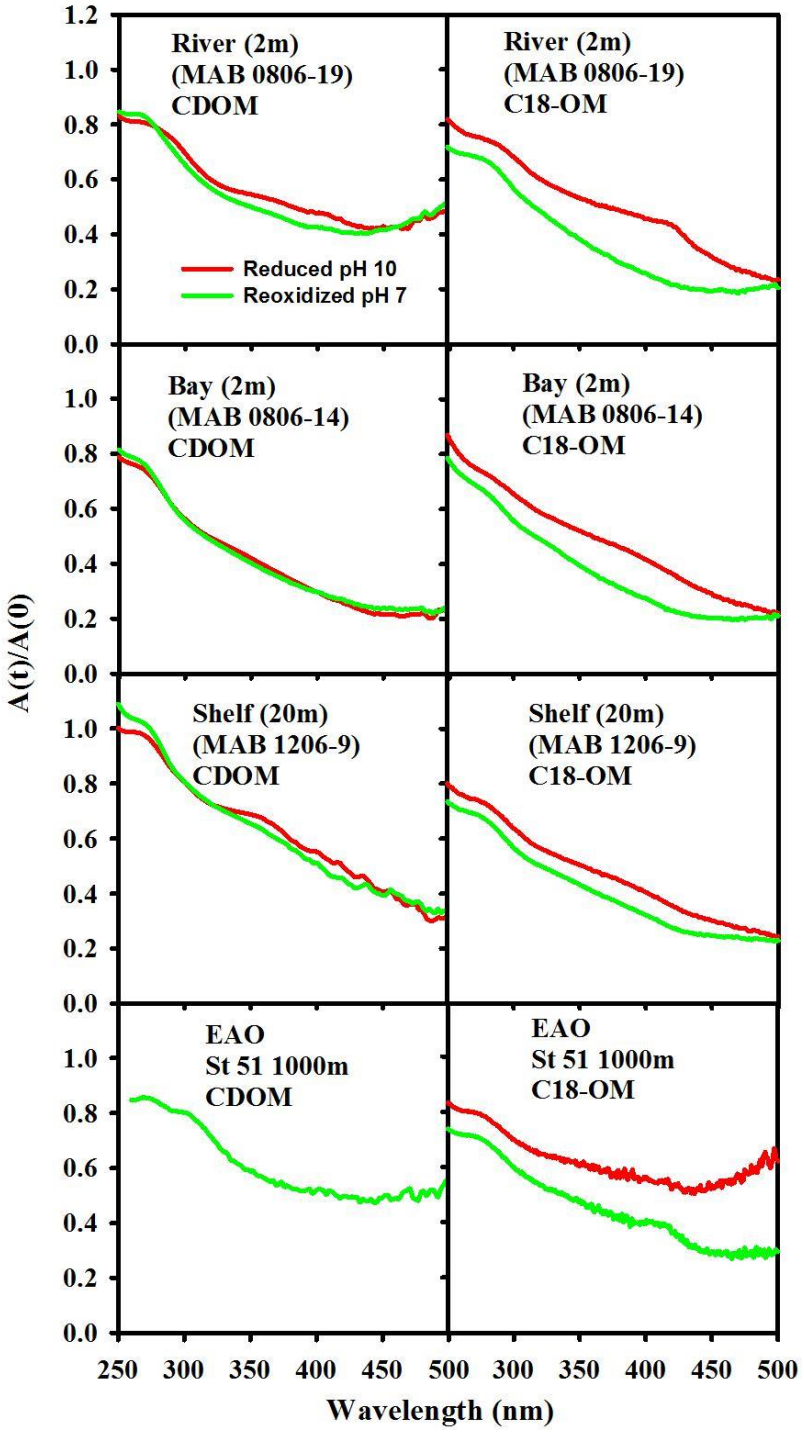

Figure 3 - 7: Wavelength dependence of fractional loss of absorbance following reduction (pH 7) of MAB CDOM and C18-OM samples from the river, mid bay, shelf and deep EAO (1000 m). The absorbance spectrum of the reduced sample (at pH 10 and pH 7) is divided by the original spectrum. Thus area below each spectra in the above plot represents fraction of absorbance remaining after reduction.

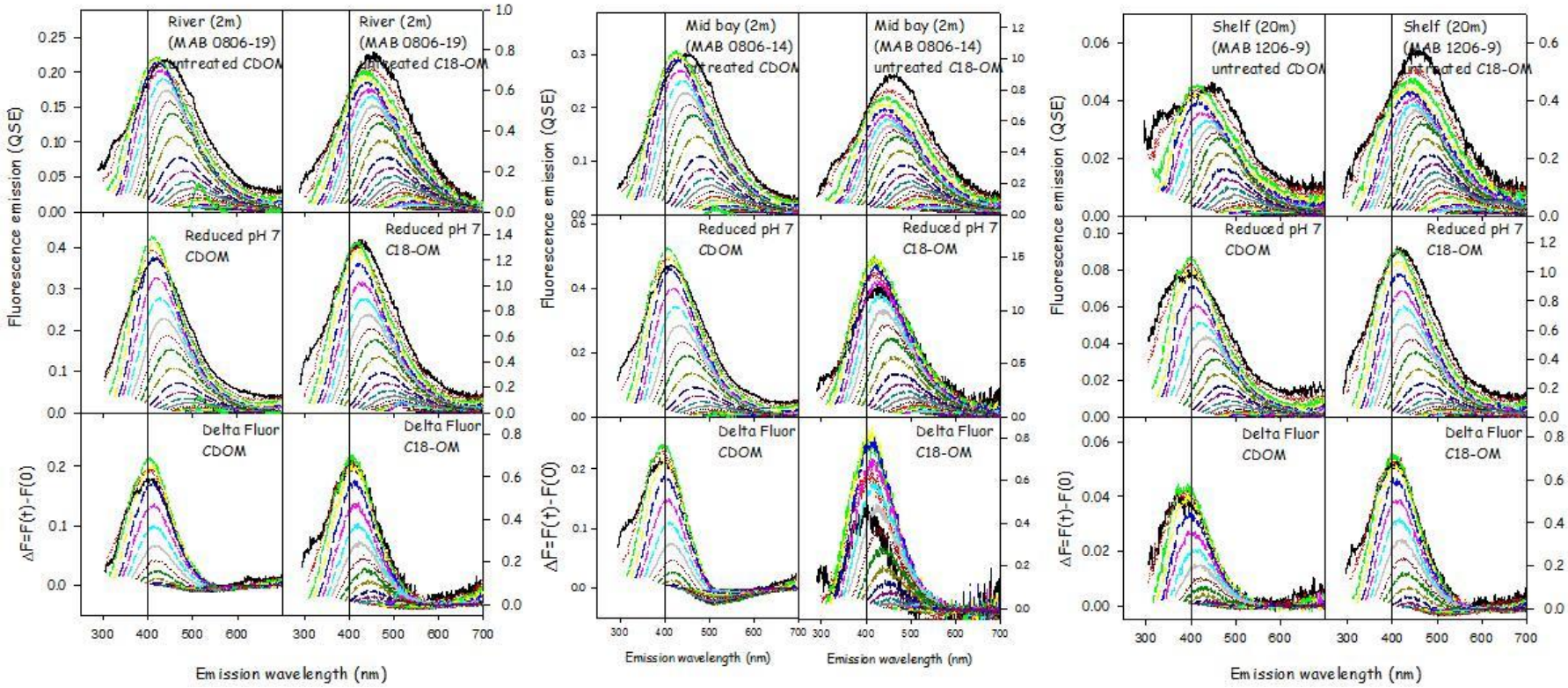

Figure 3 - 8: Comparison of changes in fluorescence emission for CDOM and corresponding C18-OM upon reduction with $NaBH_4$, for three MAB samples (river, mid bay and shelf). Original spectra (Top), Spectra of reduced sample at pH 7 (Middle) and difference spectra (bottom). Difference spectrum is calculated by subtracting the spectrum of the untreated sample from that of the reduced sample, therefore positive ΔF values represent an increase in emission.

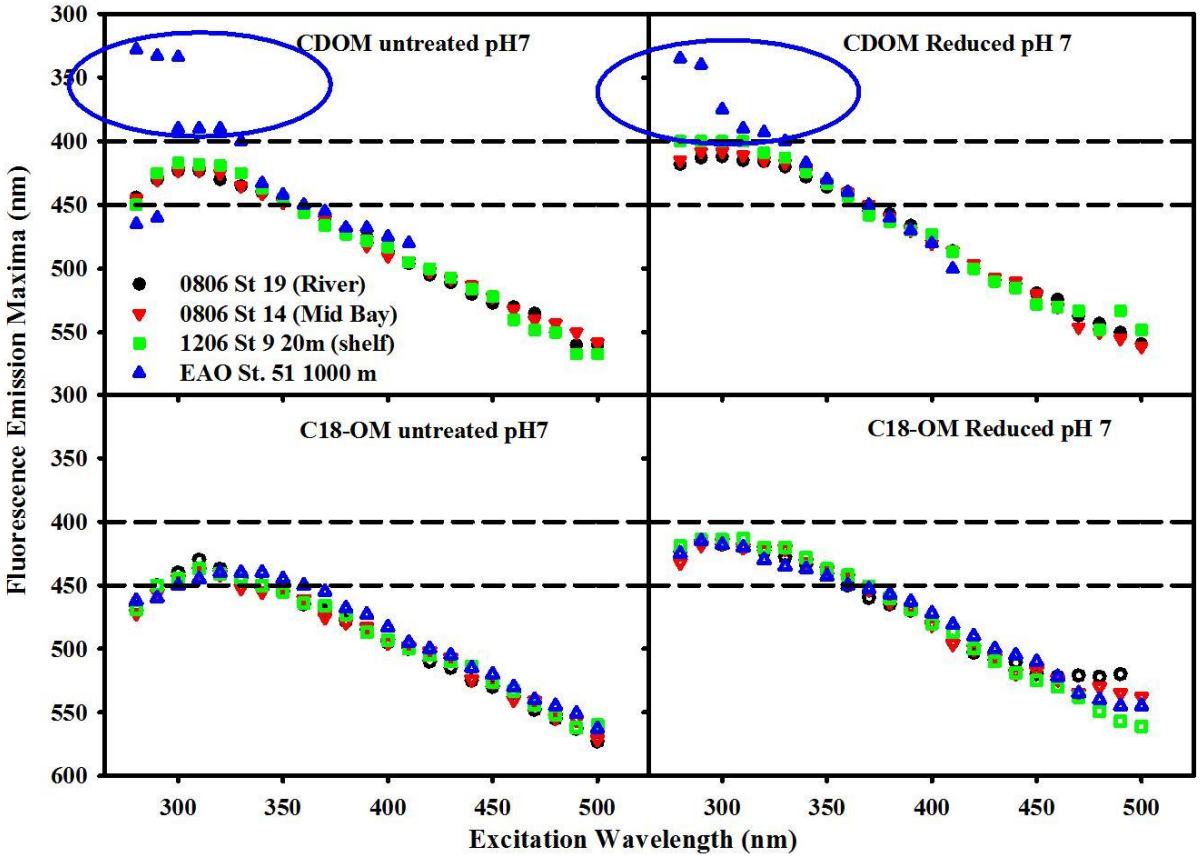

Figure 3 - 9: Wavelength dependence of fluorescence emission maxima for CDOM and C18-OM samples prior to and following $NaBH_4$ reduction. Area in the blue circle represents the emission maxima of a UV emitting species observed in the EAO CDOM sample.

Following reduction, fluorescence emission intensities increased by at least 2 fold, for both CDOM and C18-OM from the MAB and EAO, (MAB- Figure 3 - 8: $\Delta F>0$, EAO - Chapter 2 Figure 2 - 10 & Figure 2 - 11). Additionally, the emission maxima shifted to the blue by approximately 10-15 nm relative to the untreated samples (Figure 3 - 9), with a bigger shift observed for C18-OM. Interestingly, for the reduced samples, ΔF emission maxima was constant at λ_{exc} 300-330nm and red-shifted at longer λ_{exc}. This suggests that emission at λ_{exc} 300-330nm could possibly arise from a discrete fluorophore. Loss in emission intensity was observed for both CDOM and C18-OM at λ_{exc} > 410nm and > 430

nm, respectively (Figure 3 - 8 ΔF plots, Figure 3 - 10: values below the horizontal black line). These results are consistent with results previously reported by others (Ma et al., 2010; Sharpless, 2012). The wavelength dependence of fractional changes (gains and losses) in emission intensity before and after reduction were similar for both CDOM and C18-OM, although C18-OM experienced higher fractional changes (or percent) relative to CDOM (Figure 3 - 10), consistent with absorbance changes upon $NaBH_4$ reduction (Figure 3 - 7). This result could be due to the following factors: (1) Solid $NaBH_4$ was added to 30 ml CDOM sample (at low concentration, and neutral pH), thus resulting in kinetic competition between the loss of borohydride through proton reaction with water and reduction of carbonyl groups within the CDOM samples, 2) C18-OM is enriched in high molecular weight material (lower S, more visible absorption), thus greater fluorescence emission for the untreated samples at longer wavelengths, resulting in a greater blue-shift in emission maxima and emission intensity following reduction.

The fluorescence quantum yields (QY) for CDOM and C18-OM in the MAB and EAO was substantially enhanced (Figure 3 - 11) following reduction, particularly at λ_{exc} ~350 to 390 nm. In previous work done by Ma (2010), this enhancement in QY was attributed to two factors: (1) the increase in fluorescence emission at λ_{exc} less than ~450 nm, and (2) the significant decrease in absorption over these same wavelengths (Figure 3 - 10 and Figure 3 - 7 respectively).

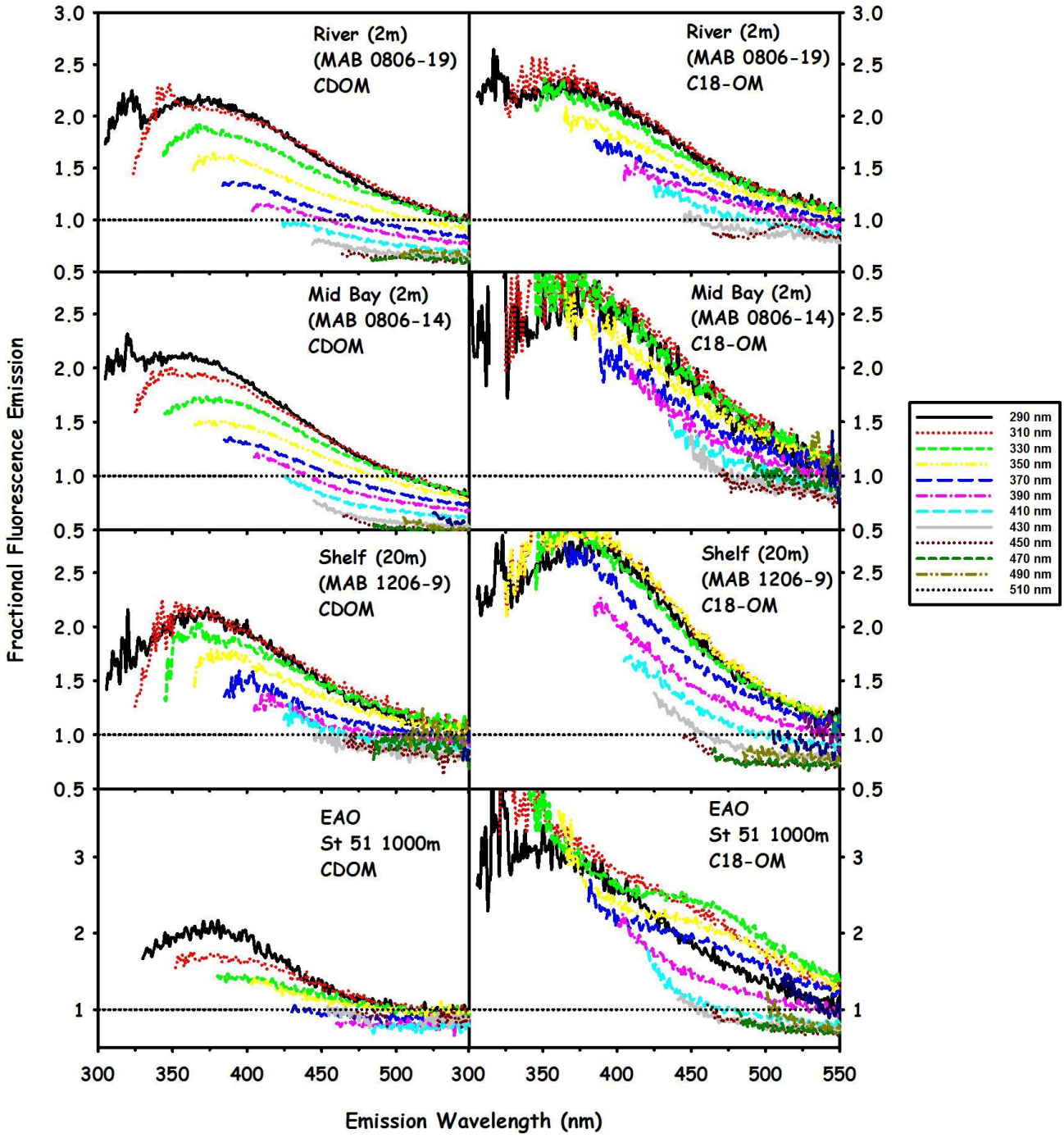

Figure 3 - 10: Fractional emission spectra for 4 CDOM samples and their corresponding C18-OM: MAB river, mid bay and shelf and EAO 1000 m sample at station 51. Fractional spectra were obtained by dividing the spectra of the reduced sample by that of the original sample. Fraction greater that 1 (horizontal black dotted line) signifies an increase in fluorescence after reduction. Spectra are presented for excitation wavelengths every 20 nm starting with λ_{exc} 290 nm.

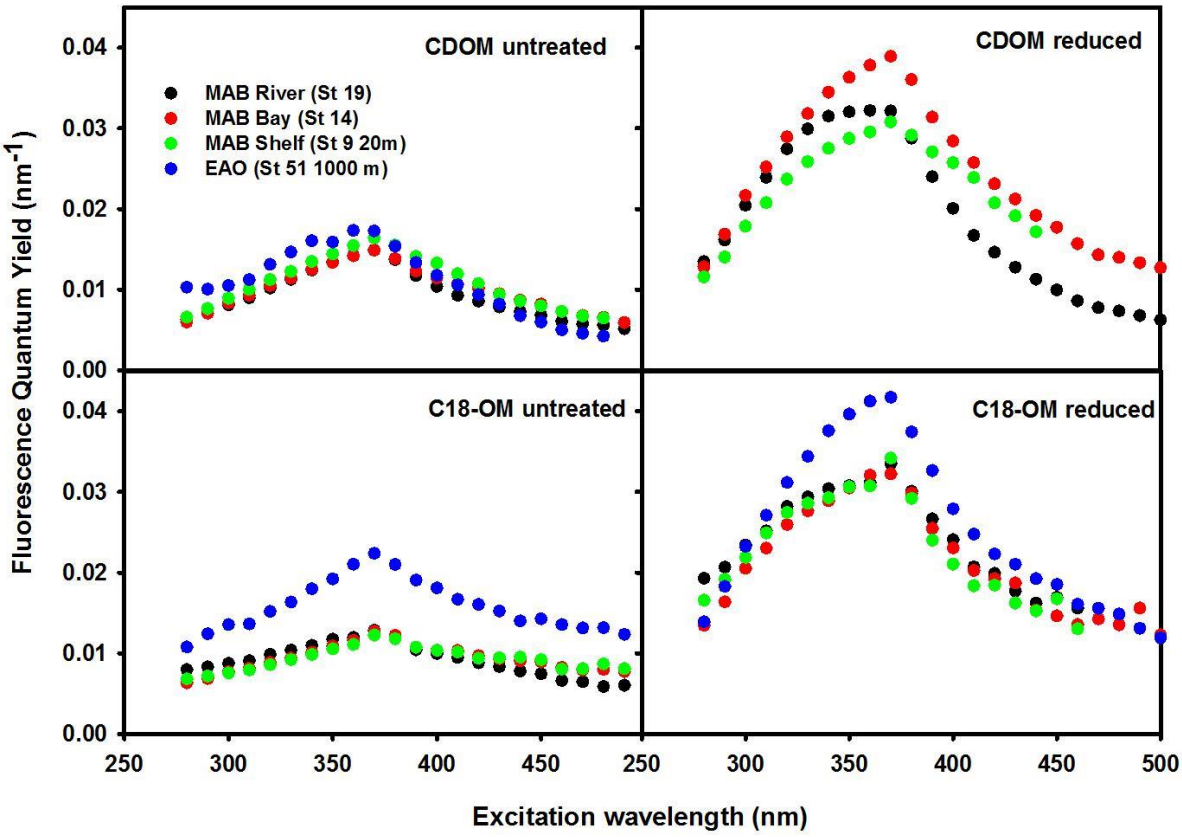

Figure 3 - 11: Wavelength dependence of fluorescence quantum yields for CDOM and C18-OM samples prior to and following $NaBH_4$ reduction.

3.5 Summary and conclusion

The results from this work provide evidence that the optical properties of C18-OM and the corresponding CDOM sample are very similar overall. The extraction efficiency (and spectral dependence of elution) as monitored by absorption, was enhanced at longer visible wavelengths for high CDOM waters, and decreased for CDOM from open ocean waters. This difference was attributed to decreasing molecular size of the organic material as a result of degradation (becoming relatively more polar), leading to a lesser degree of adsorption on the C18 column. The wavelength dependence of C18 extraction and elution were comparable, suggesting that no biasing occurs during elution of the

adsorbed organic material. Overall the wavelength dependence of absorbance, fluorescence emission and fluorescence quantum yields for CDOM and C18-OM were remarkably similar.

The results from the $NaBH_4$ reduction provide evidence that preferential enrichment of long wavelength absorbing material did not affect the chemical properties of CDOM and C18-OM. Following reduction, CDOM and C18-OM from both regions, exhibited very similar changes in optical properties. CDOM and C18-OM exhibited preferential loss of absorption in the visible, enhanced blue shifted emission, and increased apparent fluorescence quantum yields on the blue edge of the emission. Overall, the results from this study indicate that enrichment of CDOM by SPE using C18 cartridges does not substantially alter the chemical composition responsible for the optical properties of CDOM, thus C18-OM are representative of CDOM.

Chapter 4: Storage effect on the optical properties of CDOM

4.1 Introduction

The optical properties of chromophoric dissolved organic matter (CDOM) (and humic substances, HS) have been intensively studied during the last several decades (Blough and Del Vecchio, 2002; Boyle et al., 2009; Coble, 2007; Ma et al., 2010; Nelson and Siegel, 2002) and has become an important area of current oceanographic research (Nelson and Siegel, 2013). Over the years, significant progress has been made in terms of CDOM sampling and treatments, as well as development of sophisticated analytical techniques (Wurl, 2009b). These improvements have resulted in much needed insight into CDOM distribution (Nelson and Siegel, 2013), optical and chemical characterization (Coble, 2007; Nelson and Siegel, 2002), and identification of source markers (Kujawinski et al., 2009; Stenson et al., 2003) which can provide information regarding not only CDOM source but also structure. This increased knowledge has been particularly important for the characterization of marine CDOM, which has been less studied than terrestrial CDOM (Nelson and Siegel, 2002). An important factor underlying these successes (apart from the development of clean sampling, non-contaminating treatment techniques for seawater, and the development of improved analytical techniques) is the improved proper storage of CDOM samples over long periods of time. Storage practices influence sample integrity over the time period required for the successful completion of studies. This time frame may span weeks to months or even years, and therefore may affect the validity of data acquired during analysis, hence the importance of monitoring temporal stability or degradation.

Storage of CDOM samples may be inevitable for many reasons, although the ideal practice would be to measure in situ or on the research vessel at the time of collection (Nelson and Coble, 2009; Wurl, 2009b). However, there are many situations which may result in delayed measurement and analysis of CDOM samples including space constraints on the ship, breakdown of instruments, absence of clean labs, shortage of personnel and appropriate instrumentation and unfavorable conditions at sea, to mention a few. Further, researchers may simply want CDOM samples for future measurements or additional experiments which necessitate some degree of sample storage.

While protocols for CDOM sample collection and storage are very well defined and a common practice in oceanographic work, the effect of storage is less known, and there is little consensus regarding appropriate maximum storage times (Wurl, 2009a). Little or no work has been done to systematically examine the possible effects of storage practices on the optical properties of CDOM.

Green and Blough (1994) reported that values of a(300) for CDOM (southern and western coast of Florida and eastern Gulf of Mexico) measured in the lab were within 5% of those measured at sea after transport to the lab, but did not mention the length of storage. Nelson and Coble (2009) outlined many cases where little to no changes were observed in optics of CDOM samples from diverse areas stored for various short term periods from weeks to a year either refrigerated or frozen. They identified one instance where open ocean 0.2 um filtered CDOM samples from the Equatorial Pacific stored at 4°C showed no measurable change in absorbance over 1 year. Hoge et al. (1993)

observed no measureable storage effects on absorbance of CDOM samples stored for 23 days. Stedmon & Markager (2001) reported little to no changes in absorption spectra of samples from the Greenland Sea measured approximately 1 month from date of sampling. They also noted that upon reanalysis after 7 months, absorption spectra still showed no significant changes at 375 nm, but a slight decrease in S by ~7% of the mean. Previous work done on marine CDOM samples from the Equatorial Atlantic Ocean (Andrew et al., 2013) found no appreciable changes (<10%) in fluorescence or absorbance of samples repeatedly measured over a two year period.

In this work we systematically examined the effect of storage on the optical properties of CDOM samples from the Middle Atlantic Bight (MAB) stored for approximately 6 years. In this comprehensive study, absorption, fluorescence and DOC measurements for the CDOM samples were compared with measurements acquired in 2006 within two weeks or less from the time of sample collection. To our knowledge such an investigation over a similarly long time scale has not been conducted.

4.2 Material and Procedures

4.2.1 Samples

Water samples were originally collected in 2006 from the Mid Atlantic Bight (MAB) during several cruises onboard the R/V Cape Henlopen or R/V Cape Hugh Sharp from August to December (August 24-28; October 12-20; and November 30-December 4, 2006). August and October transects extended from the Delaware River (~ 40 N; -75W)

to the western boundary of the Gulf Stream (~ 36N; -72W), while December transect only extended as far as shelf break (~ 36N; -74W) (Figure 4 - 1). Of the total number of stations sampled (125 stations) on the various cruises, samples from 81 stations (65% of total) were selected for this study. Stations were selected along the complete transect to ensure true representation of the entire geographical area and seasons originally sampled. These 81 stations resulted in a total sample set of 95 samples, consisting of 81 surface (2 m) samples and 14 samples from lower depths (26-200 m). Samples were collected employing a CTD (conductivity–temperature–depth) rosette equipped with Niskin bottles (deep samples and some surface) or from the vessel's surface water pumping system (some surface samples) (Del Vecchio and Blough, 2004b). For simplicity, surface samples are referred to by only the station number, while the corresponding depth of samples below the surface are specifically mentioned when discussed.

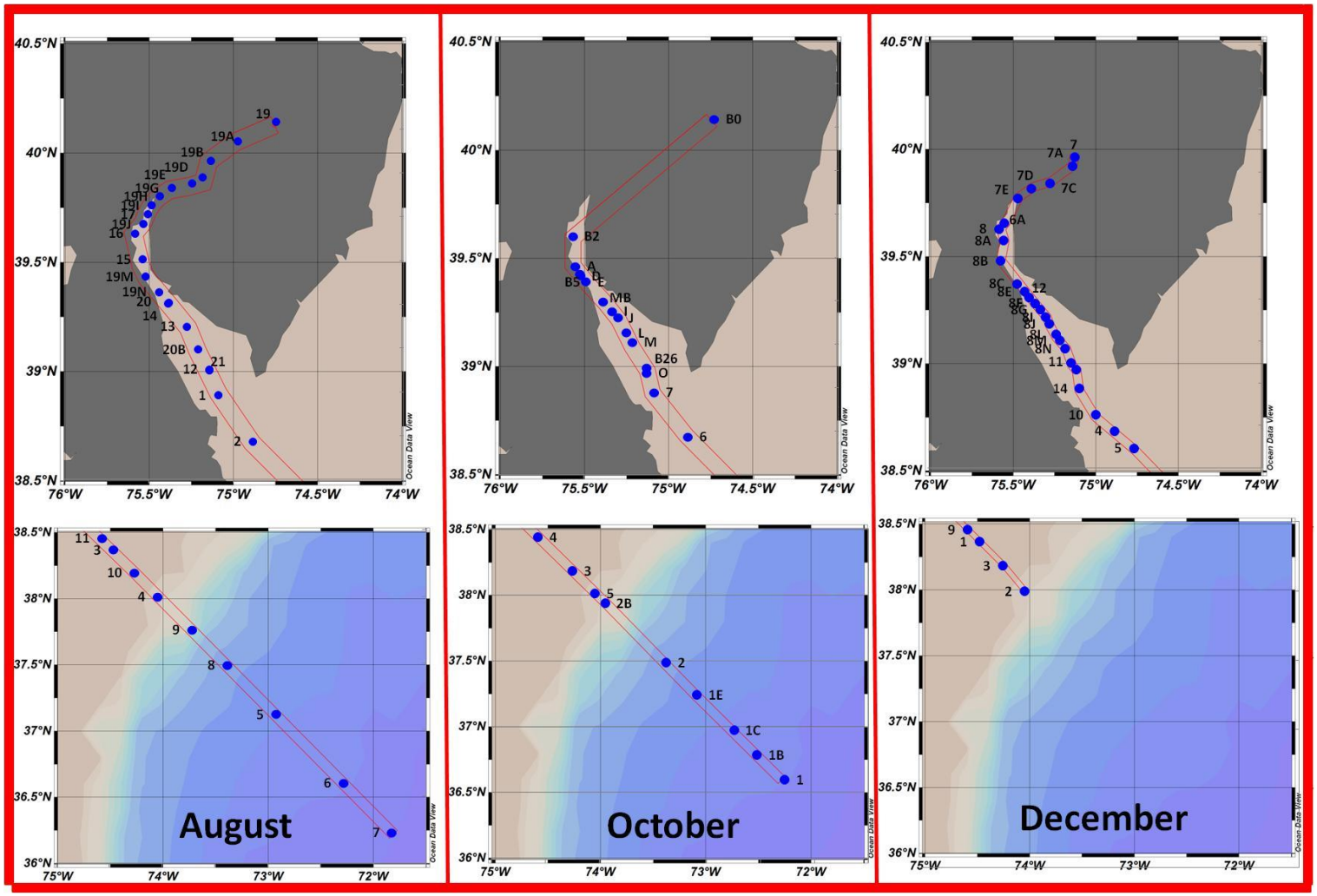

Figure 4 - 1: Map of MAB showing sampling locations in August, October and December. Inshore stations (Top panel), offshore stations (bottom panel) Inshore : 76.0°W - 74.5°W , 38.5°N - 40.5°N, offshore: 75.0°W - 72.5°W, 36.0°N - 38.5°N.

Immediately after sampling, whole water samples were filtered under low pressure, using GF/F filters (0.7-µm pore size). Acid washed bottles were rinsed (at least 3 times) with the sample before filling for storage, covered with parafilm and capped with teflon lined caps. Samples were then stored in the dark at 4 ºC to inhibit microbial growth and avoid exposure to light.

Prior to initial measurements (within 2 weeks from collection in 2006), samples were re-filtered through 0.2-µm pore-size nylon syringe filters to ensure removal of all particles, and absorbance, fluorescence, and DOC measurements were acquired as described below. Over the 6 year period, samples were stored undisturbed at 4ºC in the dark. Prior to measurements in 2013, samples were re-filtered using fully cleaned 0.2 µm polyethersulfone (PES) or nylon filters obtained from VWR (~120ml of Milli-Q water was passed through filter).

4.2.2 Measurements

Absorption spectra were acquired prior to, and following, 0.2µm filtration, with a Shimadzu 2401-PC spectrophotometer employing a 10 cm optical cell using purified Milli-Q water as the blank. The absorption spectra were recorded over the range 200–800 nm. Absorption coefficients ($a_{CDOM}(\lambda)$) were calculated using the equation $a_{CDOM}(\lambda) = 2.303 \times \frac{A_{CDOM}(\lambda)}{L}$, where $A_{CDOM}(\lambda)$ is the absorbance at wavelength λ, over path length L.

Standard deviation (σ) in absorbance measurements were obtained in two ways using a Delaware Bay CDOM sample as a standard (Figure 4 - 2). In the first method, 16 replicate absorbance spectra of the Delaware sample were acquired over the course of 3 days, with a blank (Milli-q water) taken after every replicate. In the second method, 20 replicates were acquired over a span of two days with blank measurements taken after every 4-5 replicates. The σ (λ) values obtained from the first method were lower that of the second, and were chosen for our analysis.

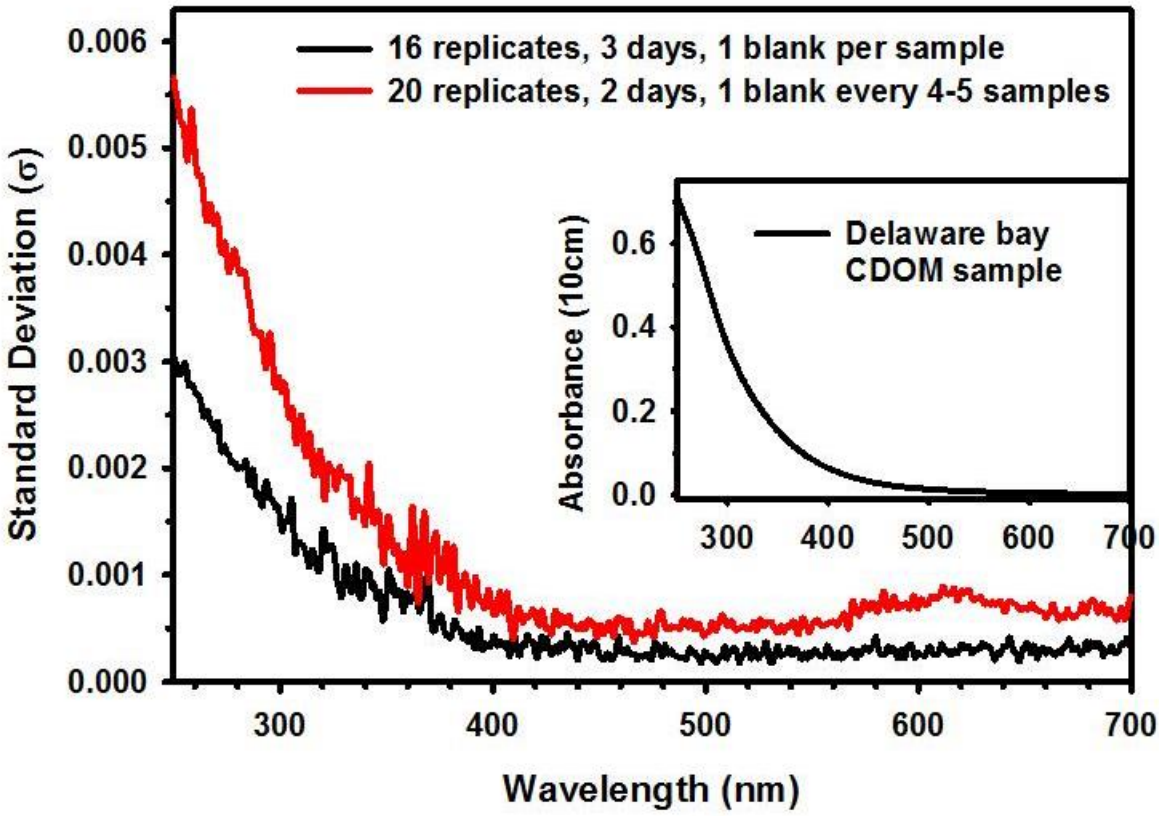

Figure 4 - 2: Wavelength dependence of the standard deviation (σ (λ)) in absorbance values obtained using a 10 cm cell. Values acquired using a CDOM sample from the Delaware bay (obtained in October 2011, 39°N, 75°W, 16.35 ppt salinity). Inset - absorbance spectrum of the CDOM sample)

Change in absorbance values (ΔA (λ)) over the six year period, (relative to 2006) was calculated for each sample over the entire UV visible regime using the equation $\Delta A(\lambda) = A(\lambda)_{2013} - A(\lambda)_{2006}$. Negative $\Delta A(\lambda)$ values indicate a loss in absorbance, while positive $\Delta A(\lambda)$ values indicate a gain in absorbance. The $\Delta A(\lambda)$ values were then divided by σ (λ) across all wavelengths ($\frac{\Delta A(\lambda)}{\sigma(\lambda)} = \Delta A^*(\lambda)$). If the resulting $\Delta A^*(\lambda)$ values were ≥ 5, then the change in absorbance over time was considered statistically significant. Percentage change in absorbance ($\%\Delta A(\lambda)$) relative to 2006 measurements was therefore calculated for $\Delta A^*(\lambda) \geq 5$ using the equation ($\%\Delta A(\lambda) = \frac{\Delta A(\lambda)}{A(\lambda)_{2006}} \times 100$.

CDOM fluorescence measurements were acquired with an Aminco–Bowman AB2 luminescence spectrometer using a 4 nm band pass for both the excitation and emission monochromator, employing a 1-cm optical cell and Milli-Q water as blank. The spectra were corrected for the instrument response using factors supplied by the manufacturer. Emission spectra were acquired over the range 365 - 700 nm at $\lambda_{exc}(355)$. Fluorescence emission values are reported relative to the integrated emission (over the range 365-690 nm) of 1 ppb quinine sulfate in 0.1 N H_2SO_4, at excitation wavelength 355 nm (thus in quinine sulfate equivalents (QSE).

Dissolved organic carbon (DOC) concentrations were obtained by high temperature catalytic oxidation and infrared detection of produced CO_2 with a Shimadzu 5000A TOC Analyzer equipped with an ASI 5000A auto-sampler as described by Del Vecchio & Blough (2004b). Each sample was injected three times, and the average was reported

as the DOC value. A maximum of five injections were executed if the coefficient of variation was greater than 3%. Potassium hydrogen phthalate (KHP) was used as the carbon standard to generate a calibration curve. To check instrument reproducibility, DOC measurements for Milli Q water and a 1mg/L KHP sample were acquired for every four CDOM samples.

4.3 Results

4.3.1 Optical properties: Absorbance

Prior to re-analysis in 2013, samples were filtered through 0.2 um filters. Absorption spectra before and after filtration overlapped over the entire wavelength range for all samples across all seasons, and were indistinguishable within the uncertainty of the absorption measurements (Figure 4 - 3).

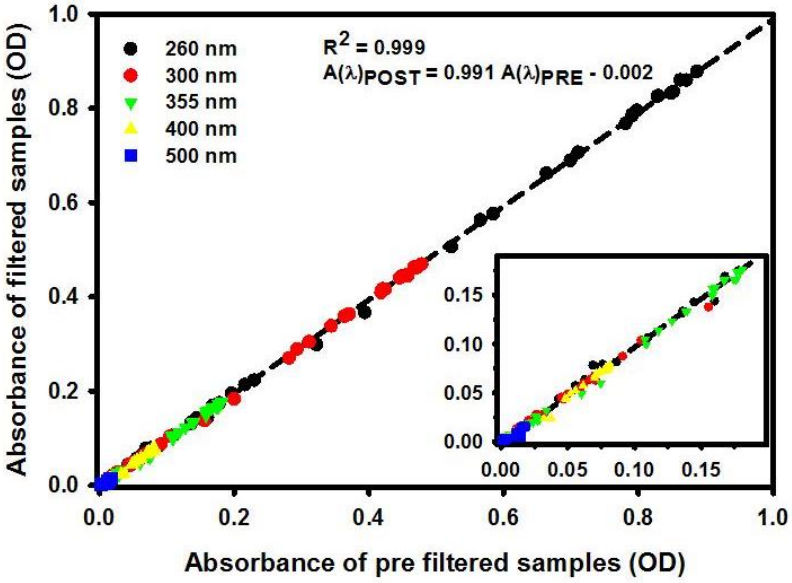

Figure 4 - 3: Comparison of absorbance values for samples prior to and after filtration at wavelengths 260, 300, 355, 400 and 500 nm

Absorption values at several wavelengths (260, 300, 355, 400 and 500 nm) showed a significant one-to-one correlation, with average slope and R^2 values of 0.991 ± 0.002 and 0.999 respectively (Figure 4 - 3). Since no change in the absorption spectra was observed upon filtration, filtered samples were used for all other measurements, calculations and comparisons.

Summary of absorbance results			
Description		Number of samples	% of total
UV (200 - 400 nm)	Vis (400 - 700 nm)		
no change*	no change*	56	58%
increase	no change*	6	6%
decrease	decrease	27	28%
new peak, 350-370 nm	no change*	6	6%
no change* : $\Delta A^*(\lambda) < 5$ OR $\Delta A^*(\lambda)$ ~constant OR $\Delta A^*(\lambda) \geq 5$ BUT $\%\Delta A(\lambda) < 15\%$			

Table 4 - 1 Summary of results from absorbance spectra comparisons

Absorbance values over the ultraviolet and visible wavelength regime for more than half of the samples studied (56 samples) showed no significant changes (Table 4 - 1). The ΔA^* values for these samples were within 5 or remained relatively constant across all wavelengths, or $\%\Delta A$ was < 15% relative to the absorbance values obtained in 2006 (Figure 4 - 4 and Figure 4 - 5). An additional 6% of samples (6 samples) also exhibited no change in absorbance in visible regime, but did experienced a 15-30% increase ($\%\Delta A$) in absorbance at short wavelengths (Figure 4 - 6). Less than a third of the samples studied (27 samples), exhibited a decreased in absorbance over the UV and visible regime relative to values in 2006 (Figure 4 - 7). For these samples, absorbance loss in the UV

was at most 30%, while in a few cases losses up to ~40% was recorded at longer wavelengths (Figure 4 - 8).

A new distinct peak at ~350 - 370 nm was observed for a few samples (6 samples, 6% of total) (Figure 4 - 9). These samples were collected during the summer, August 2006, in the shelf break and offshore waters. This observation cannot be attributed to filtration, as it was present before and after filtration. Also, these features were neither depth nor location specific as they appeared in both surface and deep samples in August but not in October 2006. Sampling stations for December did not extend to these offshore waters.

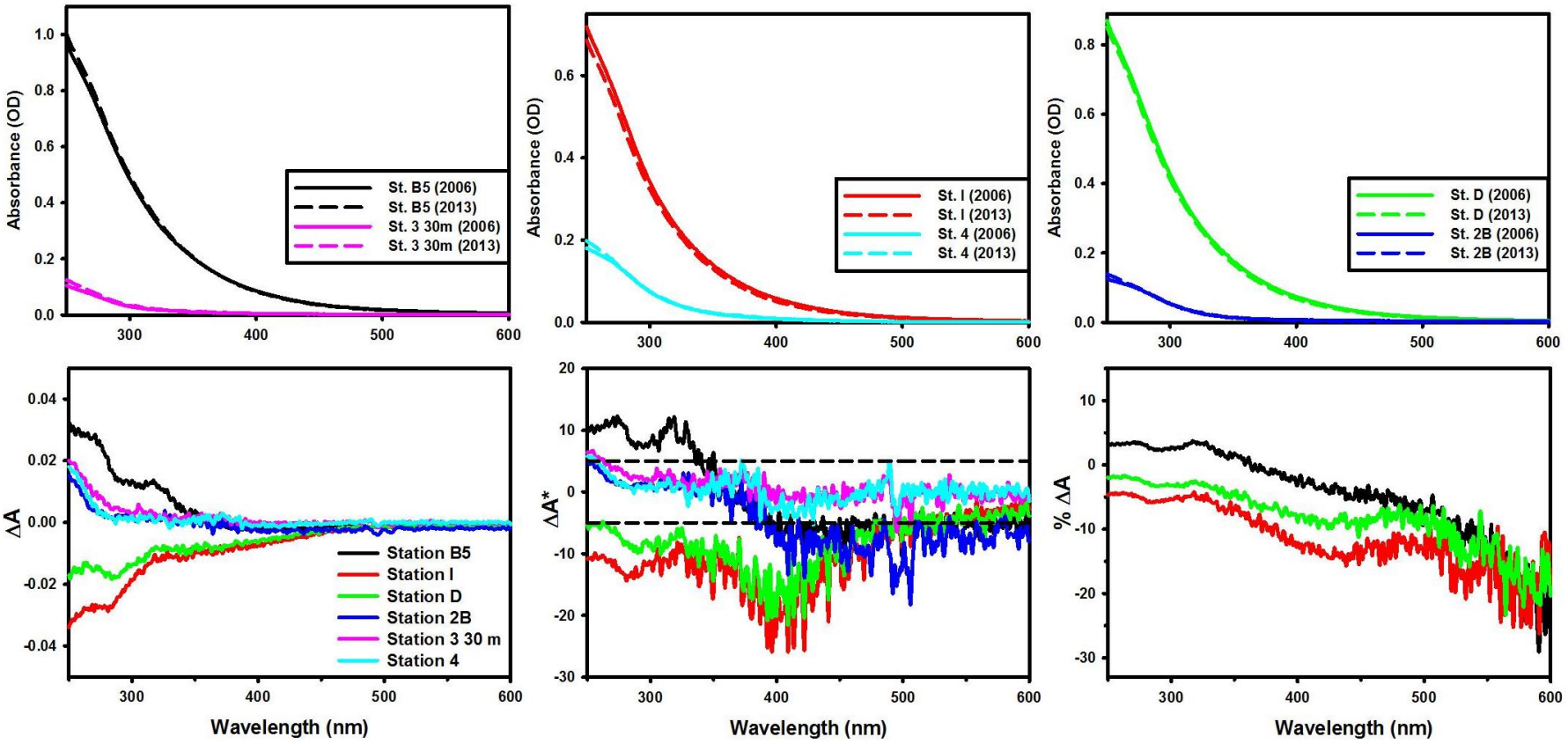

Figure 4 - 4: Select MAB samples from October 2006 showing no change in absorbance across the UV and visible regime. Top panel - comparison of absorbance spectra (10 cm), dashed lines - 2013, solid lines - 2006; Bottom panel - Plot of ΔA, Plot of ΔA* , showing ΔA*= 5 (dashed lines) and Plot of % ΔA for wavelengths where ΔA* >5, respectively. Similar plot for samples from August and December, AP5 & AP4, respectively)

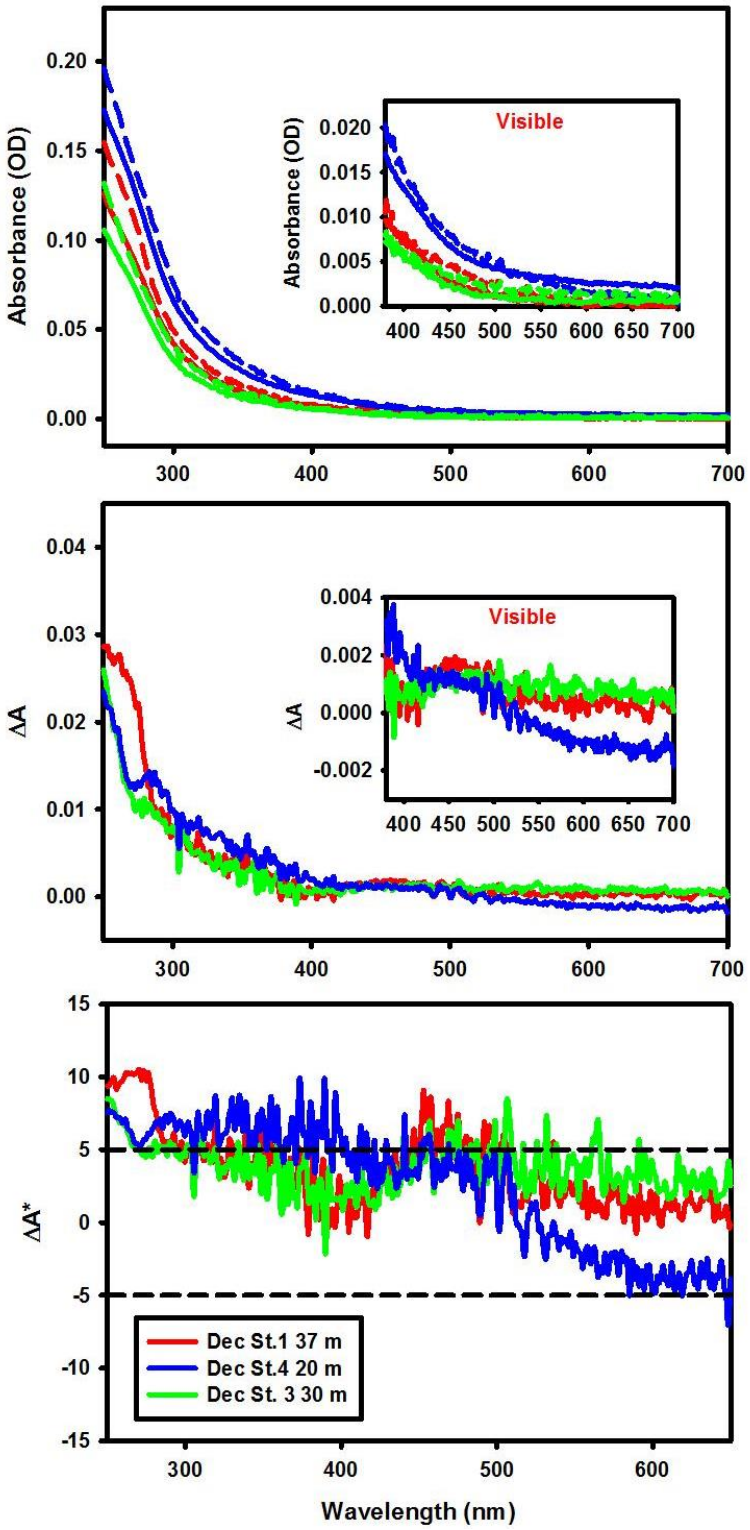

Figure 4 - 5: Comparison of absorbance spectra for select samples (December), dashed lines - 2013, solid lines - 2006. These samples displayed a relatively constant ΔA* across the UV and visible regime, indicative of a baseline offset between the two spectra.

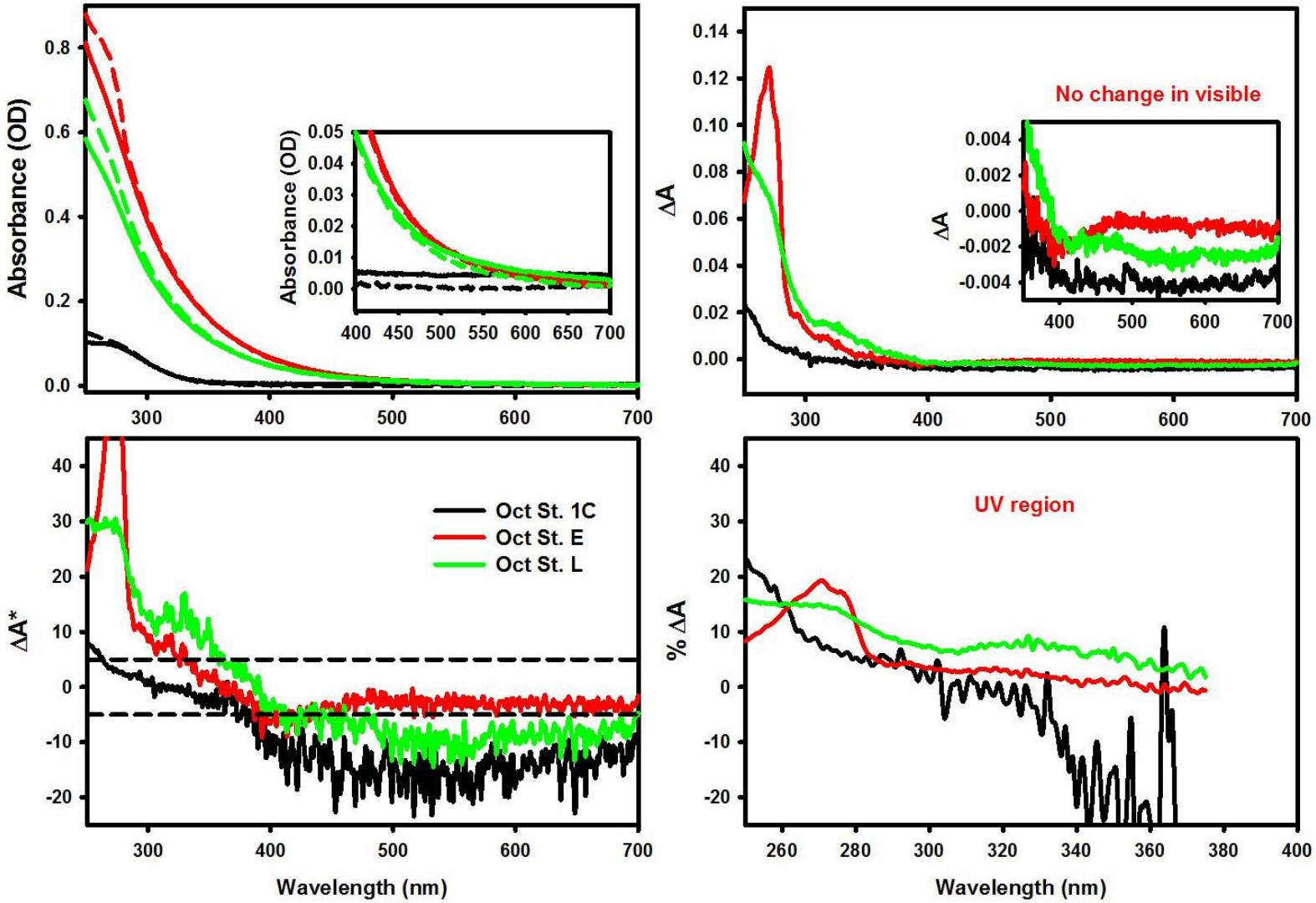

Figure 4 - 6: Small changes in UV absorbance exhibited by some samples. (A) Plot of ΔA over the UV and visible region, dashed lines represent 2013 values and solid lines represent 2006 values (B) Plot of ΔA* over the UV region and (C) Plot of %ΔA over the UV region

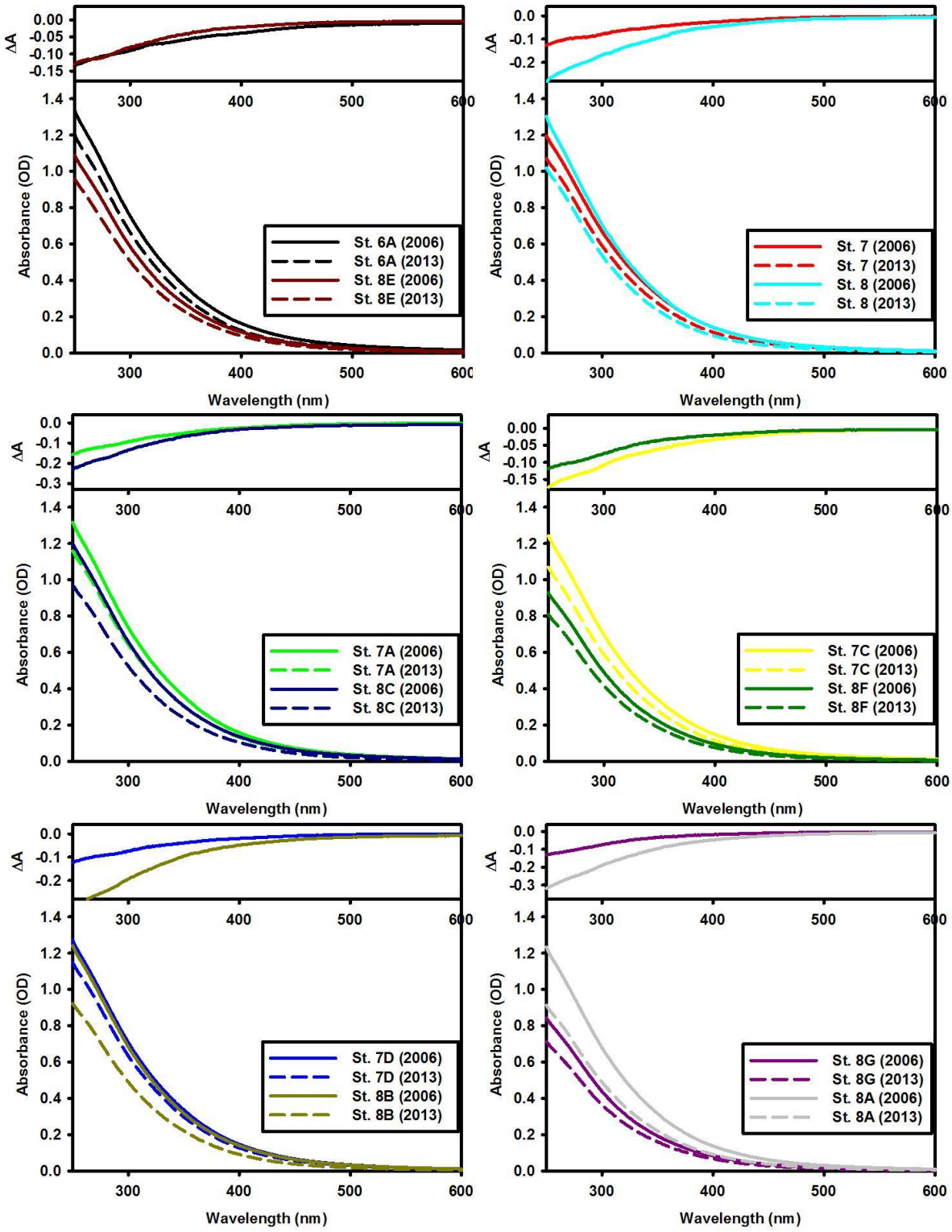

Figure 4 - 7: Absorbance spectra comparison and change in absorbance (ΔA) for select samples showing a decrease in absorbance (December season), dashed lines represent 2013 values and solid lines represent 2006 values.

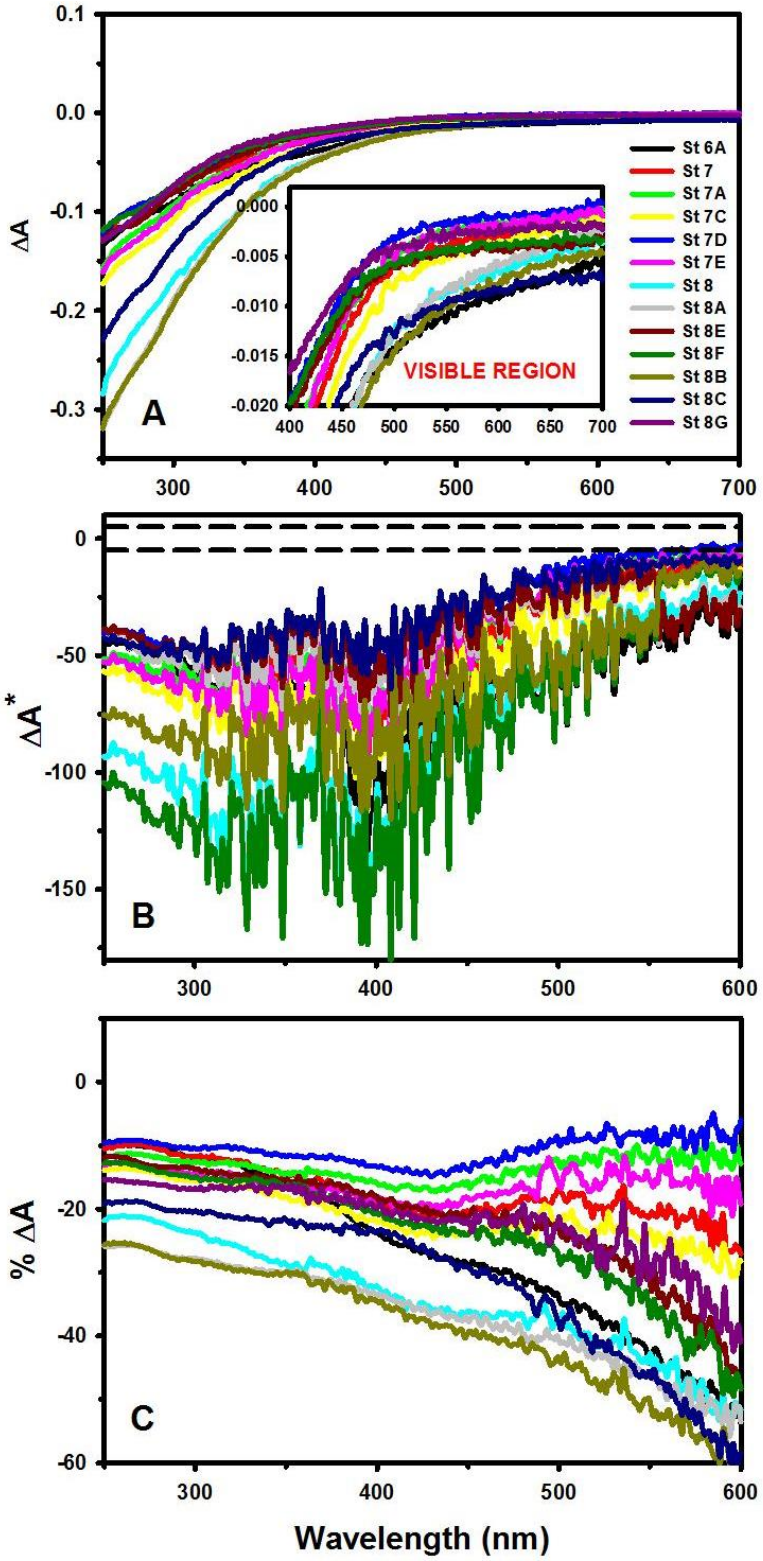

Figure 4 - 8: Decrease in UV and visible absorbance exhibited by some samples (December 2006). (A) Plot of ΔA, (B) Plot of ΔA* with dashed lines showing ΔA* >5 and (C) Plot of %ΔA across the UV and visible regime for ΔA* > 5.

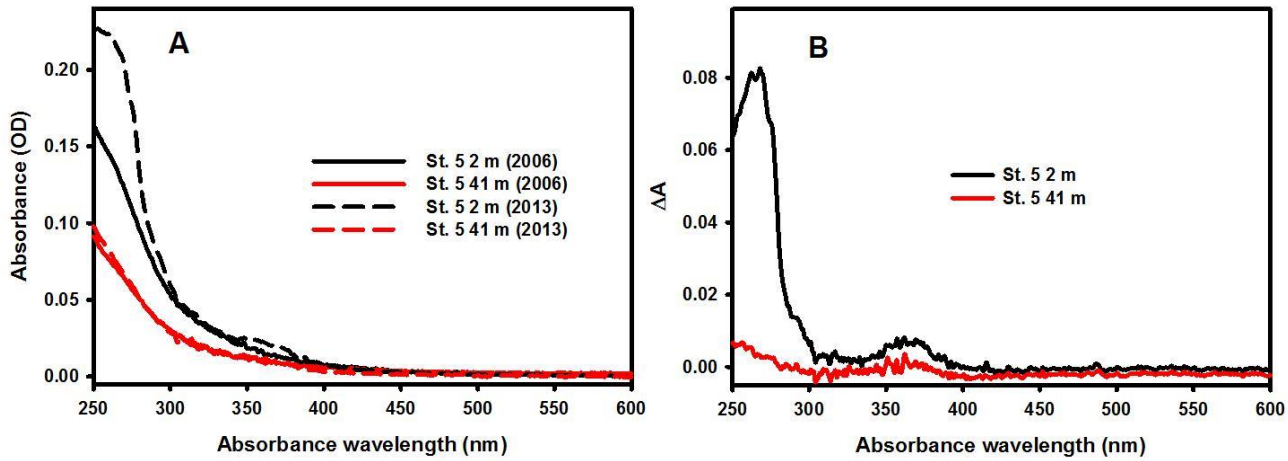

Figure 4 - 9: Plot A: New peak observed at ~350 - 370 nm for two samples in the summer season. Plot B: Delta absorbance (ΔA) more clearly depicting new peak. (August 2006, Station 5, 2 m and 41 m)

4.3.2 Fluorescence Emission

Fluorescence emission spectra were broad and unstructured with maximum in the range ~ 440 - 460 nm as previously shown for CDOM from many different geographical locales (Blough and Del Vecchio, 2002), with no new peaks observed (Figure 4 - 10). Emission intensity for more than two thirds of the samples studied (68.0%) remained within 10% of values obtained in 2006 (Table 4 - 2). However, emission maxima and spectral shape of emission at $\lambda_{exc}(355)$ remained unchanged for all samples over the six year storage period, even in cases where a change in emission intensity was observed (Figure 4 - 10).

F(355) values showed the highest correlation in August (slope 0.97±0.01), relative to October (0.89 ± 0.03) and December (0.88±0.02) (Figure 4 - 11- bottom), similar to the trends observed for absorption coefficient at 355 nm ($a_{CDOM}(355)$) (Figure 4 - 11 - top).

As a result, the ratio of F(355) to $a_{CDOM}(355)$ was relatively constant across each season, within <10% of the values in 2006 (Figure 4 - 12). A small subset of samples (13.7%) displayed a slightly different ratio of F(355) to $a_{CDOM}(355)$ relative to the bulk (Figure 4 - 12- December plot -samples in circle). Interestingly, all but one of these samples were from the December season, located in a small transect in the bay, with $a_{CDOM}(355)$ values >5 m^{-1} (in 2006) . Although it is unclear why this difference existed, it is possibly a seasonal, or less likely geographical artifact.

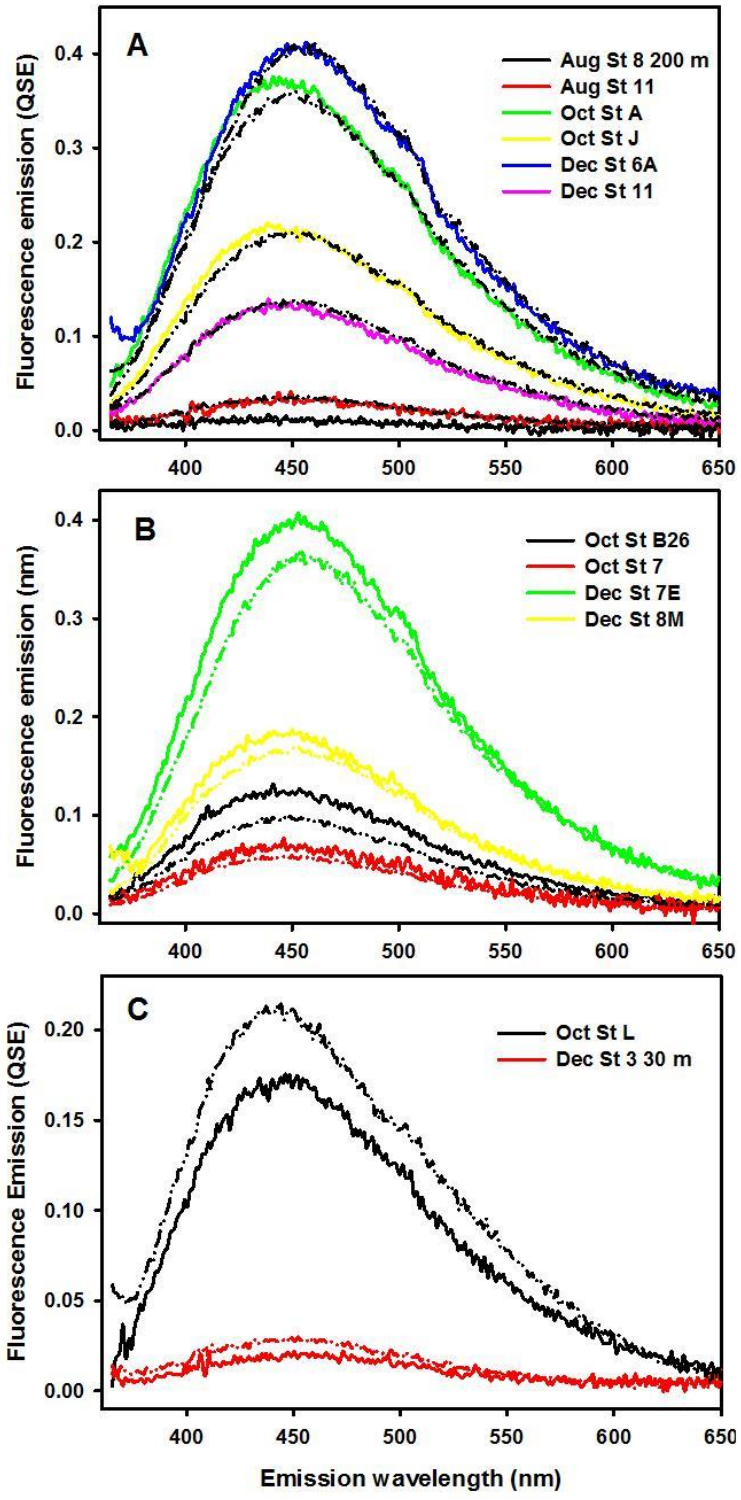

Figure 4 - 10: Comparison of fluorescence emission spectra (λ_{exc} (355)) of selected samples obtained in 2006 (solid lines) and 2013 (dashed lines). A, B and C are examples of spectra which displayed no change, decrease, and increase in emission intensity, respectively (Spectra for all samples from August, October and December, AP6 to AP11)

Percent change in fluorescence emission at λ_{exc} 355 nm					
August		October		December	
Sample	% change	Sample	% change	Sample	% change
St 11 25m	-8.74	St 2 200m	-42.13	St 8B	-16.01
St 19E	-6.39	St B2	-27.96	St 8A	-15.53
St 19H	-3.86	St 1 1000m	-27.22	St 8	-13.92
St 19B	-3.48	St B0	-26.26	St 8G	-12.36
St 8 200m	-2.96	St B26	-22.29	St 8J	-9.86
St 16	-2.95	St MB	-16.99	St 7E	-9.65
St 19D	-1.61	St 7	-16.33	St 8M	-9.03
St 19I	-1.00	St 7 21m	-11.29	St 8I	-8.99
St 19G	-0.70	St 1C	-10.30	St 7C	-7.30
St 19	-0.47	St 6	-9.92	St 12	-7.29
St 4 75m	-0.46	St 6 21m	-8.22	St 7	-7.08
St 5 41m	0.43	St D	-3.43	St 8C	-7.08
St 19M	1.45	St A	-3.39	St 8N	-4.45
St 19J	1.76	St 3 30m	-1.72	St 8E	-3.95
St 2 26.4m	1.80	St J	-1.48	St 7D	-3.33
St 19A	1.92	St 4	0.03	St 7A	-2.94
St 15	1.96	St 2	0.98	St 5	-2.01
St 17	2.06	St E	1.05	St 10B	-1.55
St 14	4.04	St I	1.06	St 6A	-1.47
St 19N	4.51	St B5A	1.47	St 8F	-0.99
St 11	4.85	St 5	1.91	St 8L	0.13
St 13	5.07	St M	4.18	St 11	4.93
St 9 35m	6.90	St 2B	4.26	St 10	7.26
St 20B	7.32	St O	4.32	St 4	7.62
St 21	8.78	St 1B	6.96	St 14	9.30
St 2	16.15	St 1E	8.78	St 9 20m	11.86
St 5	19.18	St 5 111m	16.59	St 4 20m	12.90
St 4	25.23	St 1	18.86	St 1 37m	31.47
St 6	27.22	St L	24.32	St 3	39.60
St 9	33.22			St 3 30m	39.78
St 10 35m	40.22				
St 1	67.89				
St 10	103.83				
St 8	105.63				
St 7	262.51				

Table 4 - 2 Percent change in fluorescence emission at λ_{exc} 355 nm for August, October and December samples from the MAB. Samples highlighted in red exhibited fluorescence emission within ±10% of 2006 values.

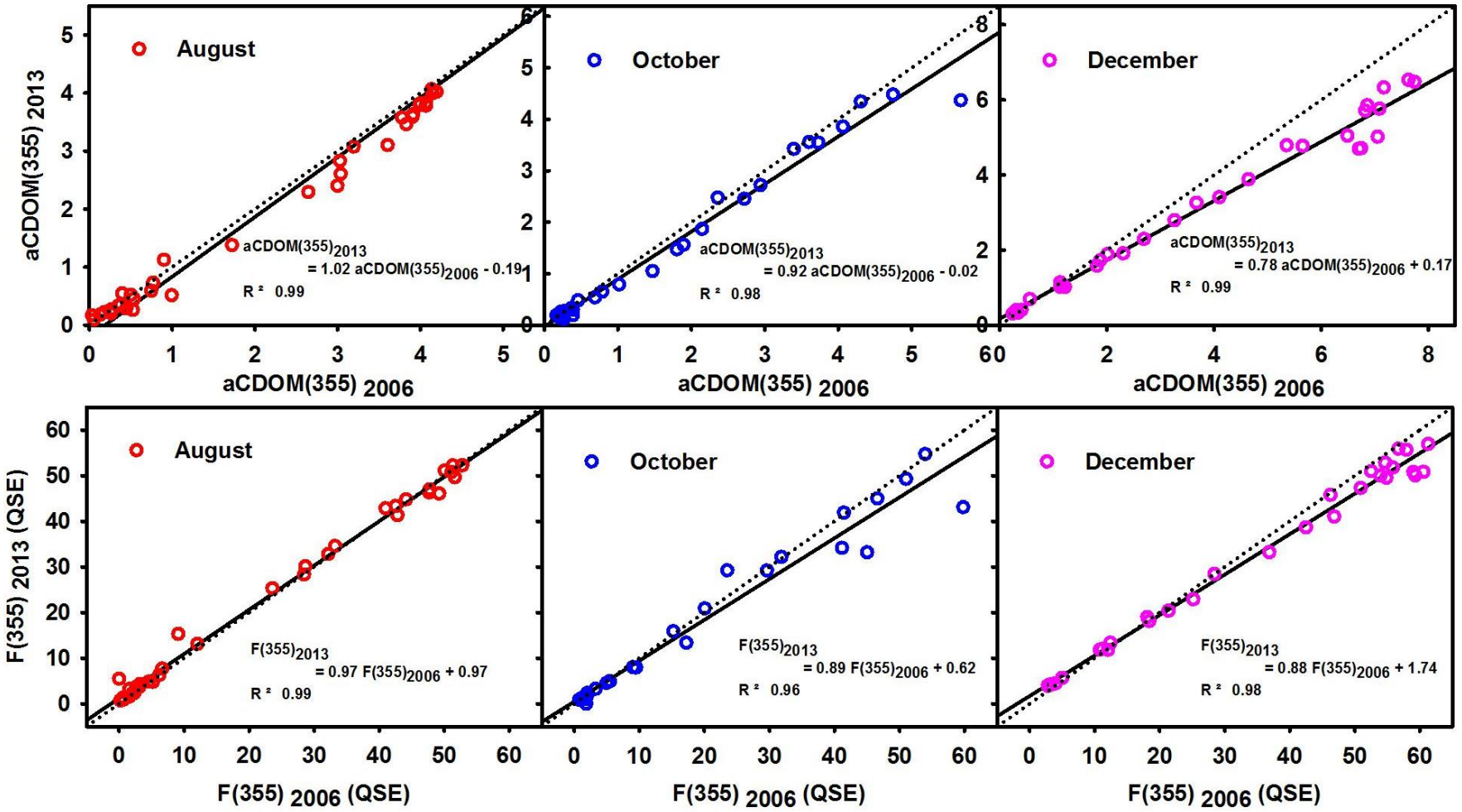

Figure 4 - 11: Comparison of $a_{CDOM}(355)$ (top) and F(355) values (bottom) obtained for August (red), October (blue) and December (pink) in 2006 and 2013, dotted is the 1:1 line.

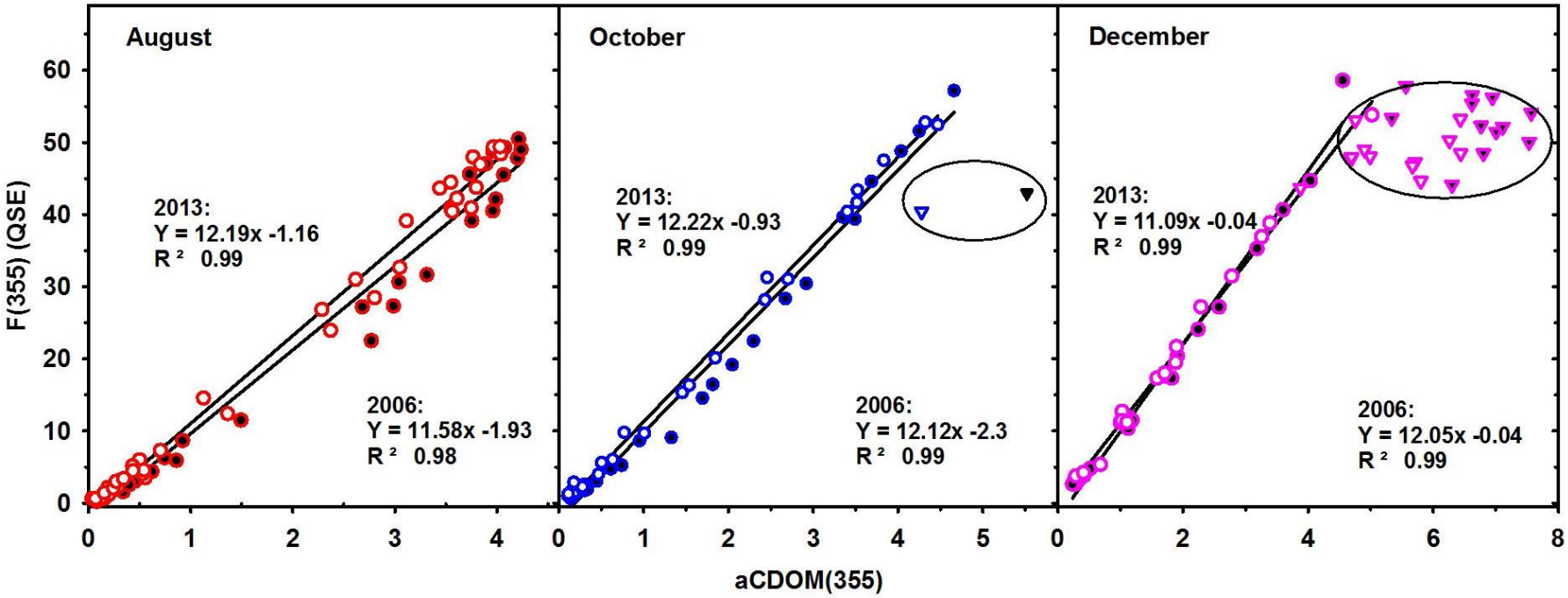

Figure 4 - 12: Ratio of F(355) to $a_{CDOM}(355)$ for August, October and December. Solid symbols - 2006 values, and open circles - 2013 values. Triangles in the December and October plots are the samples which displayed a different ratio ($a_{CDOM}(355)_{2006}$ >5m^{-1}).

4.3.3 DOC

DOC content was investigated for only a subset of samples due to unavoidable instrument problems. DOC values obtained in 2013 for August and December samples showed some correlation with 2006 measurements, although values differ by approximately ±20 % and ±10% respectively over the storage period (Figure 4 - 13). This degree of change is relatively small and reasonable considering the length of time over which the samples were stored. Further, DOC analysis is a very sensitive technique, involves many steps and samples can be easily contaminated, thus increasing the possibility of variability in measurements. The results for October samples were inconclusive, showing no correlation with 2006 values (Figure 4 - 13). The results for October samples may be due to lack of reliable measurements obtained in 2006.

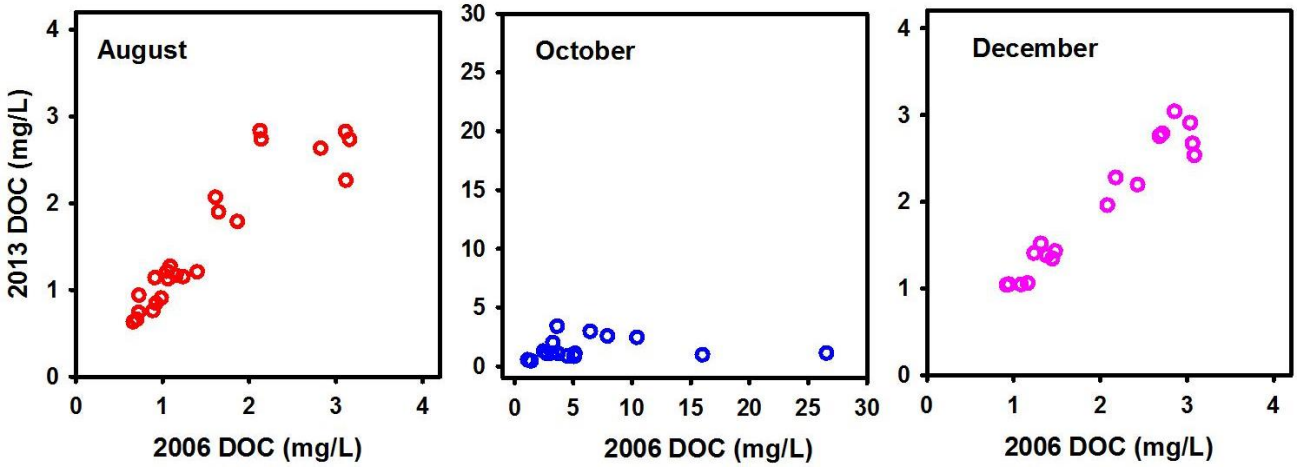

Figure 4 - 13: Comparison of DOC values obtained for August (red), October (blue) and December (pink) for 2006 and 2013

4.4 Discussion and conclusion

Overall, based on our established criteria, absorbance in the visible regime for more than two thirds of the samples were stable over the 6 year period. The increase in UV absorbance (15-30 %) observed for a small number of samples (~12%), may be associated with biological activity. However, the fact that this behavior was exhibited by only a small subset of samples, and the degree of change was small over time, this indicates that (1) filtration through 0.2 µm filters removes most bacteria and large viruses and, (2) storage at 4º C in the dark significantly inhibits growth of microbes which may have passed through the filter. Absorbance loss across the entire wavelength regime (ranging from 20-30% in the UV region and up to ~40% in the visible) were only observed for one third of the samples. These samples were located in the bay and exhibited very high absorbance, which suggests the presence of relatively higher molecular mass material. Thus this loss in absorbance may be as a result of precipitation (and sedimentation) of some of the high molecular weight organic material in these samples. Adsorption to the walls of the sample containers may be another explanation for this loss in absorbance.

The spectral line shape of emission at λ_{exc} 355 nm was unchanged for all the samples. F(355) to $a_{CDOM}(355)$ ratios were within 10 % of 2006 values implying that the apparent quantum yields were unchanged. Fluorescence quantum yield is a well-defined photophysical property that can be used as an effective tool for characterizing the nature of CDOM (Blough and Del Vecchio, 2002), thus unchanged QY values suggests relatively unchanged structure.

Results from this study highly underscore several important factors to be taken into consideration before making conclusions about what is considered to be an absolute change in absorbance values for measurements recorded over very long time intervals. Absorbance values (or changes in absorbance) must be examined relative to an established standard deviation and not just on an absolute scale. As indicated by our data, σ can be wavelength dependent and thus it is important that σ is established at each wavelength. This sets the limit on how accurately absorbance values can be measured (i.e. 3 to 5σ). Thus, absolute changes in absorbance that are smaller than the established σ are meaningless. Instead these values should be reported relative to the standard deviation in absorbance (at the respective wavelength) and to the detection limit for the spectrophotometer used. If the wavelength dependence of $\Delta A/\sigma$ shows no systematic wavelength variation, this is likely due to a systematic baseline offset.

Chapter 5: Is CDOM produced in *Pelagibacter ubique* incubations?

5.1 Overview

The work presented in this chapter was part of a collaborative project which involved several researchers, post doctorates, graduate students and technicians. The overall goal of this study was to examine the interdependence of photochemical degradation of DOM and heterotrophic metabolism of *Pelagibacter ubique* (*P. ubique*) bacteria. P. ubique is a member of the ubiquitous SAR11 clade of α-proteobacteria. Representatives of the SAR11 clade often represent the largest fraction of bacterial cells in ocean surface waters. Several specific research questions were addressed by this work including:

What are the growth substrates for SAR11 in marine CDOM?

Is CDOM produced in *P.ubique* incubations?

If so, what is structure of bacterially derived CDOM?

Incubations (growth) experiments were conducted by Stephen Giovannoni from Oregon State University. Elizabeth Kujawinski and her team from Woods Hole Oceanographic Institute (Woods Hole, MA) was responsible for FT-ICR MS analysis for structural characterization. Blough, N. V and Del Vecchio, R. (University of Maryland) were responsible for optical characterization, which was performed by Del Vecchio, R. and Andrew, A. This chapter describes the results from the optical characterization of DOM produced by SAR11 (strain HTCC 1062 in ASW) to determine whether SAR11 produces CDOM.

5.2 Introduction

Many studies have indicated that in situ biological production is the primary source of marine CDOM (Coble, 2007; Harvey et al., 1984; Yamashita and Tanoue, 2004; Yamashita and Tanoue, 2009), with terrestrial sources contributing only a small fraction. Unlike the terrestrial CDOM source and possible origin, ascertaining the source material and mechanisms or processes involved in in situ biological production of marine CDOM, has been a great challenge. Examination of the results from the plethora of studies that have been done in this area provide evidence to suggest that both of these sources may contribute to CDOM in the oceans. The extent of each individual contribution is highly debated. Additionally, the wavelength regime ($\lambda_{exc}/\lambda_{em}$ range) associated with CDOM from in situ production versus CDOM from terrestrial sources is sometimes not clearly defined.

Numerous studies (Nelson et al., 2004; Nelson et al., 1998; Ortega-Retuerta et al., 2009) have implicated several of the lower trophic groups in the production of marine CDOM including primary producers, viruses and bacteria. In fact, a recent review by Nelson (2013), stated that CDOM in oceans is produced primarily as a by-product of microbial metabolism, citing his previous work using microbial culture experiments (Nelson et al., 2004) and field data (Nelson et al., 1998). Many other studies provide primary evidence suggesting a link between bacterial production and CDOM generation. In experiments using mesocosms, Ortega -Retuerta et al. (2009) confirmed a potential role of bacteria as a CDOM source based on absorption changes of cultures at 325 and 443 nm and net decrease in $S_{275\text{-}295}$ (spectral slopes for the intervals of 275–295 nm, (Helms et al., 2008)).

Steinberg et al. (2004), implicated *Trichodesmium* and zooplankton in the production of CDOM. Their conclusions were based on observed changes in absorption spectra of the filtrate obtained during the course of incubation experiments. Additionally, other studies based on observation of absorption spectra, have also shown that *dinoflagellates* (Vernet and Whitehead, 1996; Whitehead and Vernet, 2000), and macroalgae (Hulatt et al., 2009; Shank et al., 2010) can release CDOM in significant amounts. Kitidis et al (2006), based on depth distribution paterns and correlations with $S_{290–350}$ and $S_{250–650}$ suggested the presence of two CDOM members in the waters of the Atlantic ocean. One was attributed to CDOM production by phytoplankton-derived organic matter and the other to microbes.

It is clear that some fraction of CDOM in oceans is autochthonous, and that microbial processes are possibly an important part of the production process. However the precise mechanism(s) and source material for CDOM formation within oceans remain to be determined. It is likely that autochthonous CDOM may be the result of modification of source material by microbes and /or photochemical processes, rather than direct production by microbes. Some studies indicate that terrestrial derived CDOM is largely resistant to direct microbial mineralization (Moran et al., 2000). However photochemical reactions of terrestrial CDOM produce products that can be readily consumed by bacteria (Moran et al., 2000). Contrarily, some photochemical processes have been shown to impede microbial degradation of algal-derived DOM (Benner and Biddanda, 1998; Tranvik and Kokalj, 1998).

From these studies it is evident that heterotrophic bacterial metabolism and photochemistry are two important pathways for transforming organic matter in surface oceans (Hansell and Carlson, 2002) and that these processes are often coupled in very complicated ways (Mopper and Kieber, 2002; Moran and Zepp, 1997). However, the conclusions of most of these studies are based on observed changes in absorbance spectra, often focusing on only one or two specific wavelengths. Additionally, none of these studies have examined the fluorescence properties associated with these absorbance changes. The simultaneous acquisition of complete absorbance and fluorescence emission spectra has been shown to be much more informative (Green and Blough, 1994). Observed absorbance changes or features can thus be correlated with fluorescent properties, thereby providing a clearer characterization of the newly produced absorbing/emitting material, ultimately gaining greater insight into structure and possible source of autochthonous CDOM in oceans.

In this work, we provide a systematic assessment of the complete optical properties (absorption and fluorescence emission) of CDOM produced/modified by heterotrophic metabolism/degradation by *P. ubique*. Optical measurements were obtained for the CDOM as well as for the extracted organic matter at several stages during the growth cycle of *P. ubique*. Optical properties were monitored at each stage during the extraction of the organic matter (i.e. removal of cells by filtration, subsequent acidification and PPL extraction). Results from optical measurements indicate that *P. ubique* does NOT

produce CDOM (with long-wavelength absorption and red-shifted emission) under the incubation conditions of our study.

5.3 Material and Procedures

5.3.1 Samples - Incubations

Two 10 L acid-washed & autoclaved polycarbonate carboys each containing 5 L of a nutrient limited artificial sea water (ASW) medium were supplemented with 1.0 μM NH_4Cl, 1.0 μM KH_2PO_4, 10 nM $FeCl_3$, 1000X vitamin solution (thiamine, Biotin and pantothenate), 50 μM Glycine, 10 μM Methionine and 100 μM Pyruvate. One polycarbonate carboy was inoculated with a pre-inoculated culture of HTCC 1062 (mid-log phase) to a starting concentration of ~$2x10^{-4}$ cell/mL, and the other carboy was left as a non-inoculated control. Both carboys were then placed in a 16ºC incubator on a 12 h light/dark cycle. These conditions have been shown to produce optimal cell yields for the cultivation of SAR11 on a defined artificial seawater medium (Carini et al., 2013). The medium in each of the carboy was sampled (DOM and extracted DOM) at 4 time points during the growth cycle for optical characterization. FT-ICR MS, DOC, and TOC measurements were also obtained by collaborators. The first time point, t(0), represents the point prior to inoculation with SAR11 (only the medium). The second sample, t(1), was obtained after 9 days, during the early log phase of growth. Time points t(2) and t(3) were taken in the late log and early stationary phase, respectively (at 16 & 21 days). The last time point, t(4), was taken on day 33 during the late stationary phase (Figure 5 - 1).

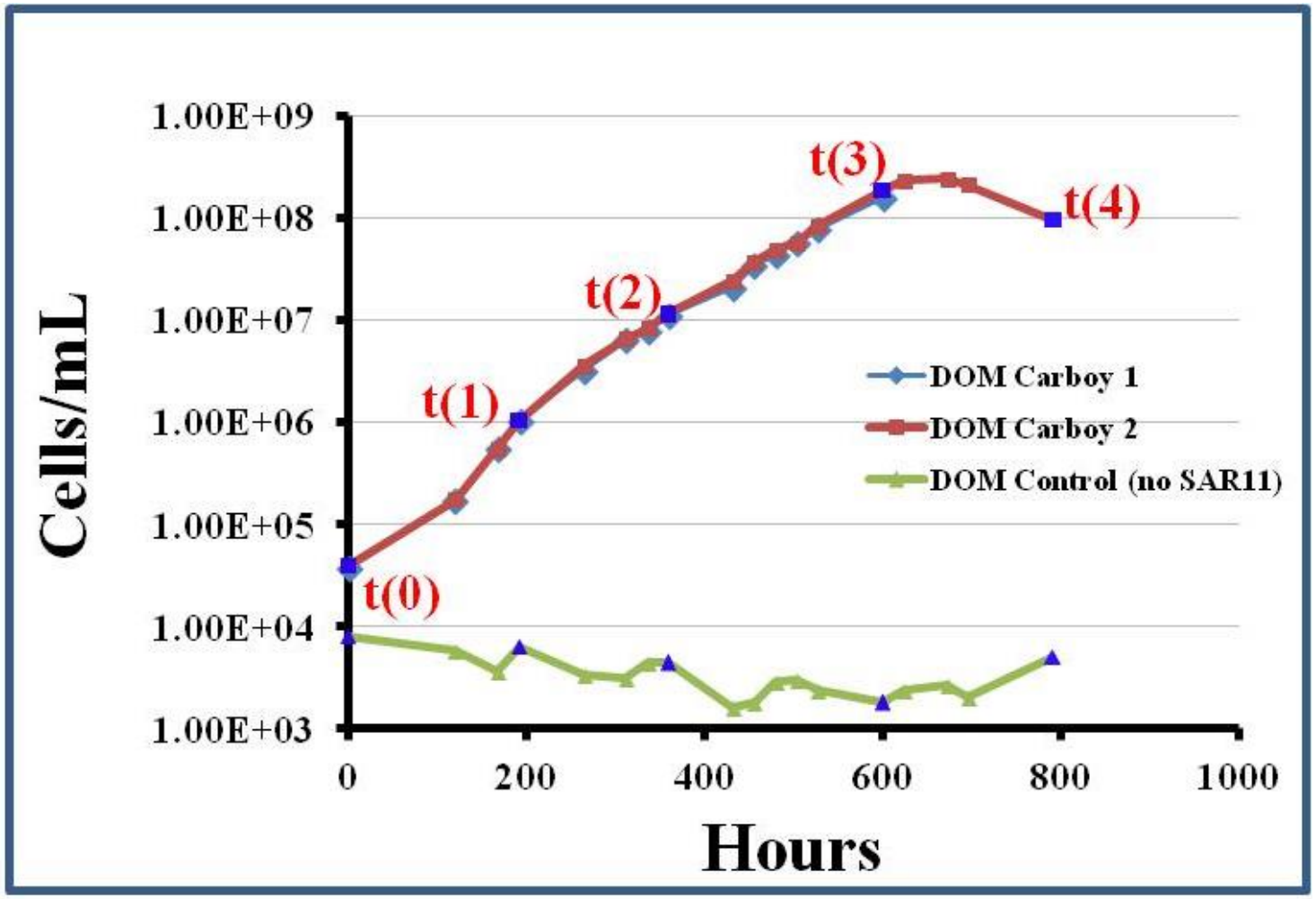

Figure 5 - 1: Growth profile of *P. Ubique* showing time point at which sampling was done.

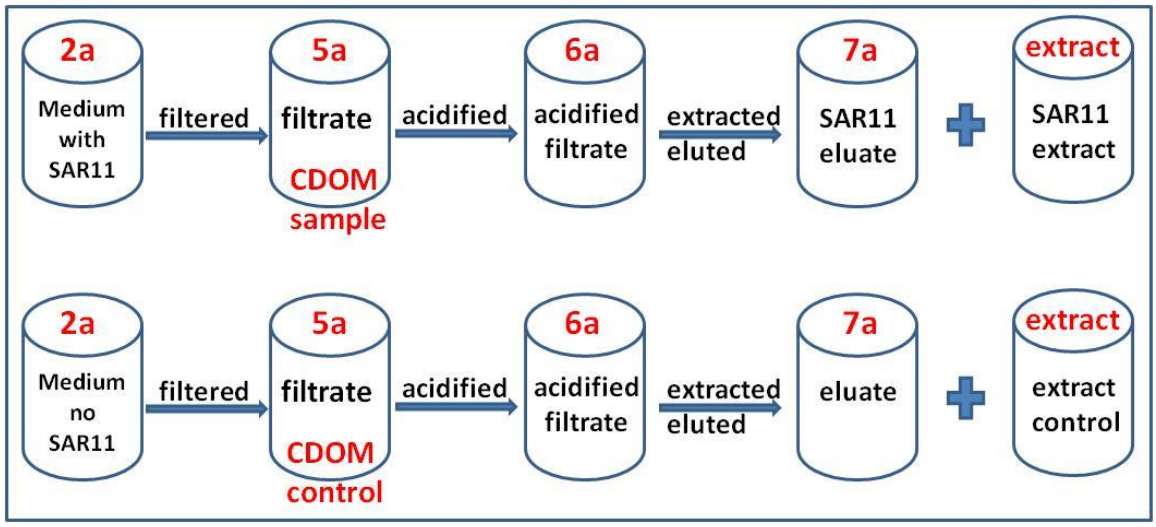

Figure 5 - 2: Sample preparation and collection. Sample 5a is the 0.2 µm filtrate and thus the CDOM sample

5.3.2 Sample preparation and collection

Incubation samples were prepared by Carter, A. (Giovannoni Lab, Oregon State University) as described below and shipped to Blough N. V (University of Maryland) for analysis by Andrew, A. At each time point, 10 samples were collected: 5 controls (samples without SAR11) and 5 samples inoculated with SAR11 as described in Figure 5 - 2 (Summary of sample description is also provided in Table 5 - 1). 1 L of medium was removed from each carboy and placed into acid-washed Polycarbonate carboys. First, 100 mL of this unprocessed sample (Sample **2a**) was placed in a 125 mL HDPE bottle (acid-washed, rinsed with HPLC grade methanol and then rinsed with nano-pure water) and stored in the dark at 4°C until processing. The remaining sample was filtered through a 0.2 µm Omnipore filter at a rate of 70 mL/min, and 100 mL of the filtrate (Sample **5a**) was stored as before. The remaining cell-free filtrate was acidified to a pH of about 2.5 – 3.0 using 10% HCl (3 mL for a 1L sample; trace metal grade). 100 mL of the acidified cell-free filtrate (Sample **6a**) was stored for analysis. PPL cartridges for

extraction of organic matter were prepared by first passing 10 mL HPLC grade methanol upward through the column. The column was then set aside (now filled with methanol) and allowed to soak for 5 - 10 min. Methanol was expelled (cartridge nose down) with air. 20 mL of nano-pure water was then passed through the column to expel the remaining water and air. Finally, the acidified cell-free filtrate was extracted by gravity at a rate of ~15 mL/min. 100 mL of the PPL eluate was collected and stored as sample **7a**. The extracted DOM was eluted off the PPL cartridge and stored as described below and was designated as SAR11 extract.

Sample Description	Sample ID
unprocessed sample	2a
filtered sample (filtrate)	5a
filtered and acidified filtrate	6a
PPL eluate	7a
PPL extract	SAR11 extract

Table 5 - 1 Description and ID of the samples (SAR11 and control) collected for analysis at each time point.

5.3.3 Sample Elution

Each cartridge was rinsed with 4 bed volumes (1 bed volume = 3 mL) of 0.01 M trace metal grade HCl using a light-vacuum. Any flow-through was discarded and cartridges were then allowed to air dry for 5 min. DOM was eluted into three 1.5 mL Teflon microfuge tubes (pre-washed with HPLC grade methanol and allowed to dry), using 3 mL of 100% HPLC grade methanol. Methanol was allowed to flow through the PPL

cartridge under gravity in order to keep the flow rate at less than 1 mL/min. The contents of the 3 microfuge tubes were combined and placed in a vacufuge (top open and facing outward) and spun until dry to remove all solvent from the DOM extracts. Dried DOM extracts was stored at -80°C until shipping and processing.

5.3.4 Optical measurements

UV-visible absorbance spectra (190-820 nm) were acquired with a Shimadzu 2401-PC spectrophotometer employing a 10 cm optical cell for CDOM samples with Milli-Q water as the blank. Spectra of extracted samples were measured using a 1 mm cell due to limited sample volume. Prior to measurements, extracted samples were dissolved in 900 μL of Milli-Q and mixed with a vortex mixer. A minimal volume of Milli-Q was used in order to maintain a high sample concentration for more reliable optical measurements. Sample pH (~pH 4.5 -5.9) was adjusted to the pH of water samples prior to extraction (~pH 7) using 2 – 4 μL of 0.250 N NaOH. Fluorescence measurements were acquired at excitation wavelengths (λ_{exc}) from 280 to 400 nm in increments of 20 nm, employing a 1-cm optical cell and Milli- Q water as blank. Both the excitation and emission monochromator bandpasses were set to 4 nm.

5.4 Results and Discussion

5.4.1 Control samples (i.e. medium without SAR11)

All the control samples (i.e. medium without SAR11) were internally consistent and the optical signature of the medium was very low. Samples displayed similar absorbance

spectra that were constant over time (Figure 5 - 3). No absorbance was evident in the visible regime, however two shoulders were observed in the UV region (~260 nm and ~ 325 nm). These shoulders experienced only minor changes during the processing of the control samples. The shoulder at 260 nm slowly decreased as the sample was filtered (5a) and acidified (6a), and was completely gone after extraction (7a), while that at 325 nm only slightly decreased. Conversely, the fluorescence emission spectra of the control samples showed no evidence of distinct emitting bands (Figure 5 - 4). Fluorescence emission intensity was extremely low and uniform with time, and was unaffected by sample processing (filtration, acidification and extraction).

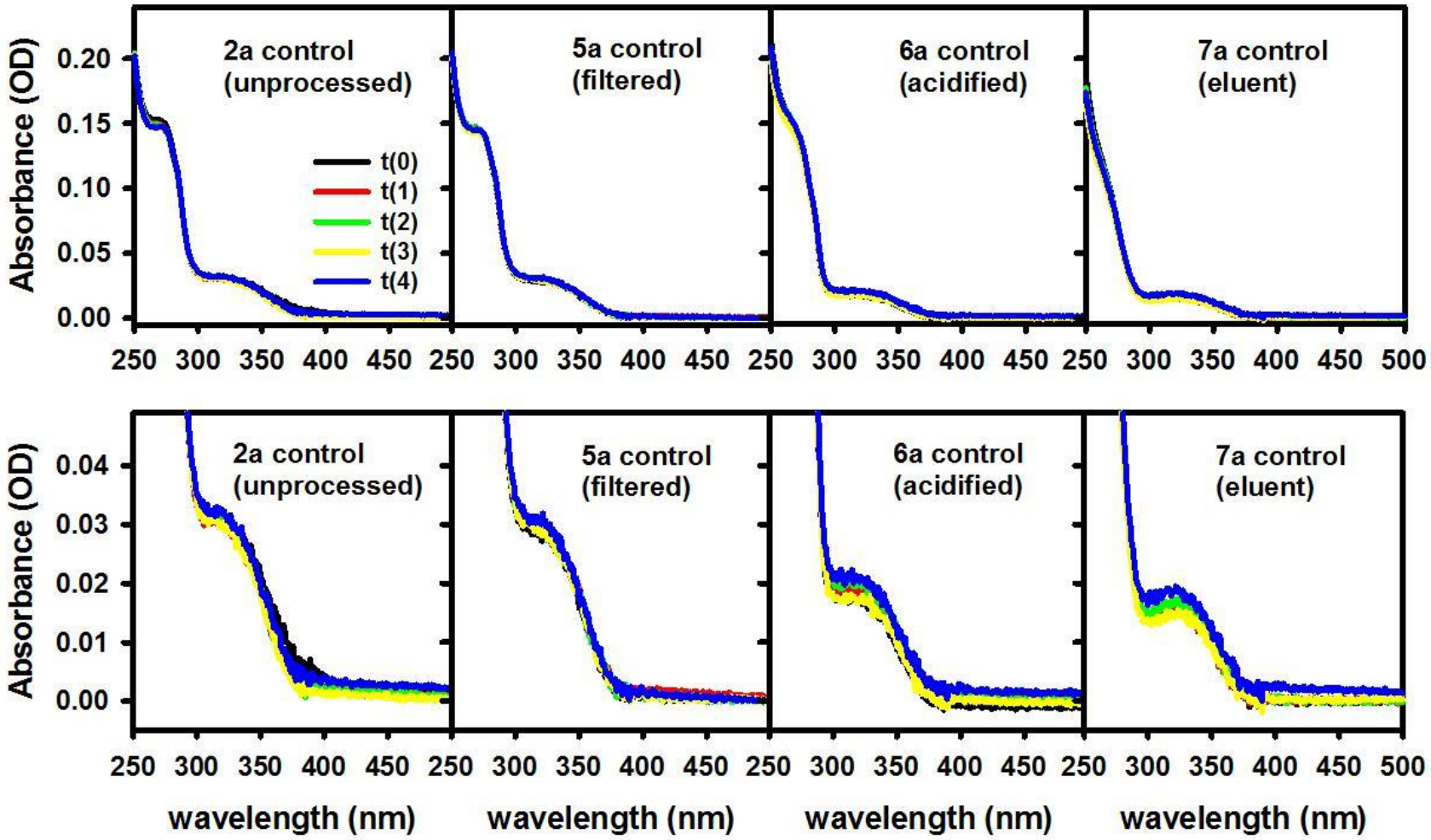

Figure 5 - 3: Absorbance spectra of controls (samples without SAR11) showing effect of processing (filtration, acidification and extraction) (bottom panel: absorbance spectra zoomed in).

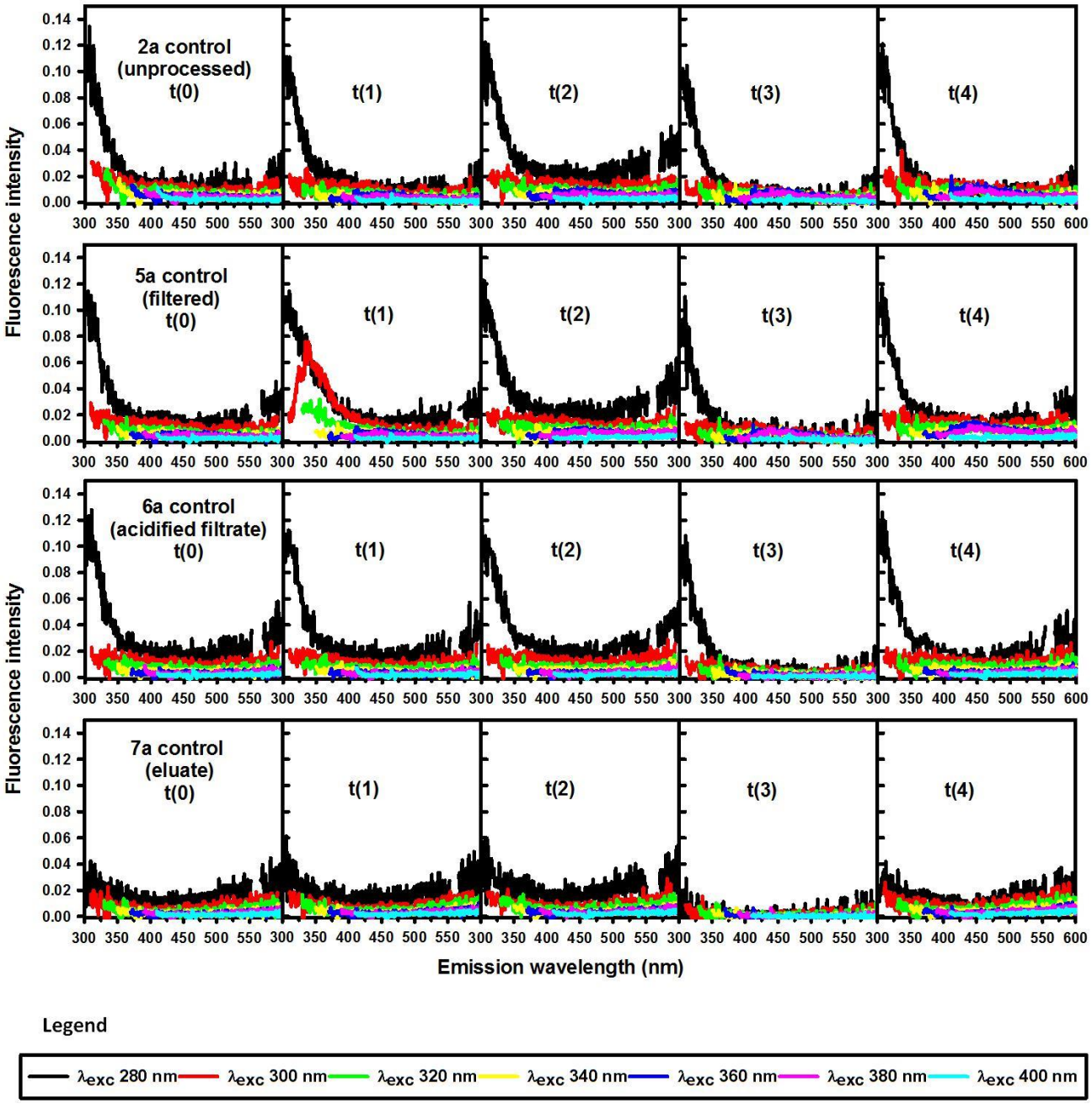

Figure 5 - 4: Fluorescence emission spectra for control samples 2a (unprocessed), 5a (filtered), 6a (filtered and acidified) and 7a (eluate). Fluorescence measurements acquired at λ_{exc} 280 to 400 nm in increments of 20 nm.

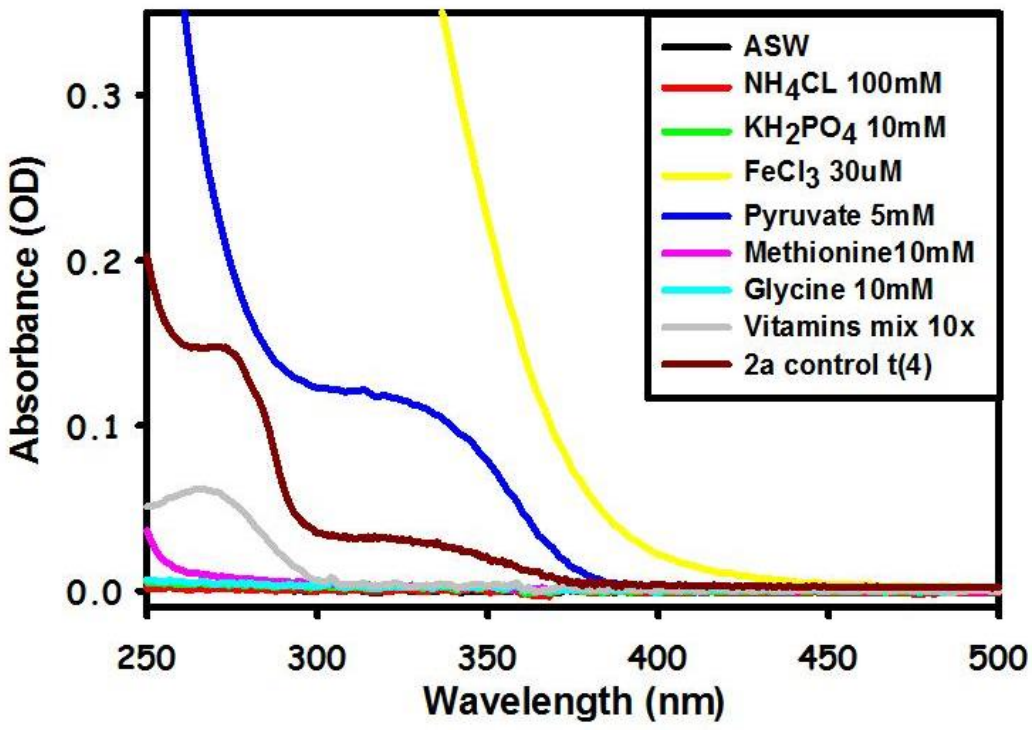

Figure 5 - 5: Absorbance spectra of the ASW and nutrients used in the SAR11 medium. Concentrations reported are much higher that what was used in the medium. Absorbance spectra for ASW and KH_2PO_4 are not visible becasue these solutions exhibited no absorbance.

An analysis of the optical properties of the artificial seawater (ASW) and nutrients used in the SAR11 medium was conducted in order to determine the possible origin of the absorbance bands observed in the control samples. The ASW showed no absorbance or fluorescence signal. Among the nutrients, only $FeCl_3$, pyruvate and the vitamins mix exhibited distinct absorbance bands over the wavelength range of interest (Figure 5 - 5). Absorbance from $FeCl_3$ was not observed in the control samples due to the much lower concentrations used in sample preparation. Based on absorbance properties observed for the vitamins mix and pyruvate standard solutions, the absorbance bands observed in the control samples at ~260-270 nm and ~300-345 nm were assigned to the vitamins mix and pyruvate, respectively.

5.4.2 Inoculated samples (i.e. medium with SAR11)

Inoculated samples, prior to filtration of cells (i.e. 2a), displayed changes in absorbance (Figure 5 - 6) and fluorescence (Figure 5 - 7) with time (and processing). While these observed changes were minor up to the late log phase, t(2), significant changes in absorbance and fluorescence occurred at the early and late log phases, t(3) and t(4), respectively. Absorbance increased across the entire UV and visible regime, with the highest gains observed over the range ~250-300 nm (Figure 5 - 6). This apparent "absorbance" may be due to scattering, as samples 2a were unfiltered (i.e. still containing SAR11 cells). Fluorescence emission exhibited a large gain at ~ 340 nm and ~ 460 nm, again most notably from time t(3) and continued to t(4) (Figure 5 - 7, black and red lines: and blue and pink lines respectively).

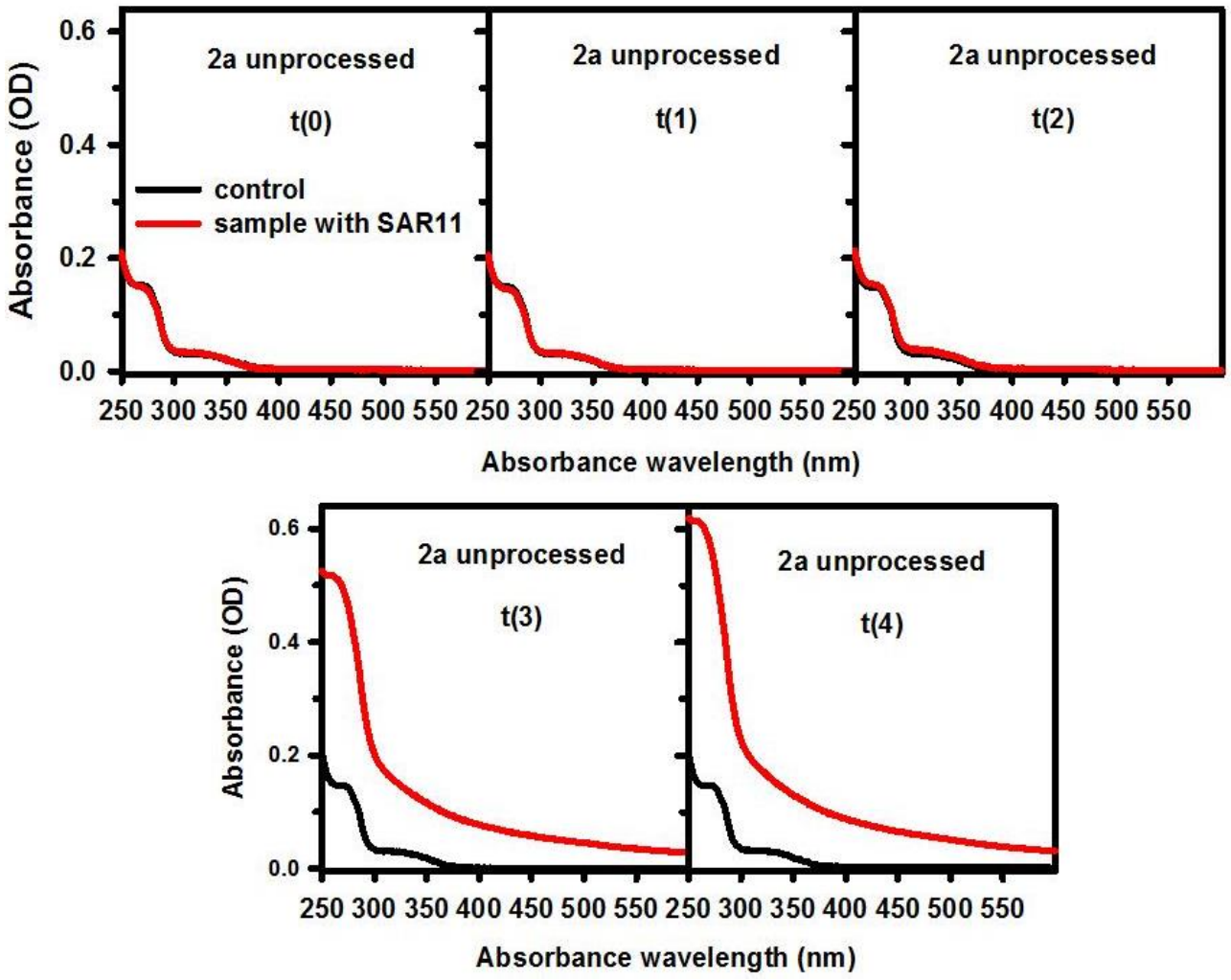

Figure 5 - 6: Absorbance spectra of unprocessed controls (black lines) and inoculated samples 2a (red lines) from t(0) to t(4). (NB: unprocessed - prior to filtration)

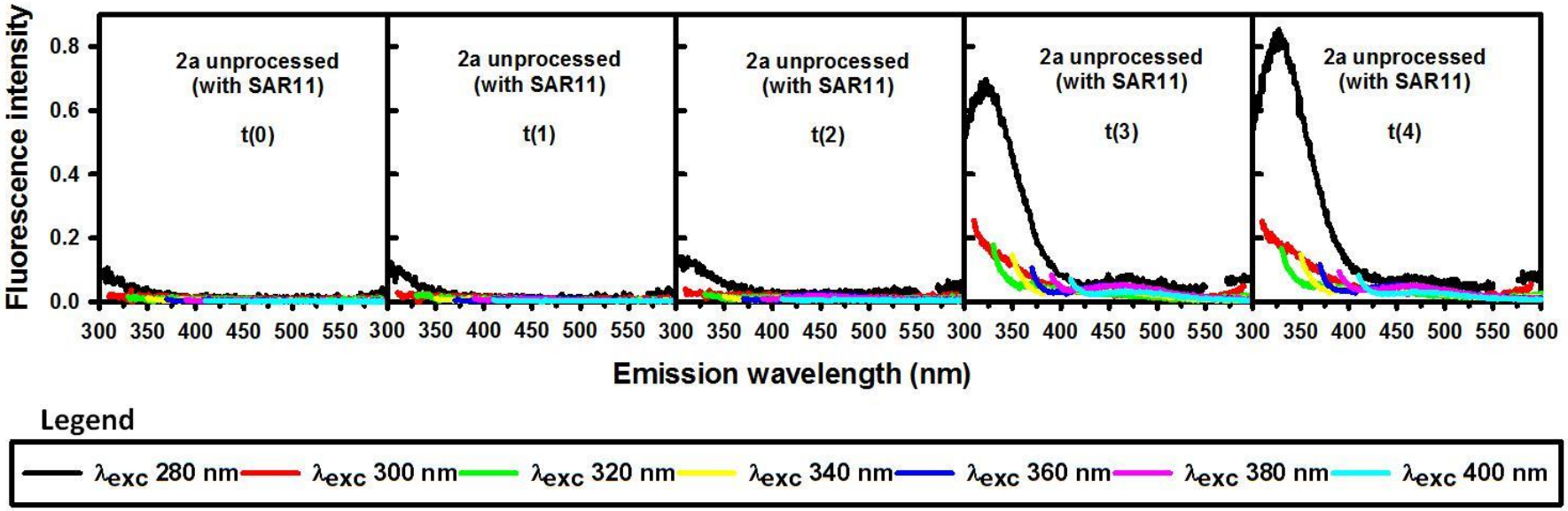

Figure 5 - 7: Fluorescence emission spectra for unprocessed (unfiltered) samples inoculated with SAR11 (sample 2a) over time. Fluorescence measurements acquired at λ_{exc} 280 to 400 nm in increments of 20 nm.

The optical properties of the inoculated samples were further investigated upon removal of SAR11 cells by filtration (5a), subsequent acidification (6a) and PPL extraction (7a). **Filtration** (sample 5a) did indeed remove the majority of the "absorbance" signal at t(3) and t(4) (Figure 5 - 8), indicating that this signal originated from the cells, most likely through scattering. However the amount of signal removed by filtration was wavelength dependent. The UV band at ~260 nm was significantly lowered from 0.62 OD to 0.23 OD, while the long wavelength absorbance signal was almost completely eliminated (Figure 5 - 8, compare 2a to 5a at t(3) and t(4)). Over time, the absorbance of the filtered samples over the 300-350 nm region decreased suggesting that this material was up taken by the cells. Similar to absorbance, filtration removed the majority of the UV emission at 340 nm (Figure 5 - 9; compare 2a to 5a at t(3) and t(4)), again suggesting that this emission also originated from particulate (intracellular) material. Because sample 5a t(4) exhibited fluorescence similar to 2a t(4), it was re-filtered to eliminate any cell material that had possibly leaked through the filter. However, no change in fluorescence emission was observed implying that this emission was indeed in the dissolved form. The emission band observed at longer wavelength (~460 nm) appeared to be less affected by filtration compared with the UV band, possibly implying that this material was not associated with cells.

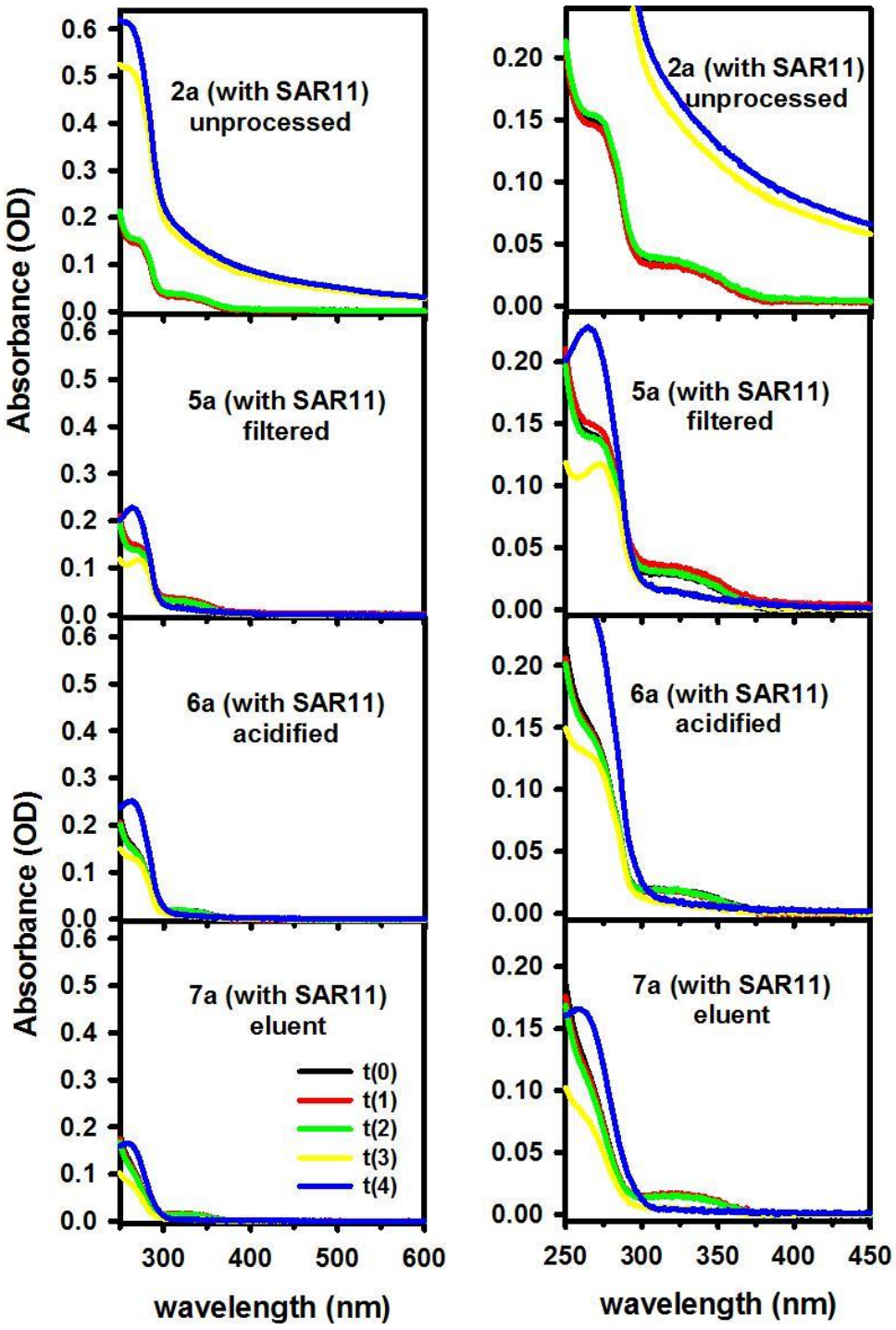

Figure 5 - 8: Effect of sample processing (filtration, acidification and extraction) on the absorbance spectra of samples inoculated with SAR11 at different stages in the growth cycle. (Right panel - zoomed in plots)

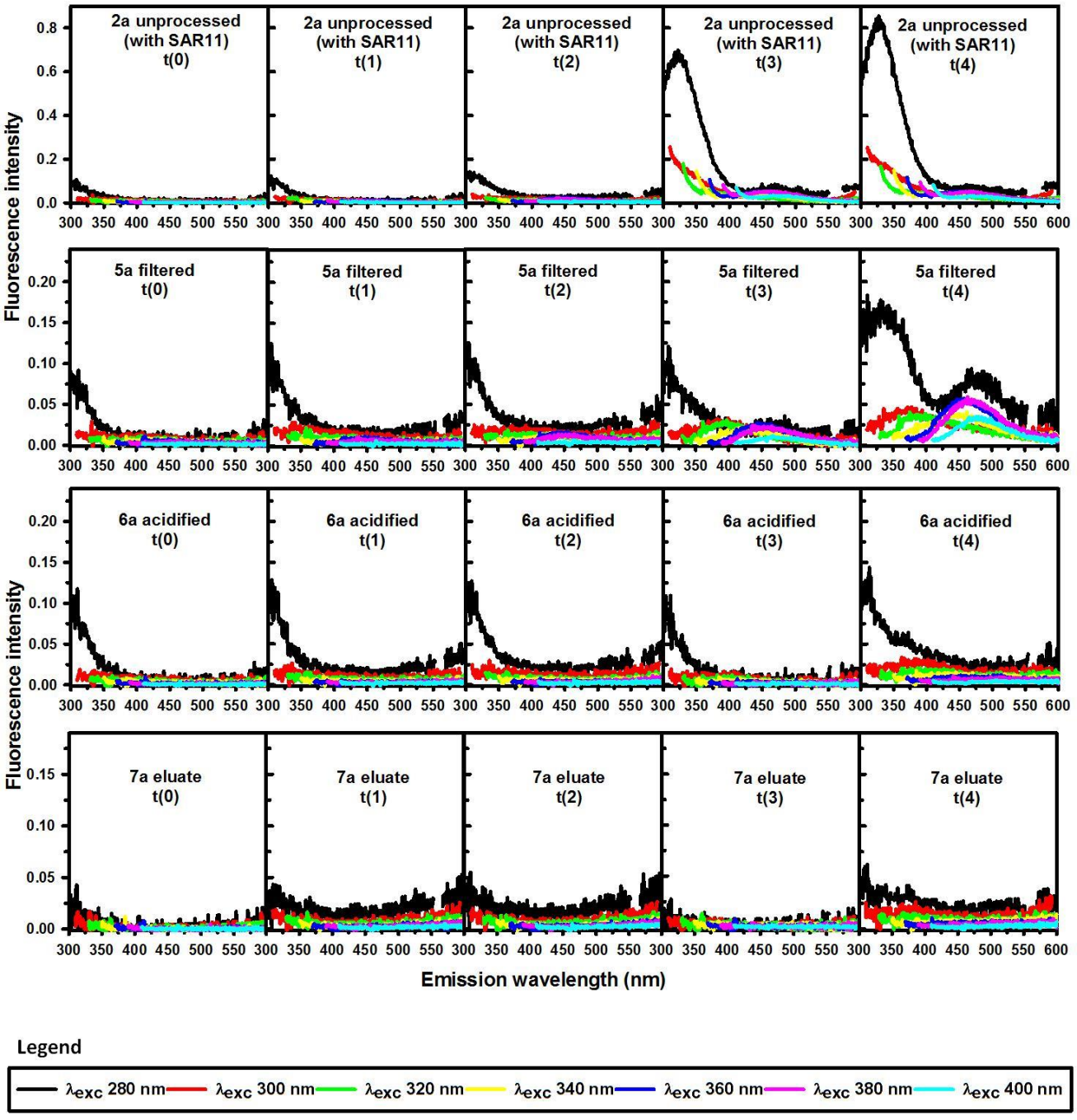

Figure 5 - 9: Effect of sample procession (filtration, acidification and extraction) on the fluorescence emission spectra of the inoculated samples.

Upon **acidification** to pH 2 (sample 6a), no major changes in absorbance were observed (Figure 5 - 8; compare 5a to 6a), except a small increase and broadening of the absorption shoulder at 260 nm. In contrast, acidification to pH 2 quenched all the emission at both short and long wavelengths (340 and 450 nm) (Figure 5 - 9; compare 5a to 6a at t(3)-t(4)). However, when the pH of the acidified sample (6a) was readjusted from 2 to 7 (Figure 5 - 10), the emission was restored at 450 nm but not at 340 nm, implying a pH effect on selected but not all emission bands.

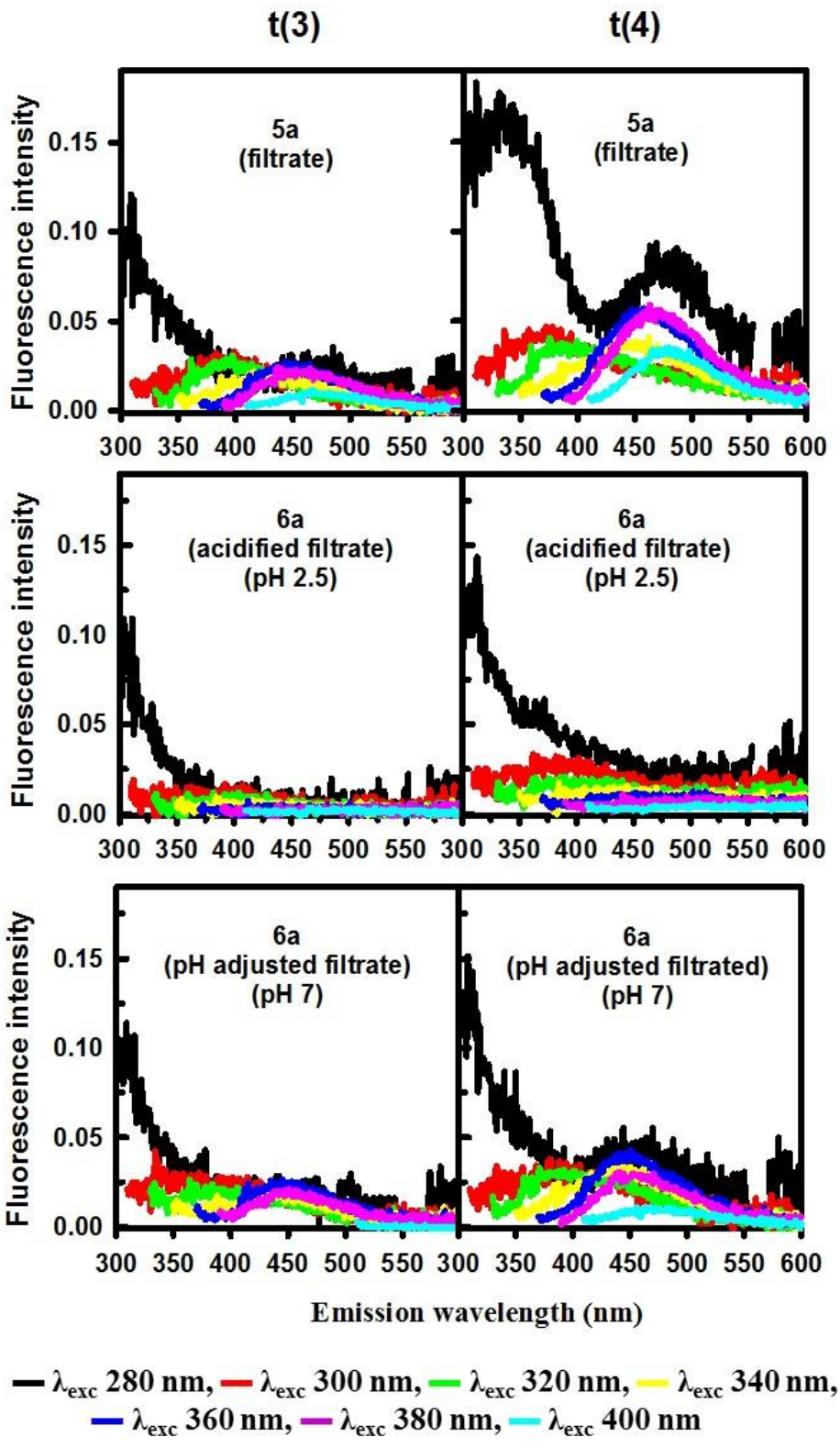

Figure 5 - 10: Effect of pH on the fluorescence emission spectra of SAR11 inoculated samples 5a (filtrate) and 6a (acidified filtrate) at t(3) and t(4).

After **extraction**, the absorbance and fluorescence spectra of the eluate **(sample 7a)** decreased over the entire wavelength range (Figure 5 - 8 and Figure 5 - 9; compare sample 6a to 7a) indicating that DOM was adsorbed onto the PPL cartridges. The pH of the eluate remained constant at ~2.5. When adjusted to pH 7, there was no change in the fluorescence emission, an indication that the previously observed pH dependent emission band at 450nm was adsorbed onto the cartridge (Figure 5 - 11).

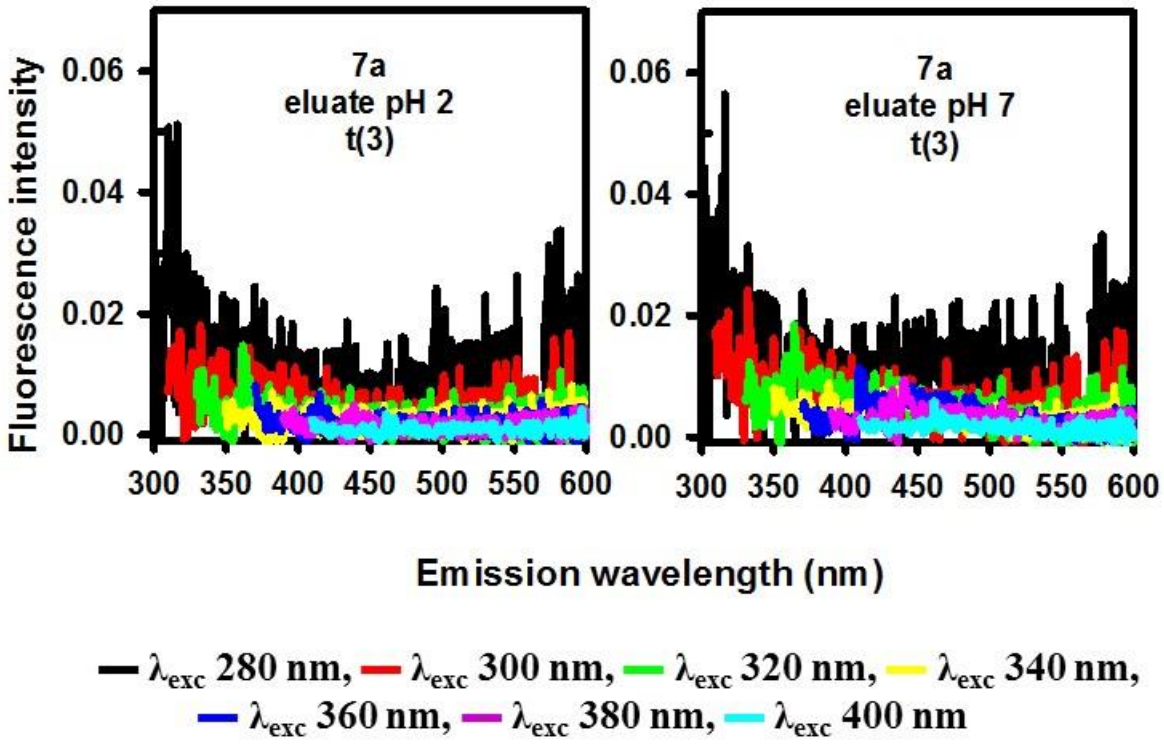

Figure 5 - 11: Effect of pH on the fluorescence emission spectra of sample 7a (eluate).

5.4.3 DOM extracts

All the control extracts (i.e. medium without SAR11) and the SAR11 inoculated extracts displayed similar absorbance spectra (Figure 5 - 12 panel A). The absorbance spectra displayed broad absorbance shoulders at ~260-270 nm and ~300-345 nm, and no long wavelength absorbance, similar to that observed for samples prior to extraction. The absorbance shoulders were again attributed to absorbance from the vitamins mix and pyruvate, respectively (Figure 5 - 5). Likewise, the wavelength dependence of fluorescence emission for both the control extracts and the SAR11 inoculated extracts were analogous and the intensity remained relatively constant with time (Figure 5 - 12, panel B and C respectively). Both fluorescence emission profiles displayed a distinct UV emitting band (excitation 280 nm/emission ~310 nm) and broad emission at wavelengths > 360 nm. While the long wavelength emission intensity remained relatively constant, the intensity of UV emitting band decreased at t(3) and t(4) (Figure 5 - 12 panel B, compare black spectra). The decrease in UV emission occurred for both the control and SAR11 inoculated extracts and may most likely result from sample processing. Overall, the comparability of the absorbance and fluorescence properties of the control and SAR11 extracts indicate that no new absorbing or emitting species were produced by SAR11 during its growth under these experimental conditions. This conclusion is further supported by the overlay of the fluorescence emission spectra of the control and the SAR11 extract at t(3) and t(4) (Figure 5 - 14). Although the emission intensities are different, the emission maxima are similar.

Interestingly, the fluorescence emission spectra for the control and the SAR11 extracts were very comparable to that obtained for the methionine and pyruvate standards (Figure 5 - 13). Although neither pyruvate nor methionine should fluoresce as they are not aromatic compounds, it is possible that these signals arise from impurities in the amino acid standard solutions. Thus, the emission observed for the extracts are attributed to the impurities in the methionine and pyruvate standards.

Although the extracts (control and SAR11 inoculated) exhibited highly similar emission properties (Figure 5 - 12, compare panels B and C), this was contrary to what was observed for the original waters prior to PPL extraction particularly in the UV region (Figure 5 - 15). This difference suggests a preferential extraction, and enrichment of selected compounds by the PPL cartridges.

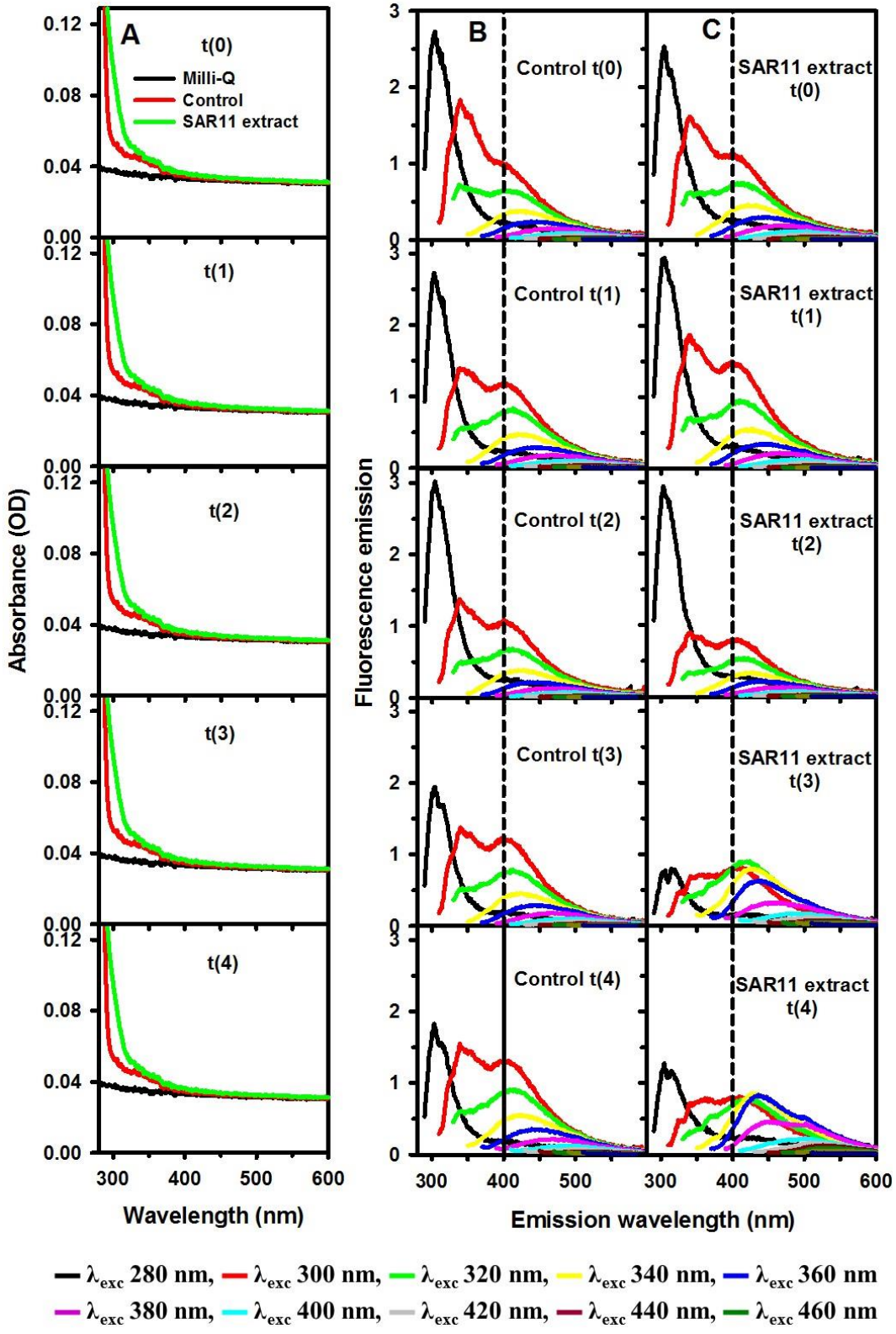

Figure 5 - 12: Comparison of absorbance spectra (panel A) and fluorescence emission spectra (panels B and C) of extracted samples over time, t(0) to t(4).

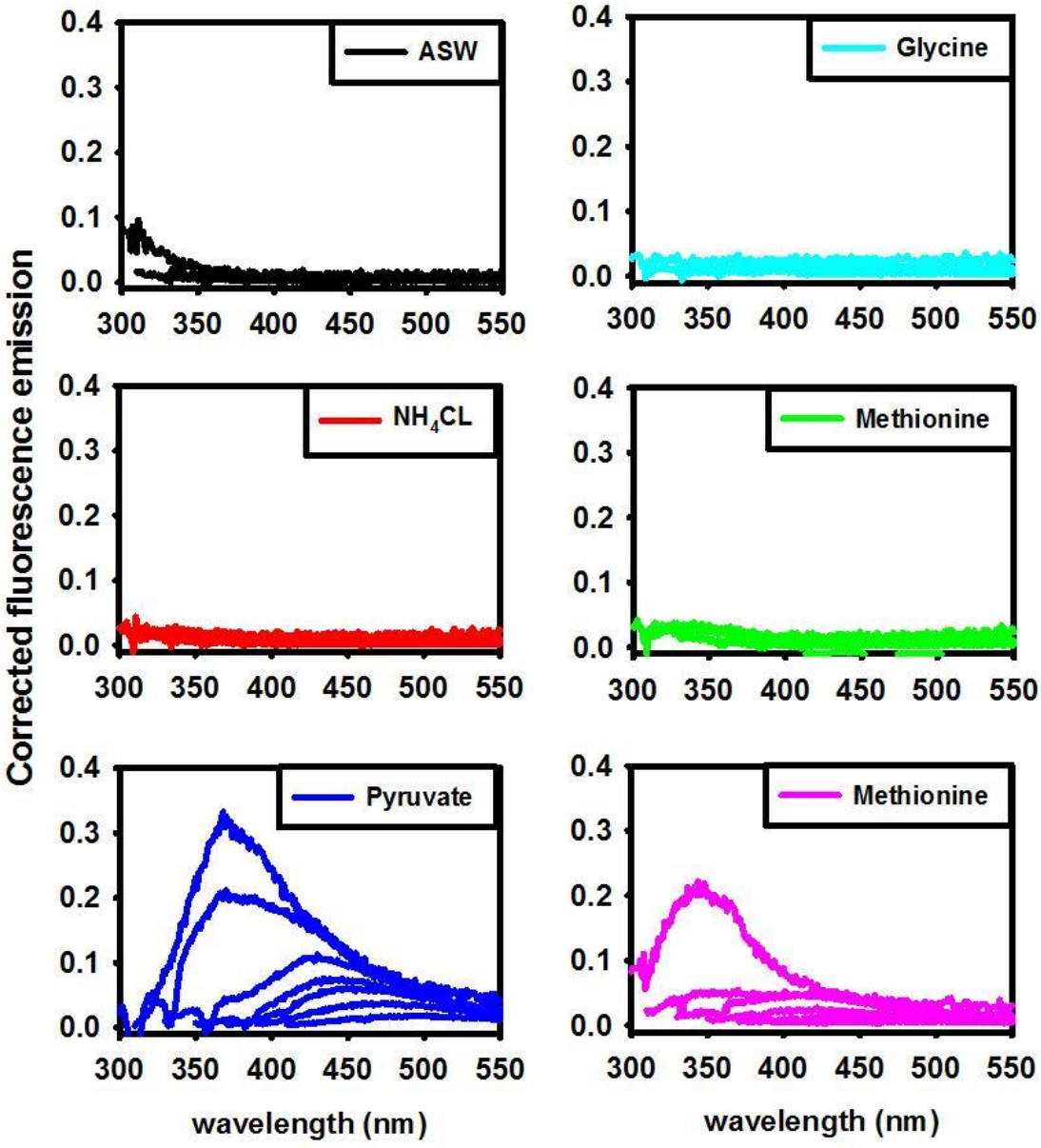

Figure 5 - 13: Fluorescence spectra of the ASW and nutrients used in the SAR11 medium.

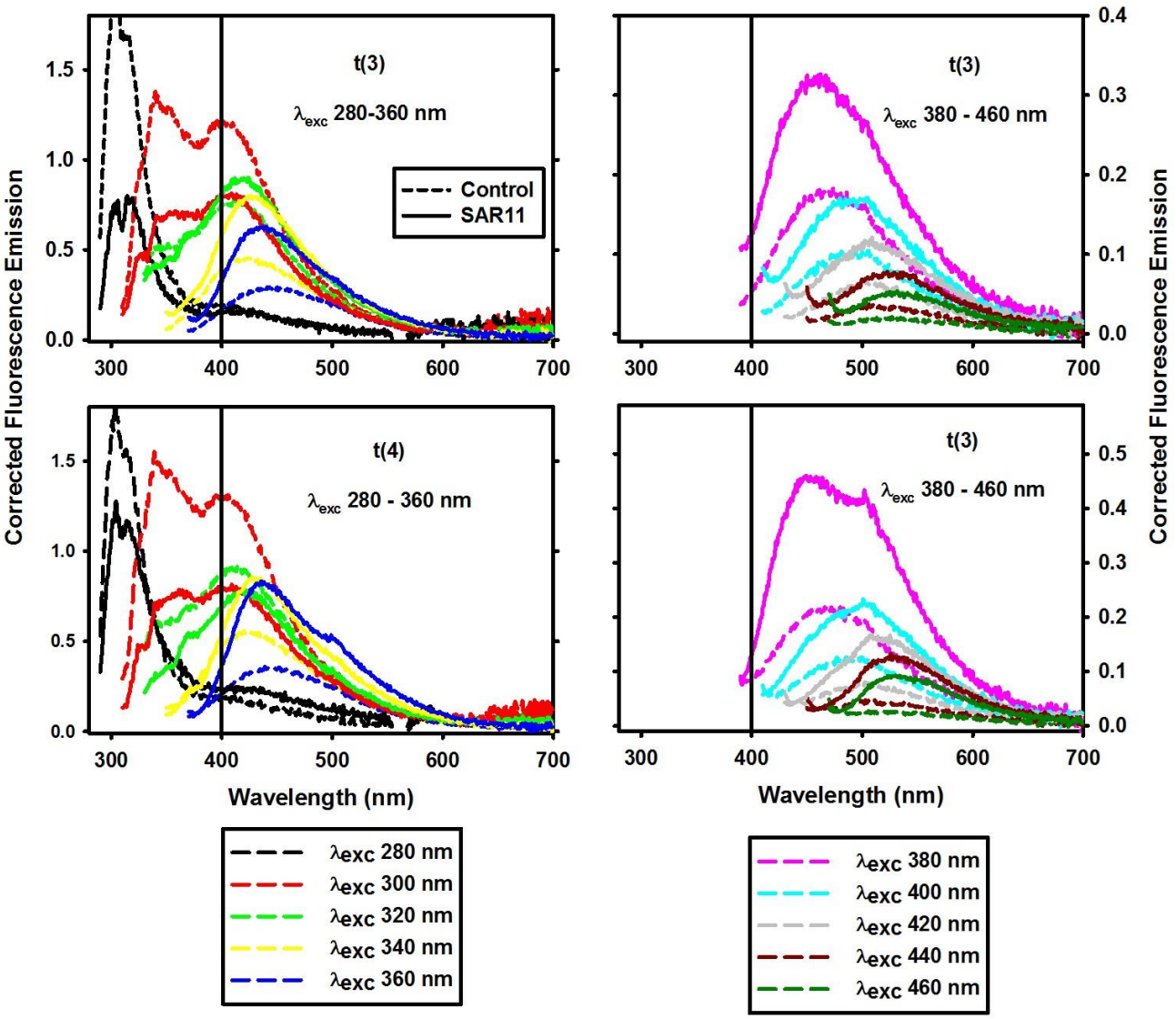

Figure 5 - 14: Comparison of fluorescence emission spectra of control extract (dashed lines) and SAR11 (solid lines) extract at t(3) and t(4).

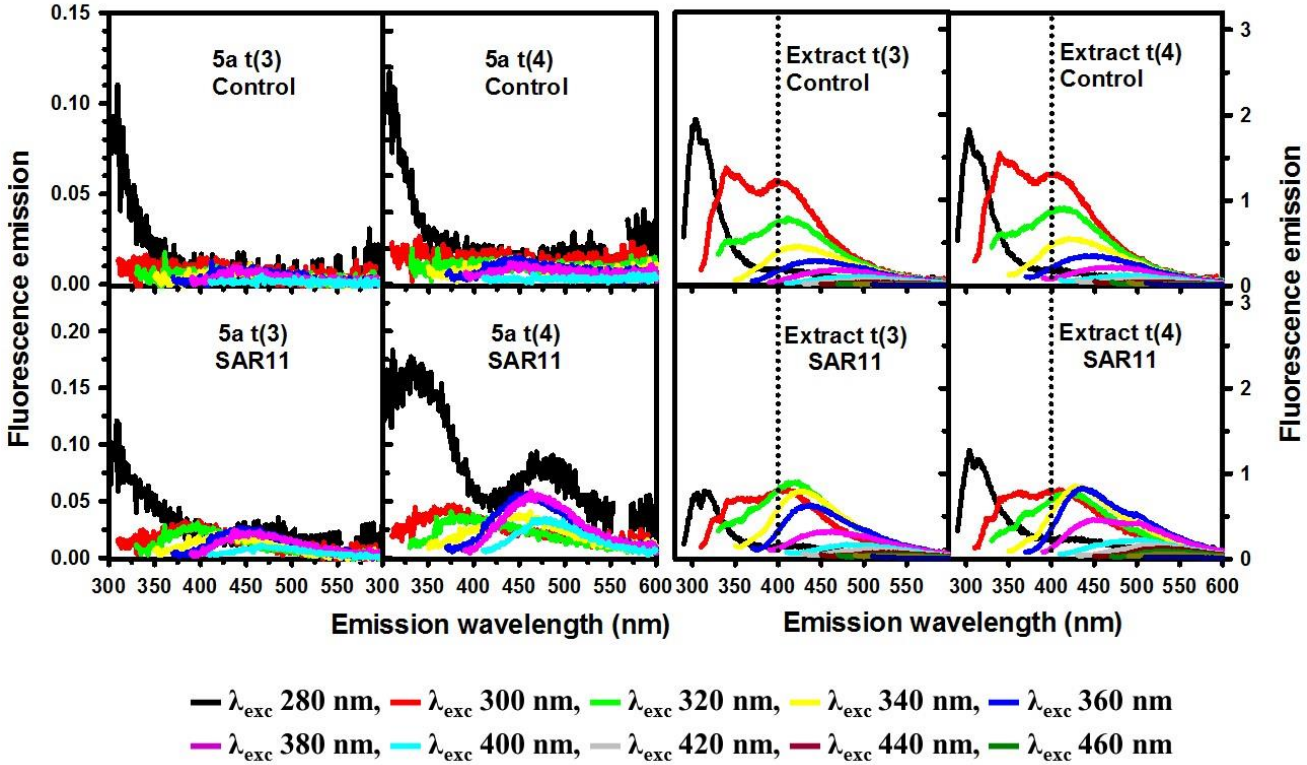

Figure 5 - 15: Comparison of fluorescence emission spectra of original waters and extracts after filtration at t(3) and t(4).

5.5 Summary and conclusions

Control samples were internally consistent, showing no significant optical changes over time. SAR11 contains fluorescing compounds that are significantly removed by filtration, some of which do however end up in the exudates. New discrete emitting bands were observed at the late stationary phase of the incubation, t(4) (at ~340 and 460 nm) that are possibly produced by SAR11. The 340 nm emission was produced upon excitation at 280 nm, thus is possibly due to fluorescence from an amino acid. That at 460 nm is excited at 360-400 nm and it is unclear what it is. No production of CDOM (with long-wavelength absorption and red-shifted emission) is evident from this experiment.

Chapter 6: Conclusions and future work

6.1 Conclusions

This work has shown that CDOM in the offshore waters of the Equatorial Atlantic Ocean is composed of a major terrestrial CDOM component that absorbs in the UV and visible and emits in the visible, as well as marine CDOM components that absorb and emit in the UV. Except in regions of upwelling or in the vicinity of the Congo River outflow, CDOM absorption coefficients and visible emission intensity were far smaller for surface waters than for waters below the mixed layer, while spectral slopes were higher, consistent with photobleaching of CDOM in surface waters. Distinct emission bands were observed in the ultraviolet, primarily at excitation/emission wavelengths ($\lambda_{exc}/\lambda_{em}$) = 280/320 nm, but also at $\lambda_{exc}/\lambda_{em}$ = 300/340, 300/405 and 320/380 nm for some stations and depths. In contrast, visible emission exhibited maxima that continuously red-shifted with increasing λ_{exc} (> 330 nm), a property characteristic of CDOM from estuarine and coastal environments. The results further demonstrated that the simultaneous acquisition of complete spectral absorption and emission properties, combined with chemical tests (C-18 extractions, borohydride reduction) provides a clearer picture of the sources and cycling of CDOM within the oceans.

Comparison of the optical properties of original water samples (CDOM) and the corresponding extracted material (C18-OM) from the MAB and EAO suggests that the extracted material does not differ significantly from the whole water. For inshore MAB samples, C18 cartridges preferentially extract higher molecular weight, long-wavelength

absorbing material. Extraction efficiency decreases with offshore distance and becomes more uniform with wavelength. Absorption and fluorescence were similarly impacted by the extraction process thus leading to essentially identical fluorescence quantum yields. Additionally, C18 extracts and corresponding water samples exhibited very similar changes in optical properties following $NaBH_4$ reduction suggesting a common structural basis for the optical properties of these materials.

Further, this data set indicates that the optical properties of CDOM over very long time periods are not highly susceptible to alteration (whether biological or not) when stored in the dark at 4°C. The majority of CDOM samples examined showed no appreciable change in optical properties over the six year storage period. The small changes that were observed were mainly association with precipitation (and sedimentation) of the organic material, or adsorption to the walls of the storage container. Additionally, this work highlighted the importance of establishing optical changes relative to the wavelength dependence of standard deviation in absorbance measurements. Absorbance measurements, particularly small changes, must be analyzed relative to the established standard deviations and not on an absolute scale.

Incubation experiments with *Pelagibacter ubique* did not provide evidence to support the production of CDOM with long-wavelength absorption and red-shifted emission properties.

6.2 Future Work

More work is needed to better understand the sources and cycling of CDOM in ocean waters. Thus, the systematic examination of the complete optical properties of absorption and emission of CDOM and changes in these properties following chemical reduction can be extended to other regions, particularly other marine regions. Additionally, ultra-high resolution mass spectral measurements can be acquired for C18 extracts, to provide structural information about the components of marine CDOM. This combined data set would facilitate a far clearer understanding of connection between CDOM optical properties and structure.

Although the question of whether bacteria can be implicated in the in situ production of CDOM was addressed in this work, it was done on a fairly limited scale using just one type of bacteria. This study can be extended to other bacterial species or other biological species in general. The effect of different substrates added to the growth medium can also be examined.

Appendix

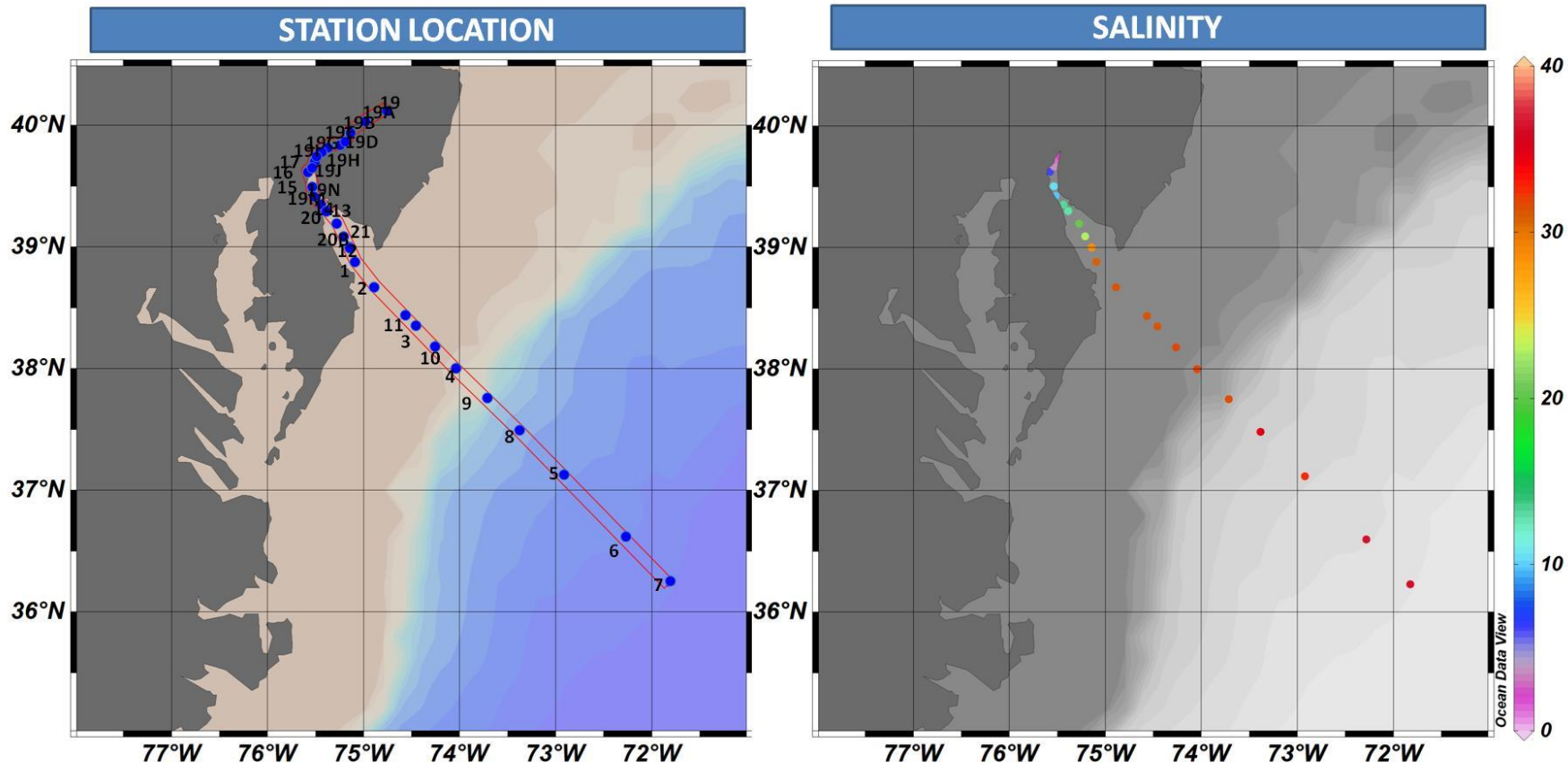

AP - 1: Map of the Middle Atlantic Bight (MAB) showing sampling station locations and salinity for August

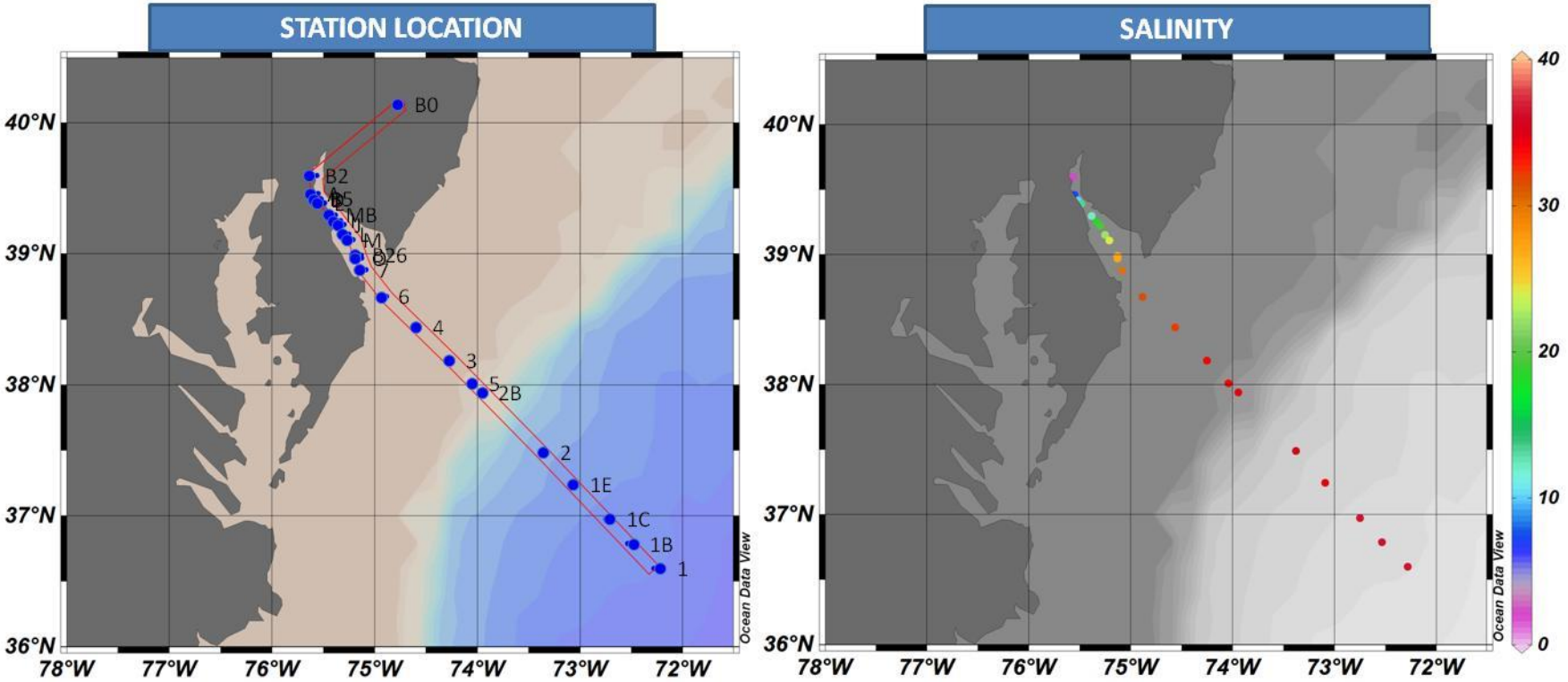

AP - 2: Map of the Middle Atlantic Bight (MAB) showing sampling station locations and salinity for October

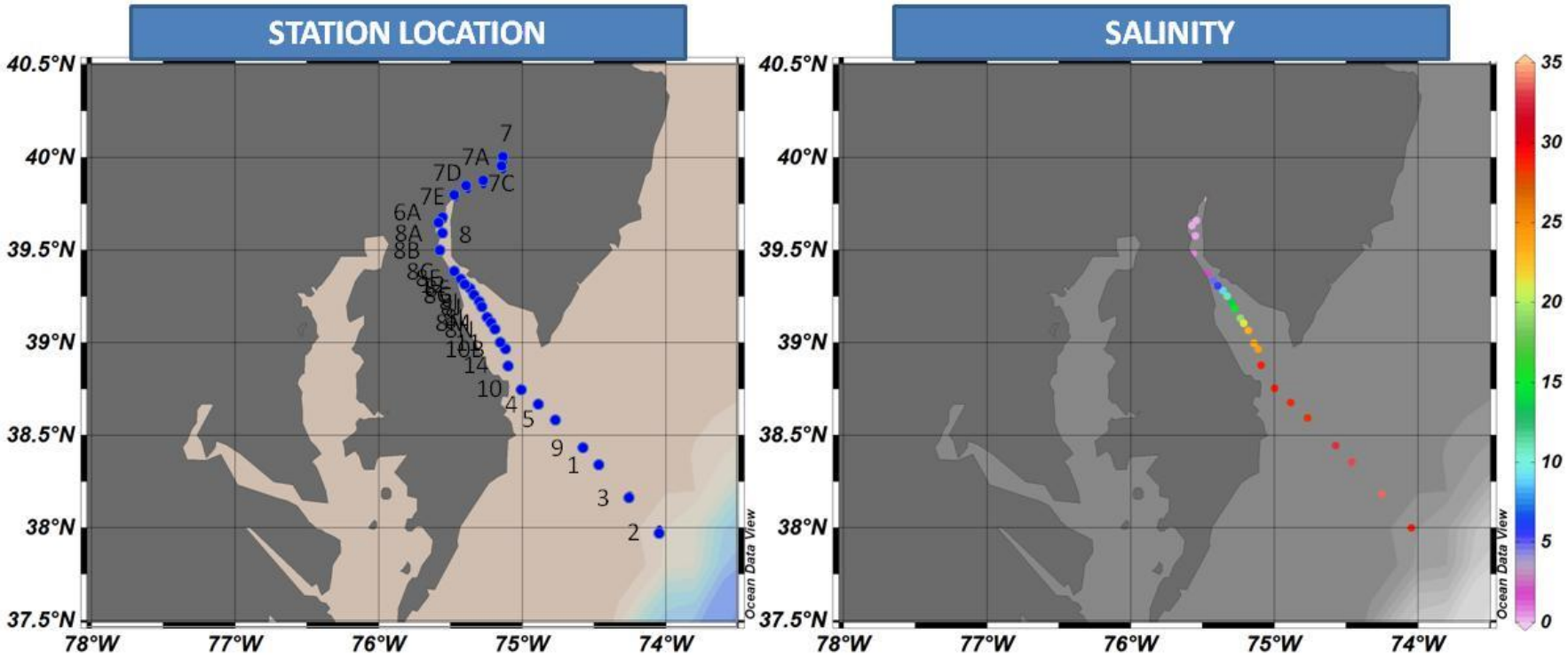

AP - 3: Map of the Middle Atlantic Bight (MAB) showing sampling station locations and salinity for December

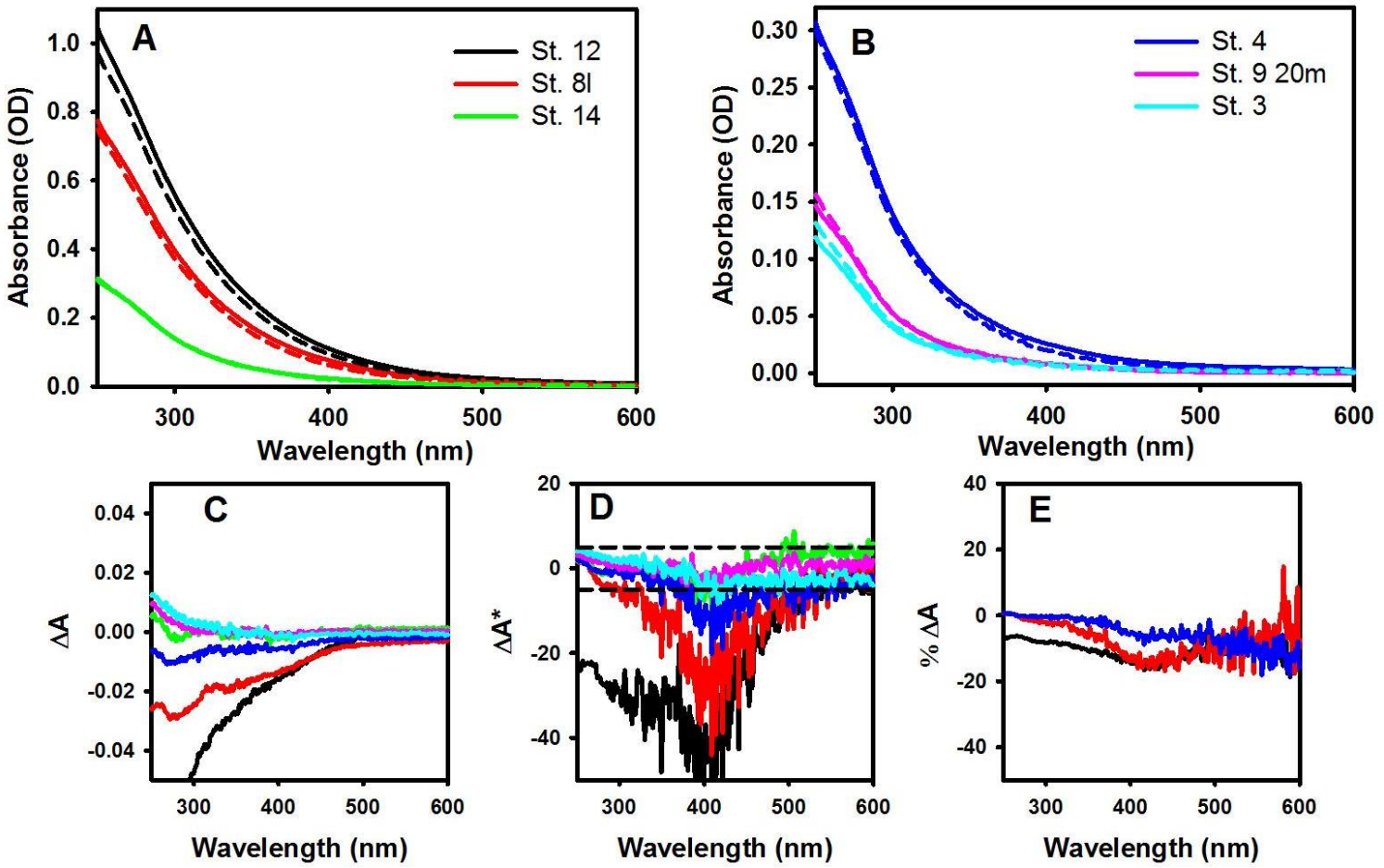

AP - 4: Select MAB samples from December 2006 showing no change in absorbance across the UV and visible regime. (A & B) Comparison of absorbance spectra, dashed lines - 2013, solid lines - 2006; (C) Plot of ΔA; (D) Plot of ΔA* , showing ΔA*= 5 (dashed lines); (E) Plot of % ΔA for ΔA* >5.

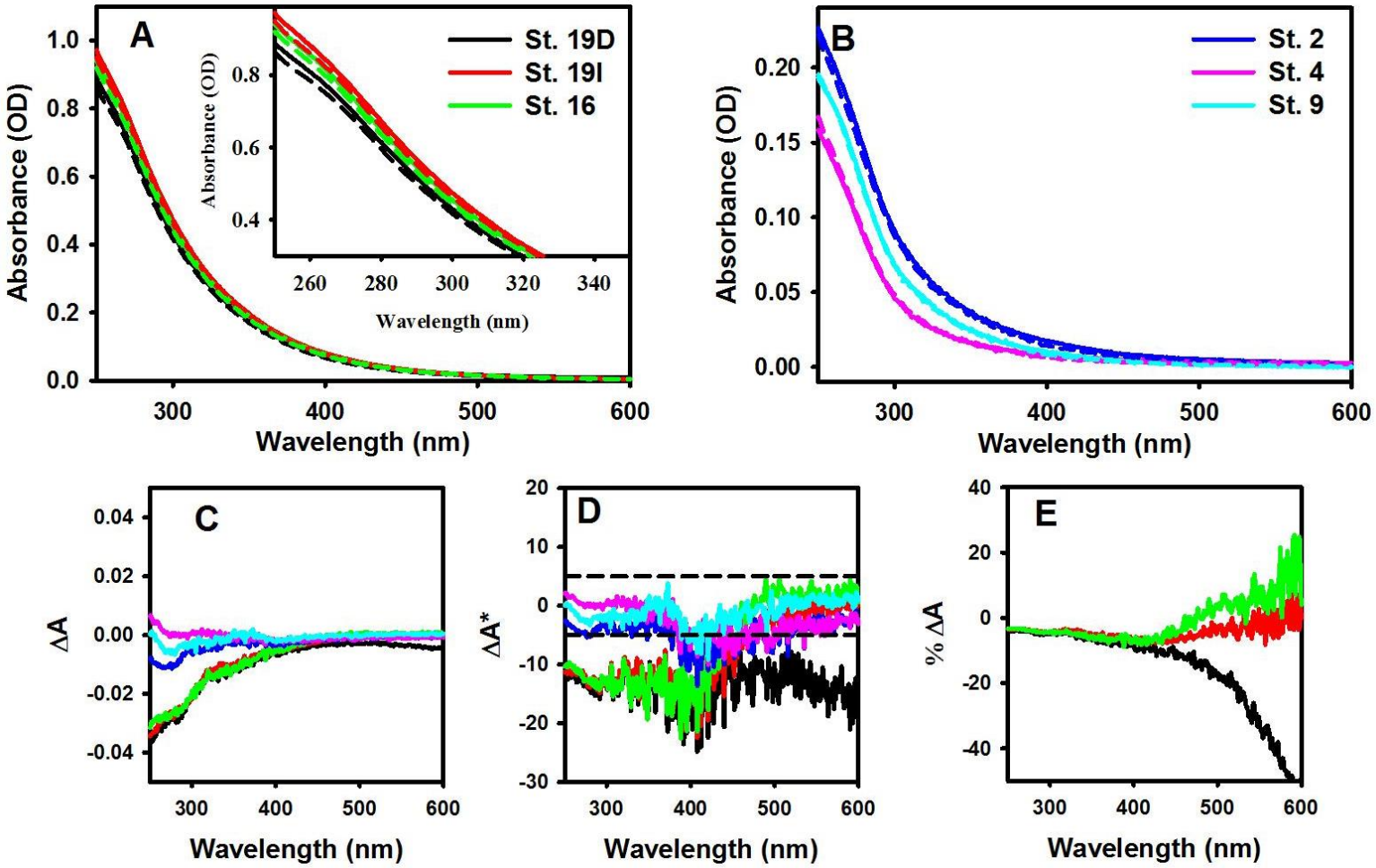

AP - 5: Select MAB samples from August 2006 showing no change in absorbance across the UV and visible regime. (A & B) Comparison of absorbance spectra, dashed lines - 2013, solid lines - 2006; (C) Plot of ΔA; (D) Plot of ΔA* , showing ΔA*= 5 (dashed lines). (E) Plot of % ΔA for ΔA* >5.

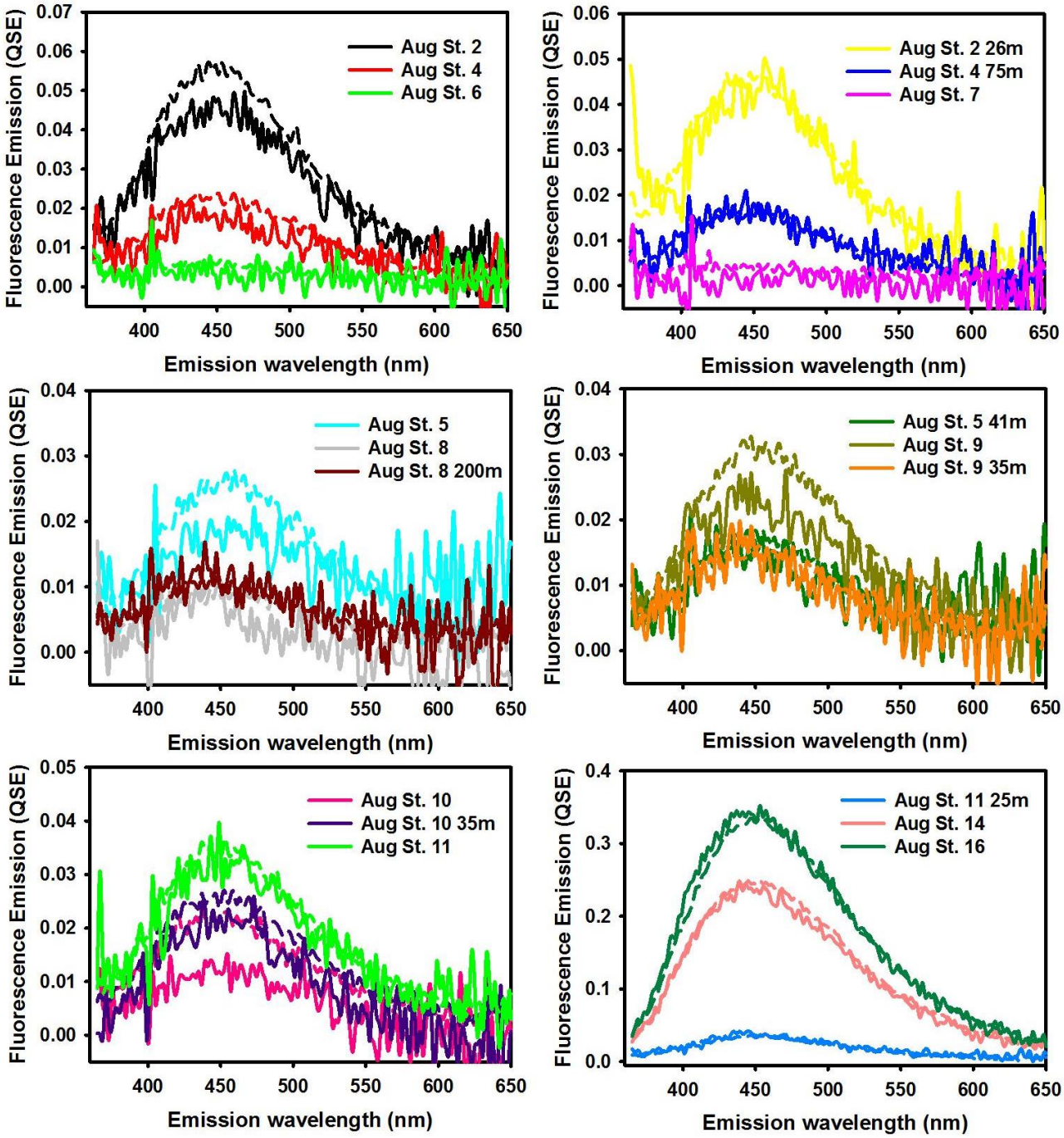

AP - 6: Comparison of fluorescence emission spectra obtained in 2006 (solid lines) and 2013 (dashed lines) for August CDOM samples.

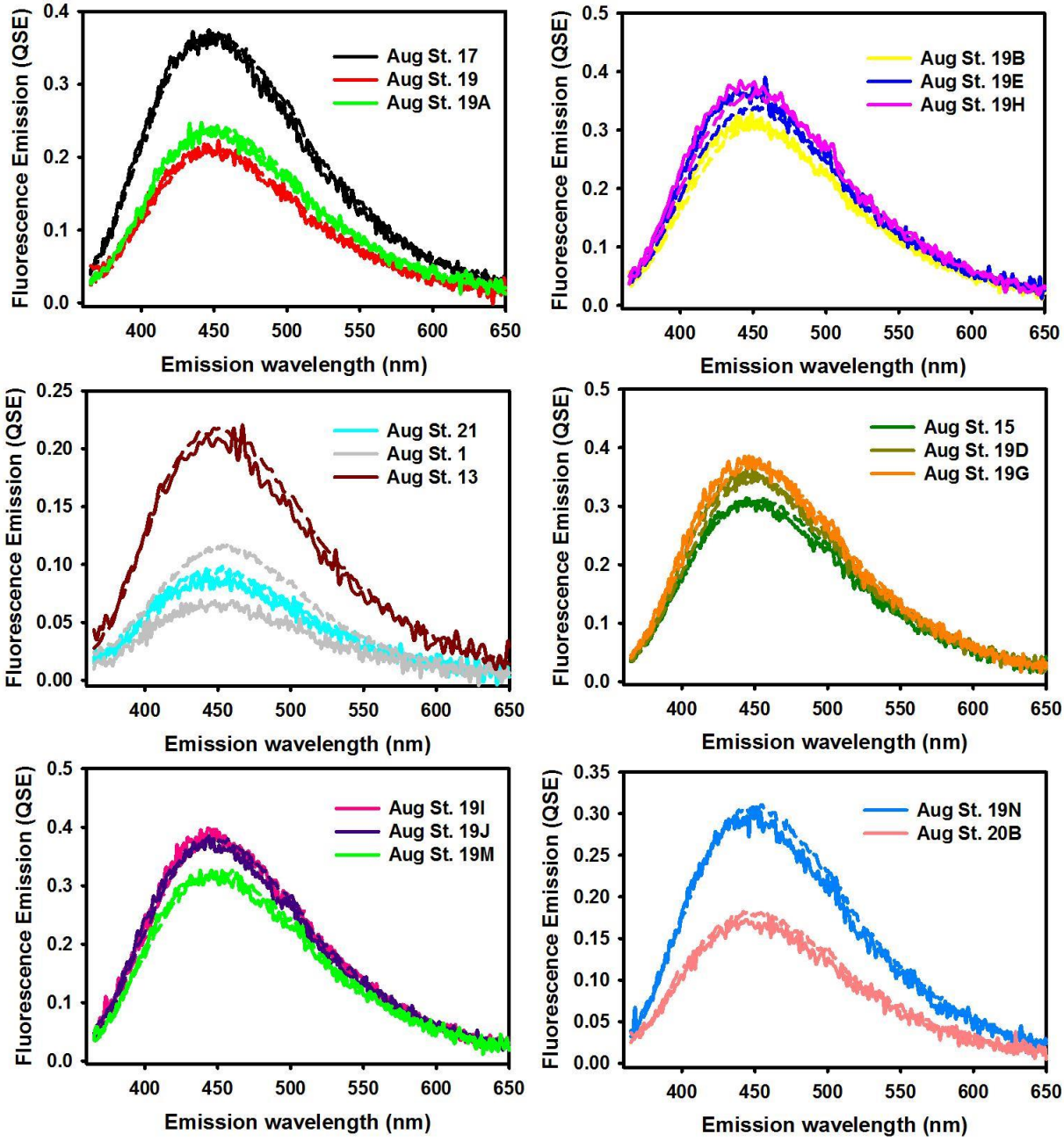

AP - 7: Comparison of fluorescence emission spectra obtained in 2006 (solid lines) and 2013 (dashed lines) for August CDOM samples contd.

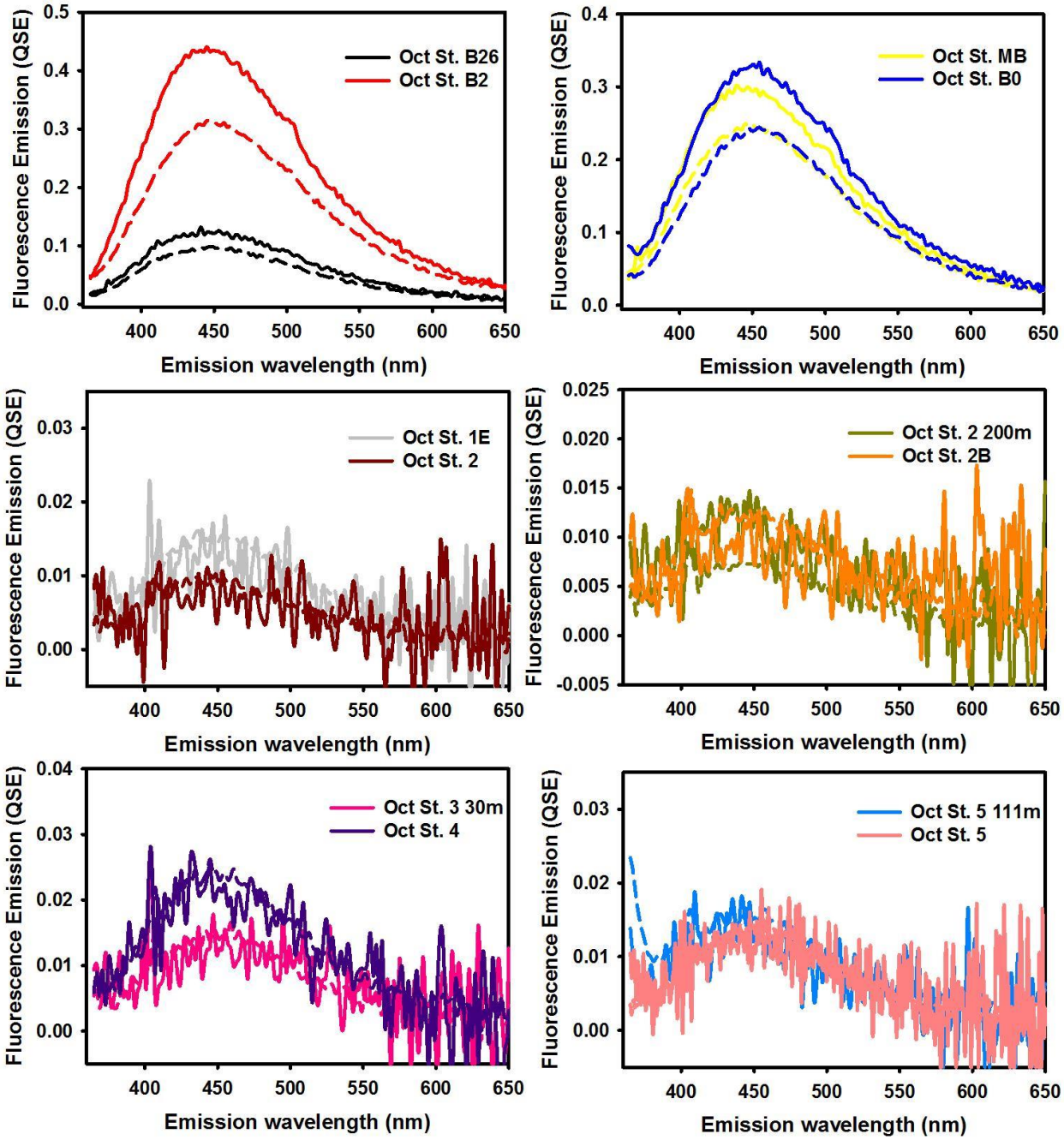

AP - 8: Comparison of fluorescence emission spectra obtained in 2006 (solid lines) and 2013 (dashed lines) for October CDOM samples.

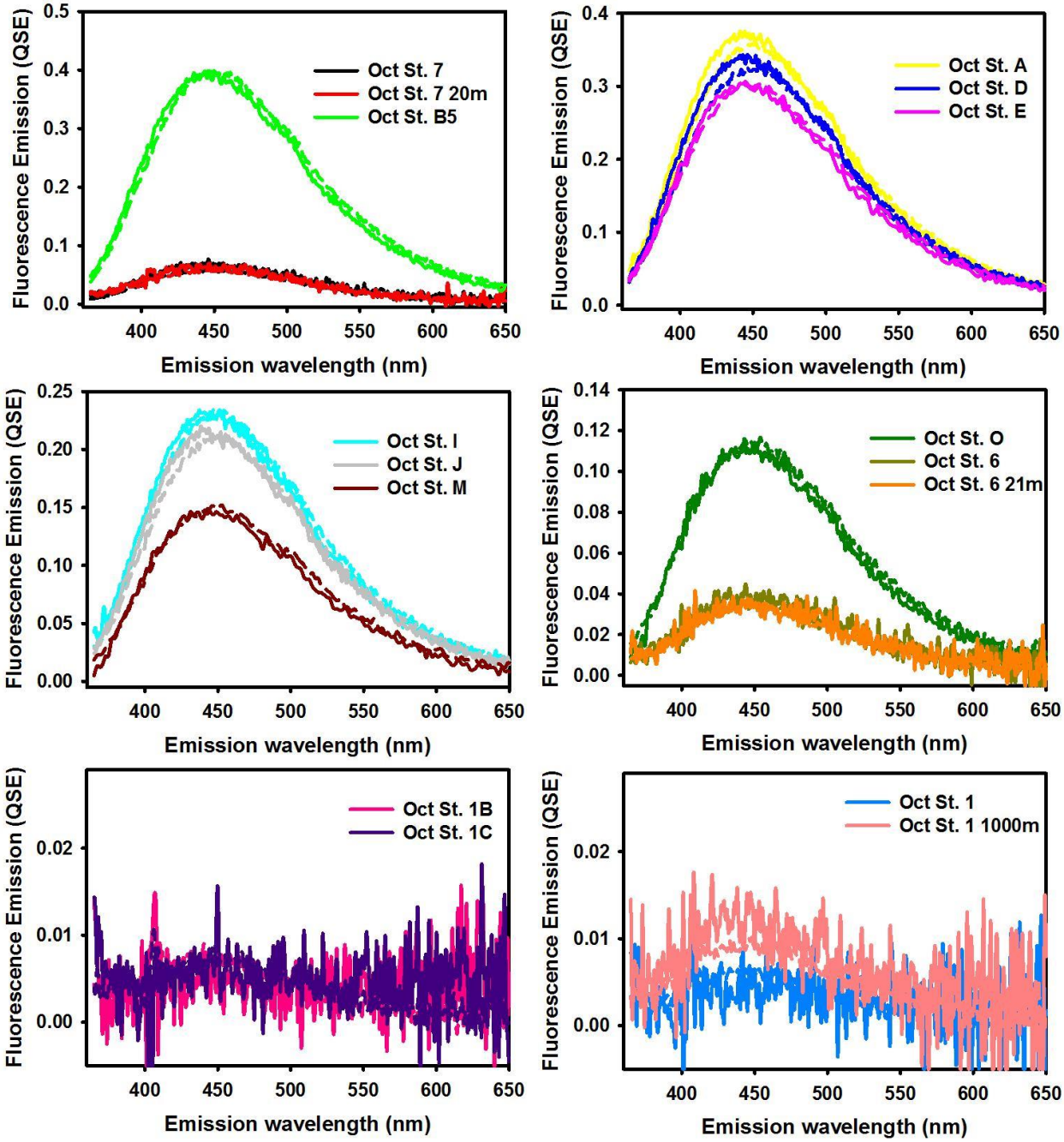

AP - 9: Comparison of fluorescence emission spectra obtained in 2006 (solid lines) and 2013 (dashed lines) for October CDOM samples contd.

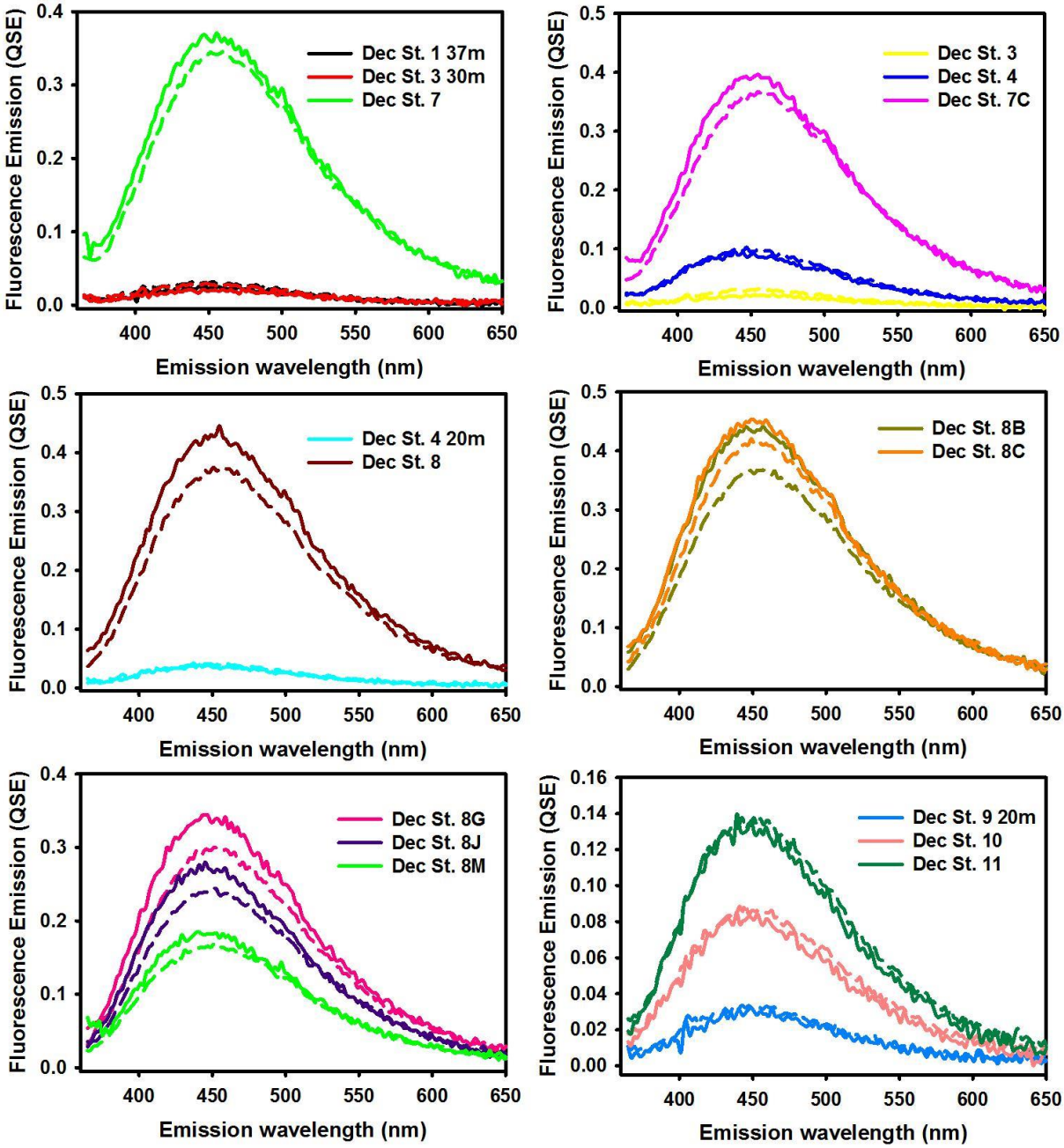

AP - 10: Comparison of fluorescence emission spectra obtained in 2006 (solid lines) and 2013 (dashed lines) for December CDOM samples.

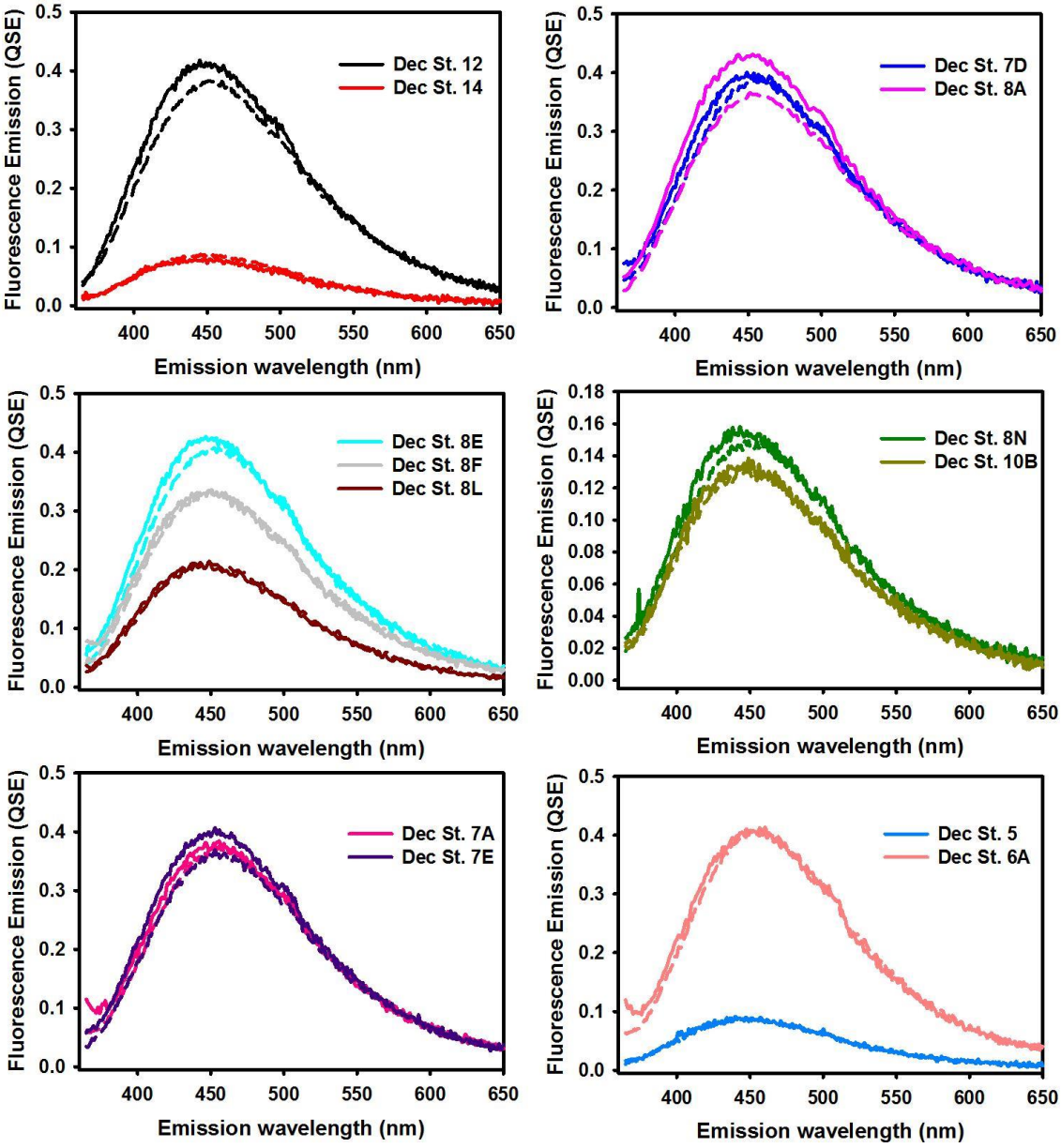

AP - 11: Comparison of fluorescence emission spectra obtained in 2006 (solid lines) and 2013 (dashed lines) for December CDOM samples contd.

Bibliography

Amador, J.A., Milne, P.J., Moore, C.A. and Zika, R.G., 1990. Extraction of chromophoric humic substances from seawater. Marine Chemistry, 29(1): 1-17.

Andrew, A.A., Del Vecchio, R., Subramaniam, A. and Blough, N.V., 2013. Chromophoric dissolved organic matter (CDOM) in the Equatorial Atlantic Ocean: Optical properties and their relation to CDOM structure and source. Marine Chemistry, 148: 33-43.

Belz, M., Dress, P., Sukhitskiy, A. and Liu, S., 1999. "Linearity and effective optical pathlength of liquid waveguide capillary cells", Part of the SPIE Conference on Internal Standardization and Calibration Architectures for Chemical Sensors, Boston, MA, pp. 271-281.

Benner, R., 2002. Chemical composition and reactivity. In: D. Hansell and C. Carlson (Editors), Biogeochemistry of marine dissolved organic matter. Academic Press, pp. 59-90.

Benner, R. and Biddanda, B., 1998. Photochemical transformations of surface and deep marine dissolved organic matter: Effects on bacterial growth. Limnology and Oceanography, 43(6): 1373-1378.

Blough, N.V. and Del Vecchio, R., 2002. Chromophoric DOM in the Coastal Environment. In: D.A. Hansel and C.A. Carlson (Editors), Biogeochemistry of Marine Dissolved Organic Matter. Academic Press, San Diego, California, pp. 509-546.

Blough, N.V. and Green, S.A., 1995. Spectroscopic characterization and remote sensing of nonliving organic matter. In: R.G. Zepp and C. Sonntag (Editors), The Role of Nonliving Organic Matter in the Earth's Carbon Cycle. John Wiley and Sons, NYC, pp. 23-45.

Blough, N.V., Zafiriou, O.C. and Bonilla, J., 1993. Optical absorption spectra of waters from the Orinocco River outflow: terrestrial input of colored organic matter to the Caribbean. Journal of Geophysical Research-Oceans, 98(C2): 2271-2278.

Blough, N.V. and Zepp, R.G., 1995. Reactive Oxygen Species in Natural Waters. In: C.S. Foote, J.S. Valentine, A. Greenberg and J.F. Liebman (Editors), Active Oxygen in Chemistry. Chapman and Hall, New York, pp. 280-333.

Boyle, E.S., Guerriero, N., Thiallet, A., Del Vecchio, R. and Blough, N.V., 2009. Optical Properties of Humic Substances and CDOM: Relation to Structure. Environmental Science & Technology, 43(7): 2262-2268.

Bricaud, A., Babin, M., Claustre, H., Ras, J. and Tieche, F., 2010. Light absorption properties and absorption budget of Southeast Pacific waters. Journal of Geophysical Research-Oceans, 115: 19.

Bricaud, A., Morel, A. and Prieur, L., 1981. Absorption by dissolved organic matter of the sea (yellow substance) in the UV and visible domains. Limnology and Oceanography, 26(1): 43-53.

Carini, P., Steindler, L., Beszteri, S. and Giovannoni, S.J., 2013. Nutrient requirements for growth of the extreme oligotroph 'Candidatus Pelagibacter ubique' HTCC1062 on a defined medium. Isme Journal, 7(3): 592-602.

Chen, R.F. and Gardner, G.B., 2004. High-resolution measurements of chromophoric dissolved organic matter in the Mississippi and Atchafalaya River plume regions. Marine Chemistry, 89(1-4): 103-125.

Coble, P.G., 1996. Characterization of marine and terrestrial DOM in seawater using excitation emission matrix spectroscopy. Marine Chemistry, 51(4): 325-346.

Coble, P.G., 2007. Marine Optical Biogeochemistry: The Chemistry of Ocean Color. Chemical Reviews, 107(2): 402-418.

Coble, P.G., Green, S.A., Blough, N.V. and Gagosian, R.B., 1990. Characterization of dissolved organic-matter in the black-sea by fluorescence spectroscopy. Nature, 348(6300): 432-435.

Daignault, S.A., Noot, D.K., Williams, D.T. and Huck, P.M., 1988. A review of the use of XAD resins to concentrate organic compounds in water. Water Research, 22(7): 803-813.

DeGrandpre, M.D., Vodacek, A., Nelson, R.K., Bruce, E.J. and Blough, N.V., 1996. Seasonal seawater optical properties of the US Middle Atlantic Bight. Journal of Geophysical Research-Oceans, 101(C10): 22727-22736.

Del Castillo, C.E., 2005. Remote Sensing of Coastal Aquatic Environments. Springer, Dordrecht, The Netherlands.

Del Castillo, C.E., Coble, P.G., Morell, J.M., Lopez, J.M. and Corredor, J.E., 1999. Analysis of the optical properties of the Orinoco River plume by absorption and fluorescence spectroscopy. Marine Chemistry, 66(1-2): 35-51.

Del Vecchio, R. and Blough, N.V., 2002. Photobleaching of chromophoric dissolved organic matter in natural waters: kinetics and modeling. Marine Chemistry, 78(4): 231-253.

Del Vecchio, R. and Blough, N.V., 2004a. On the origin of the optical properties of humic substances. Environmental Science & Technology, 38(14): 3885-3891.

Del Vecchio, R. and Blough, N.V., 2004b. Spatial and seasonal distribution of chromophoric dissolved organic matter and dissolved organic carbon in the Middle Atlantic Bight. Marine Chemistry, 89(1-4): 169-187.

Del Vecchio, R. and Subramaniam, A., 2004. Influence of the Amazon River on the surface optical properties of the western tropical North Atlantic Ocean. Journal of Geophysical Research-Oceans, 109(C11).

Del Vecchio, R. et al., 2009. Decadal time-series of SeaWiFS retrieved CDOM absorption and estimated CO2 photoproduction on the continental shelf of the eastern United States. Geophys. Res. Lett., 36(2): L02602.

Dittmar, T., Koch, B., Hertkorn, N. and Kattner, G., 2008. A simple and efficient method for the solid-phase extraction of dissolved organic matter (SPE-DOM) from seawater. Limnology and Oceanography-Methods, 6: 230-235.

Druffel, E.R.M., Williams, P.M., Bauer, J.E. and Ertel, J.R., 1992. Cycling of dissolved and particulate organic matter in the open ocean. Journal of Geophysical Research-Oceans, 97(C10): 15639-15659.

Ferrari, G.M. and Dowell, M.D., 1998. CDOM absorption characteristics with relation to fluorescence and salinity in coastal areas of the southern Baltic Sea. Estuarine Coastal and Shelf Science, 47(1): 91-105.

Golanoski, K.S., Fang, S., Del Vecchio, R. and Blough, N.V., 2012. Investigating the Mechanism of Phenol Photooxidation by Humic Substances. Environmental Science & Technology, 46(7): 3912-3920.

Green, S.A. and Blough, N.V., 1994. Optical Absorption and Fluorescence Properties of Chromophoric Dissolved Organic Matter in Natural Waters. Limnology and Oceanography, 39(8): 1903-1916.

Hansell, D.A. and Carlson, C.A., 2002. Biogeochemistry of Marine Dissolved Organic Matter. Academic Press, San Diego, Carlifonia, 774 pp.

Hansell, D.A., Carlson, C.A., Repeta, D.J. and Schlitzer, R., 2009. Dissolved organic matter in the ocean:A controversy stimulates new insights. Oceanography, 22(4): 202-211.

Harvey, G.R., Boran, D.A., Piotrowicz, S.R. and Weisel, C.P., 1984. Synthesis of marine humic substances from unsaturated lipids. Nature, 309(5965): 244-246.

Helms, J.R. et al., 2008. Absorption Spectral Slopes and Slope Ratios as Indicators of Molecular Weight, Source, and Photobleaching of Chromophoric Dissolved Organic Matter. Limnology and Oceanography, 53(3): 955-969.

Hernes, P.J. and Benner, R., 2003. Photochemical and microbial degradation of dissolved lignin phenols: Implications for the fate of terrigenous dissolved organic matter in marine environments. Journal of Geophysical Research-Oceans, 108(C9): 9.

Hernes, P.J. and Benner, R., 2006. Terrigenous organic matter sources and reactivity in the North Atlantic Ocean and a comparison to the Arctic and Pacific oceans. Marine Chemistry, 100(1-2): 66-79.

Hertkorn, N. et al., 2006. Characterization of a major refractory component of marine dissolved organic matter. Geochimica Et Cosmochimica Acta, 70(12): 2990-3010.

Hoge, F.E., Swift, R.N., Yungel, J.K. and Vodacek, A., 1993. Fluorescence of dissolved organic matter: A comparison of North Pacific and North Atlantic Oceans during April 1991. Journal of Geophysical Research-Oceans, 98(C12): 22779-22787.

Hulatt, C.J., Thomas, D.N., Bowers, D.G., Norman, L. and Zhang, C., 2009. Exudation and decomposition of chromophoric dissolved organic matter (CDOM) from some temperate macroalgae. Estuarine Coastal and Shelf Science, 84(1): 147-153.

Kieber, D.J., McDaniel, J. and Mopper, K., 1989. Photochemical source of biological substrates in sea water: implications for carbon cycling. Nature, 341(6243): 637-639.

Kitidis, V. et al., 2006. Variability of chromophoric organic matter in surface waters of the Atlantic Ocean. Deep-Sea Research Part Ii-Topical Studies in Oceanography, 53(14-16): 1666-1684.

Kowalczuk, P., Stoń-Egiert, J., Cooper, W.J., Whitehead, R.F. and Durako, M.J., 2005. Characterization of chromophoric dissolved organic matter (CDOM) in the Baltic Sea by excitation emission matrix fluorescence spectroscopy. Marine Chemistry, 96(3–4): 273-292.

Kujawinski, E.B., Del Vecchio, R., Blough, N.V., Klein, G.C. and Marshall, A.G., 2004. Probing molecular-level transformations of dissolved organic matter: insights on photochemical degradation and protozoan modification of DOM from electrospray ionization Fourier transform ion cyclotron resonance mass spectrometry. Marine Chemistry, 92(1-4): 23-37.

Kujawinski, E.B. et al., 2009. Identification of possible source markers in marine dissolved organic matter using ultrahigh resolution mass spectrometry. Geochimica Et Cosmochimica Acta, 73(15): 4384-4399.

Lin, S.Y. and Kringstad, K.P., 1970. Photosensitive groups in lignin and lignin model compounds. Tappi, 53(4): 658-&.

Liu, Z.F., Sleighter, R.L., Zhong, J.Y. and Hatcher, P.G., 2011. The chemical changes of DOM from black waters to coastal marine waters by HPLC combined with ultrahigh resolution mass spectrometry. Estuarine Coastal and Shelf Science, 92(2): 205-216.

Louchouarn, P., Opsahl, S. and Benner, R., 2000. Isolation and Quantification of Dissolved Lignin from Natural Waters Using Solid-Phase Extraction and GC/MS. Analytical Chemistry, 72(13): 2780-2787.

Lundquist, K., Josefsson, B. and Nyquist, G., 1978. Analysis of lignin products by fluorescence spectroscopy. Holzforschung, 32(1): 27-32.

Ma, J.H., Del Vecchio, R., Golanoski, K.S., Boyle, E.S. and Blough, N.V., 2010. Optical Properties of Humic Substances and CDOM: Effects of Borohydride Reduction. Environmental Science & Technology, 44(14): 5395-5402.

Maie, N., Pisani, O. and Jaffe, R., 2008. Mangrove tannins in aquatic ecosystems: Their fate and possible influence on dissolved organic carbon and nitrogen cycling. Limnology and Oceanography, 53(1): 160-171.

Matsuoka, A., Hill, V., Huot, Y., Babin, M. and Bricaud, A., 2011. Seasonal variability in the light absorption properties of western Arctic waters: Parameterization of the

individual components of absorption for ocean color applications. Journal of Geophysical Research-Oceans, 116: 15.

Maurer, F., Christl, I. and Kretzschmar, R., 2010. Reduction and Reoxidation of Humic Acid: Influence on Spectroscopic Properties and Proton Binding. Environmental Science & Technology, 44(15): 5787-5792.

Mignone, R.A. et al., 2012. Modulation of Optical Properties of Dissolved Humic Substances by their Molecular Complexity. Photochemistry and Photobiology.

Miller, R.L., Belz, M., Del Castillo, C. and Trzaska, R., 2002. Determining CDOM absorption spectra in diverse coastal environments using a multiple pathlength, liquid core waveguide system. Continental Shelf Research, 22(9): 1301-1310.

Mopper, K. and Kieber, D.J., 2002. Photochemistry and the Cycling of Carbon, Sulfur, Nitrogen and Phosphorous. In: D.A. Hansell and C.A. Carlson (Editors), Biogeochemistry of Marine Dissolved Organic Matter. Academic Press, San Diego, California, pp. 455-507.

Mopper, K., Stubbins, A., Ritchie, J.D., Bialk, H.M. and Hatcher, P.G., 2007. Advanced instrumental approaches for characterization of marine dissolved organic matter: Extraction techniques, mass spectrometry, and nuclear magnetic resonance spectroscopy. Chemical Reviews, 107(2): 419-442.

Moran, M.A., Sheldon, W.M. and Zepp, R.G., 2000. Carbon loss and optical property changes during long-term photochemical and biological degradation of estuarine dissolved organic matter. Limnology and Oceanography, 45(6): 1254-1264.

Moran, M.A. and Zepp, R.G., 1997. Role of Photoreactions in the Formation of Biologically Labile Compounds from Dissolved Organic Matter. Limnology and Oceanography, 42(6): 1307-1316.

Morris, D.P. and Hargreaves, B.R., 1997. The Role of Photochemical Degradation of Dissolved Organic Carbon in Regulating the UV Transparency of Three Lakes on the Pocono Plateau. Limnology and Oceanography, 42(2): 239-249.

Murphy, K.R., Stedmon, C.A., Waite, T.D. and Ruiz, G.M., 2008. Distinguishing between terrestrial and autochthonous organic matter sources in marine environments using fluorescence spectroscopy. Marine Chemistry, 108(1-2): 40-58.

Nebbioso, A. and Piccolo, A., 2013. Molecular characterization of dissolved organic matter (DOM): a critical review. Analytical and Bioanalytical Chemistry, 405(1): 109-124.

Nelson, N.B., Carlson, C.A. and Steinberg, D.K., 2004. Production of chromophoric dissolved organic matter by Sargasso Sea microbes. Marine Chemistry, 89(1-4): 273-287.

Nelson, N.B. and Coble, P.G., 2009. Optical Analysis of Chromophoric Dissolved Organic Matter. In: O. Wurl (Editor), Practical Guidelines for the Analysis of Seawater. CRC Press, pp. 79-96.

Nelson, N.B. and Siegel, D.A., 2002. Chromophoric DOM in the Open Ocean. In: D.A. Hansel and C.A. Carlson (Editors), Biogeochemistry of Marine Dissolved Organic Matter. Academic Press, San Diego, California, pp. 547-578.

Nelson, N.B. and Siegel, D.A., 2013. The Global Distribution and Dynamics of Chromophoric Dissolved Organic Matter. Annual Review of Marine Science, Vol 5, 5: 447-476.

Nelson, N.B. et al., 2007. Hydrography of chromophoric dissolved organic matter in the North Atlantic. Deep-Sea Research Part I-Oceanographic Research Papers, 54(5): 710-731.

Nelson, N.B., Siegel, D.A., Carlson, C.A. and Swan, C.M., 2010. Tracing global biogeochemical cycles and meridional overturning circulation using chromophoric dissolved organic matter. Geophys. Res. Lett., 37(3): L03610.

Nelson, N.B., Siegel, D.A. and Michaels, A.F., 1998. Seasonal dynamics of colored dissolved material in the Sargasso Sea. Deep-Sea Research Part I-Oceanographic Research Papers, 45(6): 931-957.

Ortega-Retuerta, E. et al., 2009. Biogeneration of chromophoric dissolved organic matter by bacteria and krill in the Southern Ocean. Limnology and Oceanography, 54(6): 1941-1950.

Rottgers, R. and Koch, B.P., 2012. Spectroscopic detection of a ubiquitous dissolved pigment degradation product in subsurface waters of the global ocean. Biogeosciences, 9(7): 2585-2596.

Schmidt, F., Elvert, M., Koch, B.P., Witt, M. and Hinrichs, K.U., 2009. Molecular characterization of dissolved organic matter in pore water of continental shelf sediments. Geochimica Et Cosmochimica Acta, 73(11): 3337-3358.

Serkiz, S.M. and Perdue, E.M., 1990. Isolation of dissolved organic matter from the Suwannee river using reverse-osmosis. Water Research, 24(7): 911-916.

Shank, G.C., Zepp, R.G., Vahatalo, A., Lee, R. and Bartels, E., 2010. Photobleaching kinetics of chromophoric dissolved organic matter derived from mangrove leaf litter and floating Sargassum colonies. Marine Chemistry, 119(1-4): 162-171.

Sharpless, C.M., 2012. Lifetimes of Triplet Dissolved Natural Organic Matter (DOM) and the Effect of NaBH4 Reduction on Singlet Oxygen Quantum Yields: Implications for DOM Photophysics. Environmental Science & Technology, 46(8): 4466-4473.

Sharpless, C.M. and Blough, N.V., 2014. The importance of charge-transfer interactions in determining chromophoric dissolved organic matter (CDOM) optical and photochemical properties. Environmental Science & Technology.

Siegel, D.A., Maritorena, S., Nelson, N.B., Hansell, D.A. and Lorenzi-Kayser, M., 2002. Global distribution and dynamics of colored dissolved and detrital organic materials. Journal of Geophysical Research-Oceans, 107(C12).

Sleighter, R.L. and Hatcher, P.G., 2008. Molecular characterization of dissolved organic matter (DOM) along a river to ocean transect of the lower Chesapeake Bay by ultrahigh resolution electrospray ionization Fourier transform ion cyclotron resonance mass spectrometry. Marine Chemistry, 110(3-4): 140-152.

Sleighter, R.L., Lie, Z.F., Xue, J.H. and Hatcher, P.G., 2010. Multivariate Statistical Approaches for the Characterization of Dissolved Organic Matter Analyzed by Ultrahigh Resolution Mass Spectrometry. Environmental Science & Technology, 44(19): 7576-7582.

Spencer, R.G.M. et al., 2009. Photochemical degradation of dissolved organic matter and dissolved lignin phenols from the Congo River. Journal of Geophysical Research-Biogeosciences, 114: 12.

Stedmon, C.A. and Markager, S., 2001. The Optics of Chromophoric Dissolved Organic Matter (CDOM) in the Greenland Sea: An Algorithm for Differentiation between Marine and Terrestrially Derived Organic Matter. Limnology and Oceanography, 46(8): 2087-2093.

Stedmon, C.A., Markager, S. and Kaas, H., 2000. Optical properties and signatures of chromophoric dissolved organic matter (CDOM) in Danish coastal waters. Estuarine Coastal and Shelf Science, 51(2): 267-278.

Stedmon, C.A., Osburn, C.L. and Kragh, T., 2010. Tracing water mass mixing in the Baltic–North Sea transition zone using the optical properties of coloured dissolved organic matter. Estuarine, Coastal and Shelf Science, 87(1): 156-162.

Steinberg, D.K., Nelson, N.B., Carlson, C.A. and Prusak, A.C., 2004. Production of chromophoric dissolved organic matter (CDOM) in the open ocean by zooplankton and the colonial cyanobacterium Trichodesmium spp. Marine Ecology-Progress Series, 267: 45-56.

Stenson, A.C., Marshall, A.G. and Cooper, W.T., 2003. Exact masses and chemical formulas of individual Suwannee River fulvic acids from ultrahigh resolution electrospray ionization Fourier transform ion cyclotron resonance mass spectra. Analytical Chemistry, 75(6): 1275-1284.

Stubbins, A. et al., 2010. Illuminated darkness: Molecular signatures of Congo River dissolved organic matter and its photochemical alteration as revealed by ultrahigh precision mass spectrometry. Limnology and Oceanography, 55(4): 1467-1477.

Sulzberger, B. and Durisch-Kaiser, E., 2009. Chemical characterization of dissolved organic matter (DOM): A prerequisite for understanding UV-induced changes of DOM absorption properties and bioavailability. Aquatic Sciences, 71(2): 104-126.

Swan, C.M., 2009. Biogeochemical and Photochemical Dynamics of Oceanic Chromophoric Dissolved Organic Matter: A Basin-scale Approach. PhD Dissertation Thesis, University of California, Santa Barbara, 51-87 pp.

Swan, C.M., Siegel, D.A., Nelson, N.B., Carlson, C.A. and Nasir, E., 2009. Biogeochemical and hydrographic controls on chromophoric dissolved organic matter distribution in the Pacific Ocean. Deep-Sea Research Part I-Oceanographic Research Papers, 56(12): 2175-2192.

Tinnacher, R.M. and Honeyman, B.D., 2007. A new method to radiolabel natural organic matter by chemical reduction with tritiated sodium borohydride. Environmental Science & Technology, 41(19): 6776-6782.

Tranvik, L. and Kokalj, S., 1998. Decreased biodegradability of algal DOC due to interactive effects of UV radiation and humic matter. Aquatic Microbial Ecology, 14(3): 301-307.

Vernet, M. and Whitehead, K., 1996. Release of ultraviolet-absorbing compounds by the red-tide dinoflagellate Lingulodinium polyedra. Marine Biology, 127(1): 35-44.

Vetter, T.A., Perdue, E.M., Ingall, E., Koprivnjak, J.F. and Pfromm, P.H., 2007. Combining reverse osmosis and electrodialysis for more complete recovery of dissolved organic matter from seawater. Separation and Purification Technology, 56(3): 383-387.

Vodacek, A., Blough, N.V., DeGrandpre, M.D., Peltzer, E.T. and Nelson, R.K., 1997. Seasonal Variation of CDOM and DOC in the Middle Atlantic Bight: Terrestrial Inputs and Photooxidation. Limnology and Oceanography, 42(4): 674-686.

Vodacek, A. et al., 1995. The use of in-situ and airborne fluorescence measurements to determine BTV absorption coefficients and DOC concentrations in surface waters. Limnology and Oceanography, 40(2): 411-415.

Wetzel, R.G., Hatcher, P.G. and Bianchi, T.S., 1995. Natural photolysis by ultraviolet irradiance of recalcitrant dissolved organic matter to simple substrates for rapid bacterial metabolism. Limnology and Oceanography, 40(8): 1369-1380.

Whitehead, K. and Vernet, M., 2000. Influence of mycosporine-like amino acids (MAAs) on UV absorption by particulate and dissolved organic matter in La Jolla Bay. Limnology and Oceanography, 45(8): 1788-1796.

Whitehead, R.F. et al., 2000. Interactions of Ultraviolet-B Radiation, Mixing, and Biological Activity on Photobleaching of Natural Chromophoric Dissolved Organic Matter: A Mesocosm Study. Limnology and Oceanography, 45(2): 278-291.

Wurl, O. (Editor), 2009a. Practical guidelines for the analysis of seawater. CRC Press, Boca ranton, FL.

Wurl, O., 2009b. Sample and Sample Treatments. In: O. Wurl (Editor), Practical guidelines for the analysis of seawater. CRC, pp. 1-32.

Yamashita, Y. et al., 2010. Fluorescence characteristics of dissolved organic matter in the deep waters of the Okhotsk Sea and the northwestern North Pacific Ocean. Deep-Sea Research Part Ii-Topical Studies in Oceanography, 57(16): 1478-1485.

Yamashita, Y., Jaffe, R., Maie, N. and Tanoue, E., 2008. Assessing the dynamics of dissolved organic matter (DOM) in coastal environments by excitation emission matrix fluorescence and parallel factor analysis (EEM-PARAFAC). Limnology and Oceanography, 53(5): 1900-1908.

Yamashita, Y. and Tanoue, E., 2004. In situ production of chromophoric dissolved organic matter in coastal environments. Geophysical Research Letters, 31(14).

Yamashita, Y. and Tanoue, E., 2008. Production of bio-refractory fluorescent dissolved organic matter in the ocean interior. Nature Geoscience, 1(9): 579-582.

Yamashita, Y. and Tanoue, E., 2009. Basin scale distribution of chromophoric dissolved organic matter in the Pacific Ocean. Limnology and Oceanography, 54(2): 598-609.

Yan, M.Q., Korshin, G., Wang, D.S. and Cai, Z.X., 2012. Characterization of dissolved organic matter using high-performance liquid chromatography (HPLC)-size exclusion chromatography (SEC) with a multiple wavelength absorbance detector. Chemosphere, 87(8): 879-885.

Zepp, R.G., Erickson III, D.J., Paul, N.D. and Sulzberger, B., 2007. Interactive effects of solar UV radiation and climate change on biogeochemical cycling. Photochemical & Photobiological Sciences, 6(3): 286-300.

Zhang, Y., Del Vecchio, R. and Blough, N.V., 2012. Investigating the Mechanism of Hydrogen Peroxide Photoproduction by Humic Substances. Environmental Science & Technology, 46(21): 11836-11843.